ANUL XLVIII **2003**

S T U D I A
UNIVERSITATIS BABEŞ–BOLYAI

PHYSICA

SPECIAL ISSUE

EDITORIAL OFFICE: Republicii no. 24, Cluj-Napoca, Romania ♦ Phone: 0264-40.53.52

SUMAR ■ CONTENTS ■ SOMMAIRE ■ INHALT

I.

II. Aniversary Communications

About EPR Laboratory

The Electron Paramagnetic Resonance (EPR) Laboratory at "Babeş-Bolyai" University was created in 1962 and conducted till 1968 by Professor I. Ursu. The EPR Laboratory was meant to bring together the physicists interested in both theoretical and experimental aspects of EPR phenomena in condensed matter.

Based on Japanese instrument (JEOL) JES-3B, the EPR group started to develop studies on paramagnetic ions in catalysis, zeolites and ferroelectrics, and on free radicals in irradiated materials. Theoretical estimations of energetic levels corresponding to ions in different crystalline fields and of forbidden EPR transitions were made by computational studies.

These results have been included in many publications, as for instance papers published in international or national journals (Appendix 1-2) and they were also communicated at international conferences and published in Proceedings (Appendix 3).

After 1968, when prof. Ursu leaved Cluj for Bucharest, the accent in EPR Laboratory moved to other modern problems in EPR as magnetic resonance of oxide glasses and non-crystalline systems, perovskites, chemical and pharmaceutical complexes, etc. (Appendix 1-4, 1970-2002).

The research activity of the laboratory co-workers was stimulated by co-operation with specialists belonging to other EPR research teams from Romania (Institutes of the Bucharest - Măgurele Platform, Institute of Isotopic and Molecular Technologies - Cluj-Napoca, University of Bucharest, Timişoara, Iaşi and from abroad (The Netherlands, Germany, England, USA, France).

The scientific results obtained in the EPR laboratory at "Babeş-Bolyai" University were included in several Ph.D. theses focused on magnetic resonance (Appendix 4).

PROF. DR. S. SIMON

PROF. DR. I. BARBUR

Appendix 1

Papers published in international journals

1965

1. A.Calusaru, I.Barbur, I.Ursu
"Recuit thermique des defaute paramagnetiques induits par irradiation gamma dans des monocristaux de (NH4)2SO4 et (ND4)2SO4 I. Verification par irradiation experimentale de la theorie de Fletcher et Brown"
J.Chem.Phys.2, 249-256 (1965)
2. A.Calusaru, I.Barbur, I.Ursu
"Thermal annealing of paramagnetic defects induced by gamma irradiation in (NH4)2SO4 et (ND4)2SO4 single crystals''
Chem. Effects. of Nucl.Transf.2, 293-311 (1965)

1966

A.Calusaru, I.Barbur, I.Ursu
"Recuit thermique des defaute paramagnetiques induits par irradiation gamma dans des monocristaux de (NH4)2SO4 et (ND4)2SO4. II. Verification experimentale de la theorie de haute zone''
J.Chem.Phys.6, 809-814 (1966)

1967

I.Ursu, V.Lupei, S.V.Nistor
"Electron Spin Resonance Study of Irradiated Semiconductors(review paper)"
Nuclear Energy Review, Viena, 5, 97 (1967)

1968

I.Ursu
"La Resonance Paramagnetique Electronique"
Dunod, Paris (1968)

1969

1. S.V.Nistor, A.Darabont
"ESR studies of the X-ray irradiated NaCl:Fe system"
Solid State Comm. 7, 363-366 (1969)
2. A.Nicula, S.I.Farcas, Al.Darabont
"ESR study of paramagnetic centers formed by introduction of Ca^{2+} in NaCl and NaBr single crystals"
Phys.Stat.Sol. 32, 741-744 (1969)
3. I.Barbur
"Paramagnetic resonance of gamma irradiated N2H6SO4 and N2D6SO4 single crystals"
Phys.Stat.Sol.34, 711-716 (1969)

1970

1. S.V.Nistor, A.Darabont
"ESR studies of X-ray irradiated NaCl crystals containing cation impurities"
Solid State Comm. 8, 451-454 (1970)
2. H. L.T.Bohan, Gh.Cristea, .J.Stapleton
"Concentration - Dependent Orbach Relaxation Rates in LMN:Nd"
Bull. Am. Phys. Soc. 15 (6), 8, 760 (1970)

1971

1. E.Burzo, I.Ursu
"Paramagnetic resonance and magnetic measurements on GdNi5 compound "
Solid State Commun. 9, 2289 (1971)
2. I.Barbur
"Electron spin resonance of gamma defects in ferroelectric ammonium hydrogen sulfate"
Phys.Stat.Sol.(b), 45, K129-133 (1971)
3. Gh. Cristea, T. H. Bohan, H. L. Stapleton
"Concentration-Dependent Orbach Relaxation Rates in Nd-Doped Lanthanum Magnesium Nitrate"
Phys.Rev. (B) 4 (7), 2081 (1971).

1972

1. S.I.Farcas, Al.Darabont, A.Nicula
"ESR study of copper doped NaCl"
Phys.Stat.Sol. (b) 50, 755-761 (1972)
2. I.Ursu, E.Burzo
"Paramagnetic resonance of Gadolinium-nickel intermetallic compounds"
J.Magnetic Resonance 8, 274 (1972)
3. E.Burzo, I.Ursu, J.Pierre
"Resonance electronique des coposes GdCu et GdAg"
Phys.Stat.Solidi (b) 51, 483 (1972)
4. I.Barbur
"E.S.R. study of the reorientational motion in N(SO3)2-2 "
Physica, 58, 324-326 (1972)
5. *V.Znamirovschi, O.Cozar, Al.Nicula*
"The ESR study of some H-D solvent isotope effects on copper ions",
Izotopenpraxiz, 1, 29(1972)

1973

V.Znamirovschi, O.Cozar
"The ESR evidence for influence of the ethanol on the hydrated complexes of copper ions"
Acta Physica Polonica, 42A, 3 (1973)

1974

V.Znamirovschi, O.Cozar, Al.Nicula
"An EPR evidence for structuring effect of alcohol in water" *Molecular Physics, 27, 73 (1974)*

1976

1. S.I.Farcas, Al.Darabont, Al.Nicula
"Electron spin resonance study of Cr^{3+} and Fe^{3+} in alums" *Phys.Stat.Sol.(b) 74, 335-339 (1976)*
2. O.Cozar, V.Znamirovschi, I.Haiduc
"ESR Investigation of the ethanol upon the structure of [Cu(trien)SCN]SCN in mixed water-ethanol solutions"
J.Molec.Structure, 31, 153 (1976)

1978

1. S.I.Farcas, Al.Darabont, A.Nicula
"Theoretical study of the forbidden ESR transitions of Cr^{3+} and Fe^{3+} in alums"
Phys.Stat.Sol. (b) 85, 75-79 (1978)
2. E.Burzo, I.Ardelean
"EPR Study of Fe^{3+} Ions in Lead Borate Glasses"
Phys. Stat Sol (b) 87, K1 137-140 (1978)
3. E.Burzo, R.Baican
"Ferromagnetic resonance study of some pseudobinary cubic compounds"
J.Less.Common.Metals 60, 315 (1978)

1979

E.Burzo, St.Vadeanu
"Magnetic properties and Ferromagnetic Resonance study of YFe2-XMn2-2x compounds"
J.Less Common.Metals 66, 111 (1979)

1980

1. I.Ardelean, Gh.Ilonca, M.Peteanu, D.Pop
"MagneticProperties of xMnO(1-x)[19TeO2·PbO] Glasses"
Solid State Commun. 33, 653-655 (1980)
2. I.Ardelean, M.Peteanu, Gh.Ilonca
"EPR Studies of Mn2+Ions Distribution in xMnO(1-x)[19TeO2·PbO] Glasses
Phys.Stat.Sol.(a) V, 58, nr.1, K 33-36 (1980)

1981

1. L.V.Giurgiu, I.Ursu, Max T.Rogers
"ESR Study of a Platinum Paramagnetic Complex in NaCl Doped with $Pt(CN)_4^{2-}$
Bull.of Magnetic Reson., 2, 171 (1981)
2. S.Simon, Al.Nicula
"The effect of melting temperature of the glasses from B_2O_3-Na_2O-CuO system studied by EPR and NMR"
Solid State Commun., 39, 1251 (1981)
3. E.Burzo, I.Ursu
"Ferromagnetic resonance studies on U(FeXCo1-X)2 compounds" *Bull.Magn.Res. 2, 240 (1981)*

1982

1. I.Ardelean, Gh.Ilonca, M.Peteanu, E.Barbos, E.Indrea
"EPR and Magnetic Susceptibility Studies of xCr2O3(1-x)[2B2O3·PbO] Glasses
J.Mat.Sci, 17, 1988-1996 (1982)

2. I.Ardelean, Gh.Ilonca, M.Peteanu
“Magnetic Properties of xCuO(1-x)[19TeO2·PbO] Glasses”
J.Non-Cryst.Solids, 51, 389-393 (1982)
3. S.Simon, Al. Nicula
“Magnetic resonance of borate glasses doped with paramagnetic ions”
Nucl. Instr. and Methods, 1-2, 199 (1982)
4. O.Cozar, I.Ardelean, Gh.Ilonca
"EPR and magnetic susceptibily studies of the interaction between Cu2+ and Mn2+ ions in x(CuO.MnO)(1-x)[2B2O3.K2O] glasses" *Solide State Commun, 44, 809 (1982)*
5. O.Cozar, I.Ardelean, Gh.Ilonca
"EPR and magnetic susceptibility studies of vanadium lead-borate glasses"
Materials Chemistry, 7, 775 (1982)

1983

1. S.Simon, Al. Nicula
“EPR study of the (100 -x) Li2O.2B2O3xTiO2.BaO glass system doped with ions from 3d group”
Glastech. Ber. 56K, 2, 904 (1983).
2. S.Simon, Al .Nicula
“Magnetic resonance of the B2O3-Na2O-MoO3 vitreous system”
J. Non-Cryst. Solids, 57, 23 (1983)
3. Al.Nicula, E.Trif, S.Simon
“The isotropy of the non-crystalline materials and the EPR spectra of S-state ions”
Bulletin of Magn. Res., 5, 314 (1983)
4. O.Cozar, V.Znamirovschi
"ESR evidence for the dimeric species of Cu(II) and VO(II) ions adsorbed on the silica surface"
Czech.j.of Physics, B 33(12), 1357 (1983)

1984

1. I.Ardelean, Gh.Ilonca, M.Peteanu
“The Valence States Of Manganese Ion in Potasium-Borate Oxide Glasses”
Solid State Commun. 52, 147-149 (1984)
2. E.Burzo, M.Chipara, I.Ardelean
“Electron Paramagnetic Resonance Study of xFe2O3(1-x)[2B2O3·PbO] Glasses”
Phys.Stat.Sol. (b) 124, K 117-120 (1984)
3. I.Ardelean, O.Cozar, Gh.Ilonca
“EPR and Magnetic Susceptibility Studies of xCuO(1-x)[2B2O3·Li2O] Glasses”
Solid State Commun. 50, 87-90 (1984)
4. S.Simon, Al.Nicula
“EPR study of Gd3+ and Cu2+ ions from litiu-borate vitroceramics”
Phys. Status Solidi (a), 81, Kl (1984)
5. E. Trif, D. Slugaru, V.Cristea, O. Cozar
"XRD and EPR study of Cr-exchaned ZSM-5 zeolite"
Procc. of XII International Conferince on “Defects in insula-tuig materials”, august 16-22, 1992, Germania, vol.2, pg. 7, 21-23, Ed. O. Kanert, J-M Spaeth.

1985

I. Ardelean, Gh.Ilonca, O.Cozar
"The influence of melting temperature on the magnetic properties of x(CuO.V2O5)(1-x) [2B2O3.PbO] glasses"
Acta Physica Polonica, A68, 163-168 (1985)

1986

Al.Nicula, O.Pana, L.V.Giurgiu
"Covalency and EPR Hyperfine Structure Constant of Eu3+ in Crystals"
Physics Lett., A119, 92 (1986)

1987

O.Cozar, I.Ardelean
"The Local Symmetry of Cu2+ Ions in Phosphate Glasses"
J. Non-Cryst. Solids, 92, 278-281 (1987)

1988

1. I.Barbur, L.Stanescu, S.Simon
"ESR evidence of ferroelectric transition in Pb3(VO4)2"
Acta Physica Polonica, A73, 4, 573 (1988)
2. S.Simon, V.Simon, I.Barbur
''Magnetic resonance on oxide vitroceramics with ferroelectric crystallits''
Ferroelectrics, 80, 39 (1988)
3. I.Ursu, E.Burzo
"Magnetic properties and resonance studies on some Gadolinium-Transition Metal-Boron compounds"
Helvetica Physica Acta 61, 521 (1988)

1989

S.Simon, Gh.Ilonca, I.Barbur, I.Ardelean, R.Redac
"EPR on Y-Ceramics and Bi-vitroceramics Doped with S-state Paramangnetic Ions"
Physica C, 162-164, 1298-1290 (1989)

1992

O.Cozar, V.Znamirovschi, L.David, L.V.Giurgiu, J.Zsaco
"EPR investigation of some cooper (II) – dioxine – dichloride compounds"
Appl.Magn.Reson. 3, 849 (1992)

1993

1. Al.Darabont, A.V.Pop, L.V.Giurgiu
"Measurements of the effective susceptibility at the surface of YBa2Cu3O7-y superconductor"
Modern Phys.Lett., B7, 1915 (1993)
2. I.Ardelean, Gh.Ilonca, M.Peteanu
"ESR studies of Mo5+ions in Potassium-borate and Soda-phosphate glasses"
Solid State Commun. 85, 461-465 (1993)

3. O.Cozar, I.Ardelean, S.Simon, L.David
"ESR Studies of Mo5+ Ions in Potassium-borate and Soda-phosphate Glasses"
Solid State Commun. 85, 461-465 (1993)
4. O.Cozar, I.Ardelean, I.Bratu, Gh.Ilonca, S.Simon
"EPR, IR and Magnetic Susceptibility Studies of xCr2O3·(1-x)[2B2O3·Li2O] Glasses"
Solid State Commun. 86, 569-572 (1993)
5. I.Barbur, I.Ardelean
"EPR of Paramagnetic Centers in Antiferroelectric Pb2MgWO6"
J. Mat. Sci. Letters, 12, 1747-1748 (1993)

1994

1. L.David, O.Cozar, V.Chis, A.Negoescu, I.Vlasin
"ESR study of Cu(II)-Indomethacin and Its Pyridine and DMF Adducts"
Appl.Magn.Reson., 6, 521-528 (1994)
2. M.Peteanu, L.Cociu, I.Ardelean
"EPR study of Borax-Glasses with addition of Fe^{3+} ions"
J.Mat.Sci.technol. 10, 97-106 (1994)
3. S. Simon, A. van der Pol, E.J. Reijerse, A.P.M. Kentgens, G.J.M.P. van Moorsel, E. de Boer
"EPR and NMR Studies of Amorphous Aluminium Borates"
J.Chem. Soc. Faraday Trans. 90, 2663-2670 (1994)
4. I.Barbur
"ESR Evidence of Low-Temperature Phase Transition in Na2SeO4" *Phase Transitions, 51, 249 (1994)*
5. E.Trif, D.Strugaru, C.Marcu
"EPR and XRD Spectroscopies of the Chromium Ions in the ZSM-5 Zeolite"
Mod.Phys.Lett.B, Vol.8, No.3, p.173-183(1994)
6. L. David, O. Cozar, V. Chis, E. Forizs, C. Cosma, G. Damian
"ESR Study of the copper(II)-diazepam complexes"
B*alkan Physics Letters, 2(2), 1091-1095 (1994)*
7. G. Damian, O. Cozar, V. Znamirovschi, L. David, C. Cosma
"IR and EPR study of DL-Ornithine-15N and DL-Lysine-15N copper(II) complexes adsorbed on NaY and HY zeolites"
Balkan Physics Letters, 2(2), 1101-1105 (1994)
8. L. David. O. Cozar, I. Bratu, D. Ciurchea, V. Chiş, D. Ristoiu
"Spectroscopic studies of Cu(II), Co(II), Cr(III) and Fe(III)-diclofenac complexes"
Balkan Phys. Lett., 2(2), 1096-1100 (1994)

1995

1. O.Cozar, L.David, V.Chis, C.Cosma, V.Znamirovschi, G.Damian, I.Bratu, Gh.Bora
"ESR study of some solvent effects on Cu(II)-Aspirinate complex" *Appl. Magn. Reson., 8, 235-242 (1995)*
2. G.Alzuet, S.Ferrer, J.Borras, D.Gatteschi, L.David, V.Chis, O.Cozar
"EPR study of bis(Methazolamidato)bipyridinaquo-copper(II)"
Indian J.Phys., 69A(4), 463-468 (1995)
3. M.Peteanu, L.Cociu, I.Ardelean
"EPR of irradiation induced centers in some Vitreous Materials containing Copper"
J.Mat.Sci.Technol. 11, 29-33 (1995)

4. S.Simon, A.Van der Pol, E.J.Reijerse, APM Kentgens, G.J.M.P. van Morsel, E.de Boer
"Magnetic Resonance Studies on Porous Alumina doped with Iron and Chromium"
J.Chem.Soc.Faraday Trans. 91, 10 1519-1522 (1995)
5. I.Barbur, I.Batiu, V.Simon
"ESR study of free radicals in some new hydrazones of terpenoids class"
J.Radioanalytical and Nucl.Chem. 196, 151-158 (1995)
6. D.Strugaru, E.Trif, V. Cristea, G.Gheorghe, R.Rusu
"EPR Study of Iteraction of Vanadium Pentoxide with H-ZSM-5 Zeolite"
Radiat. Phys. Chem. Vol.45, No.6, p. 917-922 (1995)

1996

1. O.Cozar, L.David, V.Chis, E.Forisz, C.Cosma, G.Damian "Local structure analysis of Cu(II)-diazepan complexes by ESR spectroscopy"
Fressenius Journal of Analytical Chemistry, 355, 701-702 (1996)
2. I.Ardelean, M.Peteanu, E.Burzo, S.Filip, F.Ciorcas
"EPR and magnetic susceptibility studies of Cu^{2+} ions in TeO_2-PbO-B_2O_3 glasses"
Solid State Commun. 98, 351-355 (1996)
3. M.Peteanu, I.Ardelean, S.Filip, F.Ciorcas
"Cu^{2+} containing TeO_2-B_2O_3-PbO glasses studied by means of EPR"
J. Mat. Sci. Mat. Electronics, 7, 165-170 (1996)
4. I.Ardelean, O.Cozar, S.Filip, V.Pop, I.Cenan
"EPR and magnetic susceptibility studies of Cu^{2+} ions in $Bi_2O_3 \cdot GeO_2$ glasses"
Solid State Commun, 100, 609-613 (1996)
5. V. Simon, I. Ardelean, O.Cozar, S. Simon
"Valence States of uranium and gamma irradiation defects in soda-phosphate glasses"
J. Mat. Sci. Letters, 15, 784-785 (1996)

1997

1. L.David, O.Cozar, L.Sumalean, V.Chis, R.Tetean, C.Craciun
"ESR study of some Cu(II)-4-substitude-2-thiazolyhydrazone complexes"
Appl.Magn.Reson., 13, 571-577 (1997)
2. O.Cozar, V.Chis, L.David, G.Damian, I.Barbur
"ESR investigation of gamma irradiated aspirin"
J.Radional.Nucl.Chem., 220, 241-244 (1997)
3. M.Brustolon, V.Chis, A.L.Maniero, L.C.Brunel
"New radical detected by HF-EPR, ENDOR and pulsed EPR in a room temperature irradiated single crystal of glycine"
J.Phys.Chem. A, 101, 4887-4892(1997)
4. I.Ardelean, M.Peteanu, S.Filip, V.Simon and G.Györffy
"EPR and magneic susceptibility studies of iron ions in $70TeO_2 \cdot 25B_2O_3 \cdot 5PbO$ glass matrix"
Solid State Commun. 102, 341-346 (1997)
5. M.Peteanu, V.Simon, N.Muresan, I.Ardelean, S.Filip
"EPR and magnetic susceptibility studies of Cr^{3+} ions in the $70TeO_2 \cdot 25B_2O_3 \cdot 5PbO$ glass matrix"
J. Mater. Sci. Technol. 13, 374-378 (1997)

6. D.Matulescu, M.I.Chipara, E.Burzo and I.Ardelean
"ESR and magnetic properties of xEu2O3·(1-x)[3B2O3·PbO] glasses"
Phys. Stat. Sol. (a), 161, 451-458 (1997)
7. D.Maniu, I.Ardelean, O.Cozar, V.Pop
"EPR and magnetic susceptibility investigation of $CuO-B_2O_3-K_2O$ glasses"
Supl. Balkan Phys. Lett. 5, 848-851 (1997)
8. I.Ardelean, F.Ciorcas, M.Peteanu, S.Lupsor, G.Salvan
"EPR investigation of CuO-TeO2-B2O3-SrO glasses"
Supl. Balkan Phys. Lett. 5, 860-863 (1997)
9. I.Barbur, I.Ardelean, G.Borodi, A.Veres, V.Timar
"Vanadium substitution effects on structural and electric properties of $Pb_2MgW_1-xVxO_6$ compounds"
Ferroelectrics Letters, 23, 69 (1997)
10. I.Ardelean, I.Barbur, G.Borodi, A.Veres, I.Cosma
"Structural, electric and magnetic studies on Pb2Mg1-xMnxWO6-type compounds"
J.Mat.Sci.Lett. 16, 1735 (1997)
11. E. Forizs, L. David, O. Cozar, C. Craciun, M. Venter, M. Kilyen
"IR and ESR study of Cu(II)-nitrazepam complexes"
J. Molec. Structure, 408/409, 195-199(1997)
12. M. de la Fuente, O. Cozar, L. David, R. Navarro, A. Hernanz, I.Bratu
"EPR Study of the 1:1 complexes of chromium (III) and copper(II) with 5'-GMP and 5'-CMP"
Molecular and Biomolecular Spectroscopy, Spectrochimica Acta, Part A 53, 637(1997)
13. M.Venter, I.Haiduc, L.David, O.Cozar
"IR and ESR studies on new bis-triazenido cobalt(II) and copper(II) complexes"
J. Molec. Structure, 408/409, 483-486(1997)
14. G.Damian, O.Cozar, V.Znamirovschi, L.David, V.Chis, M.Todica
"Structure and localisation of VO^{2+} ion in water adsorbed on NaY and HY zeolite"
Balkan Physics Letters, 5, 183(1997)
15. D. Maniu, I. Ardelean, I. Bratu, R. Grecu, O. Cozar, T. Iliescu "Spectroscopic investigations of x(CuO·V2O5)(1-x)[3B2O3·K2O] glasses"
Balkan Phys. Letters, 5, 199(1997)
16. L.David, O.Cozar, E.Forizs, V.Chiş, C.Crăciun
"Local structure of some Cu(II)-theophyline complexes with amine ligands"
Balkan Phys. Letters, 5, 219(1997)
17. O.Cozar, V.Znamirovschi, L.David, D.Ristoiu, L.Pop, C.Agut
"Solvent effects of some copper(II) complexes with nitrogen ligands. An EPR study"
Balkan Phys. Letters, 5, 215(1997)
18. V.Chis, M.Brustolon, O.Cozar, L.David, S.Simion, A.Darabont "Electron spin-lattice relaxation time in gamma-irradiated glycine" *Balkan Phys. Letters, 5, 223(1997)*
19. V.Chis, M.Brustolon, A.L.Maniero, L.David, O.Cozar, D.Ristoiu
"Structure and unpaired spin density of the glycine CH_2NH_2 radical" *Balkan Phys. Letters, 5, 227(1997)*
20. G.Damian, O.Cozar, V.Miclaus, Cs.Paizs, M.Todică, V.Chis
"ESR of nitroxide in the slow-motional regime adsorbed on hydrophilic and hydrophobic surfaces"
Balkan Phys. Letters, 5, 289(1997)

1998

1. G.Damian, O.Cozar, V.Miclaus, C.Paisz, V.Znamirovschi, V.Chis, L.David
"ESR study of the dynamics of adsorbed nitroxide radicals on porous surfaces in dehydration process"
Colloids and Surfaces A, 137, 1-6(1998)
2. I.Ardelean, M.Peteanu, V.Simon, C.Bob, S.Filip
"EPR and magnetic susceptibility studies of Cr_2O_3-Bi_2O_3-GeO_2 glasses"
J. Mat. Sci. 33, 357-362 (1998)
3. I.Ardelean, M.Peteanu, S.Filip, V.Simon, I.Todor
"EPR and magnetic susceptibility studies of manganese ions in Bi_2O_3-GeO_2 glasses"
Solid State Commun. 105, 339-344 (1998)
4. Rodica Micu-Semeniuc, R.Semeniuc, O.Cozar, L.David "Copper complexes of 1, 4-dihidrazinophtalazine. Synthesis and spectral characterisation"
Synthesis and Reactivity in Inorganic and Metal-Organic Chemistry 28(4), 501-513 (1998)
5. O.Cozar, L.David, V.Chis
"Structural investigations of some Cu(II)-1, 4 benzodiazepine complexes by ESR"
Balkan Physics Letters, 6(4) 231-236(1998)

1999

1. E.Forisz, L.David, O.Cozar, V.Chis, G.Damian, J.Csibi
"IR and ESR studies on novel copper(II) theophyllinato complexes containing mono or bidentate ligands"
J.Mol.Struct., 482-483, 143-147(1999)
2. G.Damian, V.Miclaus, O.Cozar, M.Todica, L.David, V.Chis, D.Ristoiu, S.Farcas
"EPR study of some copper heterocyclic azomethine complexes adsorbed on X and Y zeolites"
J.Mol.Struct., 482-483, 287-289(1999)
3. M.Todica, O.Cozar, G.Damian, L.David, V.Chis
"NMR and ESR study of local dynamics in some polyisoprene solutions"
J.Mol.Struct., 482-483, 353-357(1999)
4. E.Forisz, L.David, O.Cozar, V.Chis, C.Craciun, R.Tetean, M.Todica
"ESR studies of some Cu(II)-Oxazepan complexes"
Appl.Magn.Reson., 16, 499-506(1999)
5. O.Cozar, I.Ardelean, V.Simon, V.Mih, N.Vedean
"EPR study of phosphate glasses containing two types of transitional metal ions"
J. Magn. Magn. Mat. 196-197, 269-271 (1999)
6. O.Cozar, I.Ardelean, V.Simon, L.David, N.Vedean, V.Mih
"EPR studies of Cu^{2+} and V^{4+} ions in phosphate glasses"
Appl. Magn. Reson. 16, 473-480 (1999)
7. I.Ardelean, G.Salvan, M.Peteanu, V.Simon, C.Himcinschi, F.Ciorcas
"EPR and magnetic susceptibility studies of B_2O_3-SrO-Fe_2O_3 glasses"
Mod. Phys. Lett. B, 13, Nr. 22-23, 801-808 (1999)
8. L.David, M.Rusu, O.Cozar, D. Rusu, M.Todica, C. Balan "Spectroscopic and magnetic Investigations of Some Transition Metal Complexes with N-4-methoxyphenyl-N-4-chlorophenyl hydrazine as ligands"
J.Molec.Structure, 482(1), 149-152 (1999)

9. I.Haiduc, L.David, O.Cozar, R.Micu-Semeniuc, M.Armeneanu "Spectroscopic and magnetic studies of some copper (II), chromium (III) and iron (III) complexes with dithiophosponate as ligand" *J.Molec.Structure, 482(1), 153-157 (1999)*
10. V.Chis, M.Brustolon, C.Morari, O.Cozar, L.David "Experimental and theoretical structural parameters of the glycine CH_2NH_2 radical"
J.Molecular Structure, 482(1), 283-286 (1999)
11. O.Cozar, I.Ardelean, V.Simon, L. David, V. Mih, N. Vedean
"The local structure and interactions between V^{4+} ions in soda-phosphate glasses"
Appl. Mag. Reson., 16, 529-537 (1999)
12. L.David, O.Cozar, E.Forizs, C.Craciun, D.Ristoiu, C.Balan "Local structure analysis of some Cu(II) theophylline complexes" *Spectrochimica Acta, Part A, 55, 2559-2564 (1999)*
13. I.Ardelean, M.Peteanu, O.Cozar, V.Simon, V.Mih, G. Botezan
"Structural and Magnetic Properties of MnO-P2O5-PbO glasses"
J. Mater. Sci. Technol., 15(5), 453-456 (1999)

2000

1. I.Ardelean, M.Peteanu, V.Simon, S.Filip, M.Flora, S.Simon ''EPR and magnetic susceptibility studies on MnO-B2O3-SrO glasses"
Phys. and Chem. of Glasses, 41, 3, 153 (2000)
2. S.Simon, I.Ardelean, M.Peteanu, M.Pop, R.Stefan
''EPR study on Fe3+ and Mn2+ doped alumina and aluminum-borates"
Mod. Phys. Lett. B, 14, 2, 59 (2000)
3. I.Ardelean, O.Cozar, Gh.Ilonca, V.Simon, V.Mih, C.Craciun, S.Simon
''EPR and magnetic susceptibiliy studies on V_2O_5-P_2O_5-PbO glasses"
J. Mat. Sci.: Mat. Electronics, 11, 401 (2000)
4. I.Ardelean, M.Peteanu, S.Simon, V.Simon, F.Ciorcas, C.Bob, S.Filip
"EPR and magnetic susceptibiliy study of manganese ions in Bi_2O_3.PbO.As_2O_3 glass matrix"
Indian J. Phys., 74A (5), 467 (2000)
5. I.Ardelean, M.Peteanu, R.Ciceo-Lucacel, I.Bratu
"Structural investigation of CuO containing strontium-borate glasses by means of EPR and IR spectrometry"
J. Mat. Sci.: Materials in Electronics 11, 11-16 (2000)
6. I.Ardelean, M.Peteanu, V.Simon, F.Ciorcas
"EPR and magnetic susceptibility investigations of iron containing TeO_2-B_2O_3-SrF_2 glasses"
J. Mat. Sci. Techn. 16(b), 596-600 (2000)
7. I.Ardelean, F.Ciorcas, M.Peteanu, I.Bratu, V.Ioncu
"The structural study of Fe_2O_3-TeO_2-B2O_3-SrF_2 glasses by EPR and IR spectroscopies"
Mod. Phys. Lett. B, 24(17, 18) 653-661 (2000)
8. I.Ardelean, M.Peteanu, V.Simon, C.Borsa, F.Ciorcas, V.Ioncu
"Influence of melting temperature on the iron distribution in Bi_2O_3.PbO.As_2O_3 glass matrix studied by EPR"
Mod. Phys. Lett. B, 14(22, 23) 785-791 (2000)
9. S.Simon, I.Ardelean, S.Filip, I.Bratu, I.Cosma
"Structure and magnetic properties of Bi_2O_3-GeO_2-Gd_2O_3 glasses"
Solid State Comun., 116, 83 (2000)

10. L. David, C. Crăciun, M. Rusu, O. Cozar, P. Ilea, D. Rusu "Spectroscopic and electrochemical investigations of the K8[P2VMoW16O62]·31H2O heteropolyoxometalate"
Polyhedron, 19, 1917-1923 (2000)
11. L. David, C. Crăciun, M. Rusu, D. Rusu, O. Cozar
„Spectroscopic and Magnetic Investigation of the K5[PMo2VW9O40]·24H2O Heteropolyoxometalate and its Monoprotonated Form"
J. Chem. Soc., Dalton Trans., 4374-4378 (2000)
12. Letiția Ghizdavu, Crăița Bălan, L. David, Carmen Bâtiu, O. Cozar, D. Ristoiu
„Spectroscopic, Magnetic and Thermal Investigations on Cu(II), Mn(II), Co(II) and Fe(III) Complexes with Glutamyl Nitroanilide"
Journal of Thermal Analysis, Calorimetry, 62, 2000 (in press)
13. C Craciun. L. David, D. Rusu, M. Rusu, Ocular, V. Chis "FT-IR, UV-VIS, and ESR Investigation of Three Vanadium(IV) Substitued Keggin Polyoxometalate"
Balkan Phys. Letters (2000)
14. C. Agut, C. Craciun., L. David, M. Rusu, V. Chis, , Ocular "Spectroscopic Investigation of Cu(H3C-CO-CH-CO-CH3)2 complex"
Balkan Phys. Letters (2000)

2001

1. R.Stefan, S.Simon - "EPR of Mn^{2+} and Fe^{3+} ions doped in Bi_2O_3-B_2O_3 vitreous matrices"
Mod. Phys. Lett. B, 15, 3, 111 (2001)
2. O.Cozar, I.Ardelean, I.Bratu, S.Simon, C. Craciun, L. David, C. Cefan
"IR and EPR studies on some lithium-borate glasses with vanadium ions"
J. Mol. Struct., 563-564, 421 (2001)
3. S. Simon, D. Eniu, A. Pasca, D. Dadarlat and V. Simon
"EPR and photopyroelecric investigations of Fe_2O_3-CaO-P_2O_5-SiO_2 glass and glass-ceramic systems"
Mod. Phys. Lett. b, 15, 21, 921 (2001)
4. O.Cozar, I.Ardelean, V.Simon, G.Ilonca, C.Craciu, C.Cefan
"EPR and magnetic susceptibility investigations of some vanadate-lithium-borate glasses"
J.Alloys and Compounds, 326, 124-127 (2001)
5. I.Ardelean, M.Peteanu, V.Simon, F.Ciorcas, V.Ioncu
"Structural investigation of Fe2O3-TeO2-B2O3-SrO glasses by EPR"
J. Mat. Sci. Lett. 20, 947-949 (12001)
6. I.Ardelean, M.Peteanu, R.Ciceo-Lucacel
"EPR of Cu^{2+} ions in B_2O_3-SrO glasses"
Mat. Sci. Forum 373-376, 261-264 (2001)
7. O.Cozar, I.Ardelean, I.Bratu, S.Simon, C.Craciun, L.David, C.Cefan
"IR and EPR studies on some lithium-borate glasses with vanadium ions"
J. Mol. Structure, 563-564, 421-425 (2001)
8. I.Ardelean, M.Peteanu, V.Ioncu, N.Muresan
"EPR and magnetic susceptibility studies of Cr^{3+} ions in the $70TeO_2.25B_2O_3.5SrFe_2$ glass matrix"
Mod. Phys. Lett. B, 15 (22), 941-947 (2001)
9. O.Cozar, L.David, V.Chis, G.Damian, M.Todica, C.Agut
"IR and ESR studies on some dimeric copper(II) complexes"
J.Mol.Struct., 563-564, 371-375 (2001)

10. S.Simon
"Local structure characterization of gadolinium doped amorphous and crystalline alumina"
Mod. Phys. Lett.B, 12&13, 375(2001)
11. L.David, C.Crăciun, C.Bălan, O.Cozar, L.Ghizdavu, C. Bâtiu
"New Transition Metal Complexes Of γ-L-Glutamyl-5-(2-Methoxy-*P*-Nitroanilide): Synthesis, Spectroscopic, Magnetic and Thermal Investigations"
Acta Chim. Slov. 48, 407-415 (2001)
12. O. Cozar, I. Ardelean, I. Bratu, S. Simon, C. Crăciun, L. David, C. Cefan
"IR and ESR studies on some lithium-borate glasses with vanadyl ions"
J. Mol. Struct., 563-564, 421-425 (2001)
13. L. David, C. Craciun, O. Cozar, V. Chiş, C. Agut, D. Rusu, M. Rusu
"Spectroscopic studies of some oxygen-bonded copper(II) β-diketonates complexes"
J. Mol. Struct., 563-564, 573-578 (2001)
14. D. Rusu, C. Craciun, A.L. Barra, L. David, C. Rosu, O. Cozar, Gh. Marcu
„Spectroscopic and electron paramagnetic resonance behaviour of trinuclear metallic cluster encapsulated in $[M^{n+}{}_3(H_2O)_x(BiW_9O_{33})_2]^{(18-3n)-}$ heteropolyanion ($M^{n+} = VO^{II}$, x = 0, $M^{n+} = Cr^{III}$, Mn^{II}, Fe^{III}, Co^{II}, Ni^{II}, Cu^{II}, x = 3)"
J. Chem. Soc. Dalton Trans., 19, 2879 (2001)
15. O. Cozar, I.Bratu, L.David, C. Craciun, A. Mernanz, R. Nenaro, M. De la Fuente, C. Balan
„EPR Investigations of Cu(II) Complexes with 5I-CMP and 5I-GMP"
Appl. Mag. Resonance 21, 71-78 (2001)

2002

1. I.Ardelean, M.Flora
"EPR and magnetic investigations of MnO-B2O3-PbO glasses"
J.Mat.Sci.: Mat. in Electronics 13, 357-362 (2002)
2. I.Ardelean, P.Pascuta, M.Peteanu
"EPR and magnetic susceptibility studies of calcium-borate oxide glasses containing iron ions"
Mod. Phys. Lett. B, 16(7), 231-239 (2002)
3. I.Ardelean, M.Peteanu, V.Simon, G.Salvan
"EPR and magnetic susceptibility investigation of Fe ions in B_2O_3-SrF_2 glass matrix"
J. Mat. Sci. Technol. 18 (3), 231-233 (2002)
4. I.Ardelean, O.Cozar, C.Craciun, C.Cefan
"EPR and magnetic susceptibility studies of V^{4+} ions in $2B_2O_3$-SrO glass matrix"
Int. J. Mod. Phys. B, 16 (19) 2807-2813 (2002)
5. S.Simon, C.Neamtu, D.Eniu, D.Dadarlat, V.Simon
"Local order and thermal diffusivity in iron containing lime-phosphate-silicate ceramics"
Mod. Phys. Lett.B, 16, 17, 631(2002)
6. O. Cozar, R. Micu-Semeniuc, L. David, I. Haiduc
„Local structure and metal-metal interaction in some Cr(III)-dithiophosphonate compounds"
Modern Physics Letters B, 16, 401-407 (2002)

Appendix 2

Papers published in romanian journals

1962

I.Ursu, I.Pop, A.Nicula, D.Barb
„Studiul proprietatilor magnetice ale catalizatorilor de nichel-trioxid de crom”
Stud.Cerc.Fiz.13, 349 (1962)

1963

I.Ursu, I.Barbur
„ Rezonanta electronica de spin a sistemului Pt – C in atmosfera de diferite gaze”
Com.Academiei RSR, 13, 805-809 (1963)

1964

1. Gh. Cristea
„Studiul spectrului de rezonanta electronica de spin al ionului V^{3+} în corindon ($Al_2O_{3)}$”
Studia UBB, Math-Phys (2), 117 (1964).
2. Al. Nicula, Gh. Cristea
„Dependență de temperatură a spectrului RES al ionului Cu^{2+} în zeoliți”
Studia UBB, Math-Phys (2), 11 (1964).
3. I.Ursu, A.Nicula
„RES a ionului de Mn(II)in zeoliti”
Rev.Roum.Phys.9, 343 (1964)

1965

1. I.Ursu, V.Grecu, I.Barbur
„The study of ESR signal of active charges on oxigene atmosphere”
Rev.Roum.Phys. 10, 585-591 (1965)
2. I.Ursu, Al. Nicula, S. V. Nistor, Gh. Cristea
„RES a ionului Cu^{2+} în compuşi cristalini de tipul MX_6 - parțial covalenți”
Studia UBB, Math-Phys. (2) (1965).
3. V.Grecu, R.V.Deutsch, S.V.Nistor
„Contribution to the study of crystal fields by the method of equivalent operators”
StudiaUBB, Math.-Phys. (1), 131-140 (1965)
4. I.Ursu, A. Nicula, S. V. Nistor
„Forbidden transition in the ESR spectra of Mn^{2+} ions in zeolites”
Rev.Roum.Phys. 10, 229-237(1965)

1966

1. Al. Nicula, Gh. Cristea, I. Ursu
Rezonanța electronica de spin a ionului VO^{4+} în zeoliți de tip X si Y.
Studia UBB, Math-Phys. (1), 109 (1966).
2. I.Ursu, O.Pop, L.Stanescu, I.Pop
„Studiul unor proprietati electrice si magnetice ale sistemului Cr_2O_3-BeO”
Rev.Roum.Phys. 11, 751(1966)

3. I.Ursu, V.Lupei
„Electron spin resonance of Mn^{2+} in polycrystalline As_2S_3"
Rev.Roum.Phys. 11, 165(1966)
4. I.Ursu, V.Lupei, A.Lupei
„Forbidden hyperfine transition in the ESR spectra of Mn^{2+} in calcite"
Rev.Roum.Phys. 11, 875(1966)

1967

I.Ursu, S.V.Nistor, A.Nicula, V.Niculescu
„Studiul prin rezonanta magnetica a distorsiunilor campului cristalin in sistemul LiF: Fe^{3+}"
Rev.Roum.Phys. 12, 931(1967)

1968

1. I.Barbur
„Efecte feroelectreice in $(NH_4)_2SO_4$ si $(ND_4)_2SO_4$iradiat"
Studia UBB, Math-Phys. (2), 139-141 (1968)
2. Al.Darabont, S.V.Nistor
„The atmosphere influence on the decomposition of Mn^{2+} ions aggregates in LiF-MnF_2 system"
Studia UBB, Math-Phys. (1), 81-83 (1968)
3. A.Nicula, I.Darabont, S.I.Farcas
„Influenta radiatiilor UV asupra halogenurilor alcaline impurificate cu cationi"
Studia UBB, Math-Phys. (2), 107-112 (1968)
4. S.V.Nistor
„Contribution to the energetic levels calculation for $^6S_{5/2}$ ions in cubic crystalline fields with axial symmetry of <110>type"
Rev.Roum.Phys. 13, 539-548 (1968)
5. S.V.Nistor
„Magnetic resonance studies of zeolites.(review)"
Rev. Chim., Bucuresti, 19, 117-119 (1968)
6. S.V.Nistor, G.Mihali
„Calculation to the energetic levels of a $^6S_{5/2}$ ions in cubic crystalline fields with axial deformation in a <111>direction"
StudiaUBB, Math-Phys. (1), 123-129 (1968)
7. V.Lupei, A.Lupei, I.Ursu
„Spin hamiltonian description of the ESR spectra of the $^6S_{5/2}$ ions in trigonal crystalline fields"
Rev.Roum.Phys. 13, 327 (1968)

1969

1. A .Suteu, Gh. Cristea
„Etude du $H_2(PW_{10}V_2O_{40})$ par methode RES"
Rev.Roum.Chim. 14 (2), 209 (1969).
2. Gh. Cristea, Darabont
„ESR Spectrum of Mn^{2+} în $(NH_4)Cd(SO_4)_3.nH_2O$"
Studia UBB, Math-Phys. (2) 87 (1969).

3. N.M.Grecu, Al. Darabont
„ESR in neutron irradiated $NaNO_2$ single crystals"
Rev.Roum.Phys.14(3), 313-315 (1969)
4. S.V.Nistor, G.Mihali
„Calculation to the energetic levels of a $^6S_{5/2}$ ions in cubic crystalline fields with axial deformation in a <111>direction"
StudiaUBB, Math-Phys. (2), 149-150 (1969)
5. S.V.Nistor, L.V.Giurgiu
„Energetic level calculation for $^6S_{5/2}$ ion situated in a cubic or axially deformated crystalline field"
Rev.Roum.Phys.14, 638 (1969)
6. Al.Nicula, S.I.Farcas, M.Paladi
"The explicit form of the Euler rotation for the equivalent operators"
Studia UBB, Phis.(2), 95-101 (1969)

1970

1. Al.Darabont, S.V.Nistor
„ESR study of NaCl single crystals doped with manganese and iron"
Rev.Roum.Phys.15(6), 641-647 (1970)
2. S.V.Nistor
„An ESR cavity for low temperature studies"
Rev.Roum.Phys. 13, 603-609 (1970)
3. Al.Nicula, S.I.Farcas
"Tensorul g in studiile RES"
St. Cerc.Fiz. 22, nr.1, 105-116 (1970)

1971

1. I.Barbur, E. Trif
„Electron spin resonance of Mn^{2+} ion in $NH_4NaSO_4 2H_2O$ ferroelectric compound"
*Studia UBB, Phys.2, 49-51 (*1971)
2. L. Ciociu, Gh. Cristea
„Determinarea timpilor de relaxare T_1 si T_2 in$(NH_4)Cd(SO_4)_2.12H_2O$ prin metoda parametrului *n*"
Studia UBB, Phys. (1), 73 (1971).
3. Al.Nicula, O.Cozar
„Linii satelit în spectrele RES ale atomilor de hidrogen în CaF_2 „
Studia UBB, Phys. (2), 35 (1971)
4. D. Strugaru
„Studiul RES a ionului Co(II) în complexul [Ce(CN)2dyp]''
Studia UBB (2), 91 (1971)
5. S.V.Nistor
„Studiul defectelor punctuale in cristale ionice prin RES(rezumat teza doctorat)"
St. Cerc.Fiz. 23, 1033-1074 (1971)
6. S.V.Nistor, Gh.Stoicescu
„Theory of ESR parameters for O^- centers in axial crystal fields"
Rev. Roum.Phys. 16, 495-510 (1971)

7. S.V.Nistor, I.Ursu
„ESR parameters analysis of oxygen color centers in doped NaCl"
Rev.Roum.Phys.16, 515-519 (1971)
8. Al.Nicula, M.Peteanu, S.T.Farcas
„Spectrul RES al ionilor de Gd^{3+} in cristale de CaF_2"
Studia UBB, Phys.(1), 7 (1971)

1972

1. Gh. Cristea
„Asupra teoriei fenomenului de limitare fononică în relaxarea Orbach"
Studia UBB, Phys. (2) 45 (1972).
2. V.Znamirovschi, O.Cozar
„RES a ionului Cu(II) în complecsii partial covalenti formati în solutii amoniacale si alcoolice la 77K"
Studia UBB, Phys. (1), 53 (1972)
3. O.Cozar, N.Vezentan
„Studiul RES al bis-(monotiodibenzoilmetanato)-Cu(II)"
Studia UBB, Phys. (2), 71 (1972)

1973

1. Gh. Cristea
„Influența efectului de bottleneck asupra lucrului maserului pe solid cu trei nivele"
Studia UBB, Phys. (1), 79 (1973).
2. Gh. Cristea, Gitta Samson.
„On Phonon Limitation of Orbach Spin Lattice Relaxation"
Studia UBB, Phys. (2), 57 (1973).
3. N.Vezentan, O.Cozar
„ESR study of two cupric complexes with nitrogen and oxigen ligands"
Studia UBB, Phys. (2), 3 (1973)
4. Al.Nicula, M.Peteanu, R.I.Campeanu
„Formarea prin iradiere a centrilor paramagnetici n NaCl-Ca"
Studia UBB, Phys.(1), 69 (1973)
5. M.Peteanu, L.Stanescu, I.Ardelean, C.Kovacs
„Investigation of some electronic and structural properties of V_2O_5 based semiconducting glasses. Correlation with catalytic activity"
Rev.Roum.Phys. (20), 67 (1973)

1974

O.Cozar, N.Vezentan
„RES a bis-(acetilaceton-etilendiamino)-Cu(II) în solutii''
Studia UBB, Phys. (1), 19 (1974)

1975

1. O. Cozar, V.Znamirovschi, I.Haiduc
„On the metal-ligand bonding in copper (II)-bis(8-hydroxyquinolinate)"
Studia UBB, Phys., 29 (1975)

2. N.Vezentan, O.Cozar, I.Milea
Studiul RES al dietilditiofosfonatului de Cu(II)
Studia UBB, Phys., 10 (1975)
3. D. Strugaru
„Rezonanța electronică de spin in studiul unor complecşi ai ionului Co(II)"
Rev.Roum.Phys. nr.4, 425 (1975)

1976

1. L.Stanescu, Gh. Cristea, I. Ardelean, N. Bassanyi.
„Spectre de transfer de sarcină în sisteme cristaline şi vitroase pe baza de V_2O_5"
Studia UBB, Phys. (2), 6 (1976)
2. V. Znamirovschi, O.Cozar, Al.Nicula
„EPR of Mn(II) ions in water-ethanol mixtures"
Studia UBB, Phys., 70 (1976)
3. O.Cozar, V.Mercea
„Determinarea coeficienților orbitalilor moleculari din date RES şi optice"
St.cerc.fiz. 29, 143 (1976)
4. O.Cozar, V.Znamirovschi, V.V.Morariu
„EPR of Cu(II) into layers of water adsorbed on silica surface"
Rev.Roum.Phys., 21, 579 (1976)
5. Al.Nicula, M.Peteanu
„Paramagnetic resonance of Fe^{3+} and Mn^{2+} ions in borate glasses"
Studia UBB, Phys.(1), 42 (1976)

1977

1. V.Znamirovschi, O.Cozar
„ESR evidence for some structural H-D isotope effects in aqueous solutions"
Studia UBB, Phys. (1), 22 (1977)
2. V.Znamirovschi, O.Cozar, V.V.Morariu
„The freezing properties of water adsorbed on silica in presence of paramegnetic ions"
Studia UBB, Phys. (2), 24 (1977)
3. D. Strugaru, Al Nicula
„Studii RES a stărilor de valența a nichelului a nichelului în zeolit x"
Studia UBB, nr.1, p.56 (1977)
4. V.Simon, D. Strugaru, E.Trif şi, Al Nicula
„Rezonanta protonică a zeoliților sintetici dopați cu Cu(II) şi Co(II)"
St.Cerc.Fiz. 29, p. 235 (1977)

1978

1. O.Cozar, V.Znamirovschi, I.Haiduc
„Solvent dependent EPR spectra of Cu(II)-monoethanolamine complexes in water-ethanol mixtures"
Studia UBB, Phys. (1), 6 (1978)
2. O.Cozar, Gh.Ilonca
„Studiul RES a $(NH_4)_3AlF_6$:Ca"
Studia UBB, Phys. (1), 79 (1978)

3. O.Cozar, V.Znamirovschi
„EPR evidence for two cupric complexes in water-ethanol mixtures at 77K"
Rev.Roum.Phys., 23, 87 (1978)
4. I. Nicula, Lavinia Cociu, I. Milea, Al. Nicula
„UV Transmission of Borate Glasses"
Studia UBB, Phys. 23, 32-34 (1978).
5. L.V.Giurgiu, Al.Nicula
„Molecular g value calculation for axially distorted d^7 low spin configuration crystal field"
Studia UBB, Phys. (2), 63 (1978).
6. Al.Nicula, M.Peteanu, C.Hagan
„Superhyperfine interaction in KDP: Cu^{2+} single crystals"
Studia UBB, Phys.(2), 46 (1978)

1979

1. O.Cozar, R.Semeniuc
„Studiul RES al unor cianati complecsi de Cu(II) în solutii"
Studia UBB, Phys. (1), 31 (1979)
2. O.Cozar, V.Znamirovschi
„Studiul RES al [Cu(trien)SCN]SCN în apa adsorbită pe SiO_2"
Studia UBB, Phys. (1), 41 (1979)
3. D.Strugaru
„Studiul nichelului in zeoliti sintetici prin spectroscopia optica"
Studia UBB (2), 61, 1979
4. S.Simon, V.Simon, Al.Nicula
„Influenta ionilor de Mn2+ si Gd3+ asupra unor sticle borice"
Studia UBB, Phys.24, 77 (1979)
5. S.Simon, F.Tolea, I.Duca, Al.Nicula
„RES a ionului Gd3+ in sistemul de sticla B_2O_3-Li_2O-SiO_2"
Studia UBB, Phys. 24, 37 (1979)
6. Al.Nicula, M.Peteanu, I.Ardelean
„Hyperfine Splitting of the g ~ 4.3 line a TeO_2-PbO:Mn^{2+} Glass"
Studia UBB, Phys. (2), 65-69 (1979)
7. E.Burzo, I.Ursu
„Magnetic resonance in gadolinium and yttrium crystalline compounds"
Rev.Roum.Phys., 24, 265 (1979)
8. Lavinia Cociu, L. Trif, Al. Nicula
„EPR of Chromium in B_2O_3-Li_2O-Al_2O_3-Cr_2O_3 Glasses"
Studia UBB, Phys. 24, 77-79 (1979).
9. Al.Nicula, M.Peteanu, C.Hagan
„High temperature phase transition of KH_2PO_4 studied by NMR"
Studia UBB, Phys.(1), 45 (1979)
10. Al.Nicula, M.Peteanu, C.Hagan
„Irradiation centers in KDP single crystals"
Studia UBB, Phys.(1), 49 (1979)
11. M.Peteanu, I.Ardelean, Gh.Ilonca, I.Luca
„Comportarea magnetica a unor sticle din sistemul $xFe_2O_3(1-x)[0.95TeO_2 \cdot 0.05PbO]$"
Studia UBB, Phys.(1), 65-68 (1979)

12. M.Peteanu, I.Ardelean, Al.Nicula
„Hyperfine splitting of the g≈4.3 line a TeO_2-PbO:Mn^{2+} glass”
Studia UBB, Phys.(2), 65-69 (1979)

1980

1. O.Cozar, V.Znamirovschi
„Studiul RES al $[Cu(NH_2CH_2CH_2OH)_4]Cl_2$ adsorbit pe SiO_2 si Al_2O_3”
Studia UBB, Phys. (1), 25 (1980)
2. O.Cozar, I.Ardelean, M.Coldea
„RPE a ionilor Cu^{2+} în sticle din sistemul $xCuO(1-x)[2B_2O_3.K_2O]$”
Studia UBB, Phys. (2), 52 (1980)
3. S.Simon, Al.Nicula
„Effect of some paramagnetic ions on the structure of some borate vitreous matrices”
Studia UBB, Phys. 25, 63 (1980)
4. S.Simon, Al.Nicula
„EPR study of soda-borate glasses with copper and titanium”
Studia UBB, Phys. 25, 39 (1980)
5. Lavinia Cociu, A. Marton, Al. Nicula
"Study of the ageing of stratified-electro-insulating materials by electron-spin resonance method”
Studia UBB, Phys.25, 57-62 (1980).

1981

1. S.Simon, Al.Nicula
„RPE pe sticle litiu-borice cu ioni paramagnetici ’’
Studia UBB, Phys. 26, 54 (1981)
2. I.Ardelean
„Studiul unor proprietati magnetice si radiospectroscopice ale sticlelor semiconductoare din sistemul Fe_2O_3-B_2O_3-PbO”
St. Cerc.Fiz. nr.1, 55-100 (1981)
3. I.Ursu, E.Burzo, D.Ungur, I.Ardelean
„Physical Properties of B_2O_3-PbO-Fe_2O_3 Glasses”
Rev. Roum. Phys. 26, nr.8-9, 801-813 (1981)
5. Lavinia Cociu, I. Ciogolas, Al. Nicula
„Rezonanta paramagnetica electronica a centrilor de argint în sticle de tipul B_2O_3-Li_2O-SiO_2 si B_2O_3-Li_2O-Al_2O_3 iradiate gamma”
Studia UBB, Phys.26, 57-62 (1981).
6. M.Peteanu, Al.Nicula
„RPE in sticle oxidice impurificate cu ioni de fier”
St.Cerc.Fiz.33(1), 29 (1981)
7. M.Peteanu, Al.Nicula
„EPR investigation of Mn^{2+} ions in xMnO(1-x)”
Studia UBB, Phys. (1), 63 (1981).
8. M.Peteanu, Al.Nicula
„Paramagnetic resonance of Mn^{2+} ions in polycrystalline and amorphous materials”
Rev.Roum.Phys.26(8-9), 1047 (1981).

1982

1. I.Barbur
„Fenomene critice in feroelectrici studiate prin rezonanta paramagnetica electronica”
St.Cerc.Fiz.34, 753-769 (1982)
2. O.Cozar, I.Ardelean
„Studiul RES al formarii perechilor mixte de ioni Cu^{2+}-V^{4+} si Cu^{2+}-Mn^{2+} în matricea $2B_2O_3.K_2O$”
Studia UBB, Phys., 27, 41 (1982)
3. O.Cozar, V.Znamirovschi, M.Gridan
„ESR study the dispersion mode of Cu(II) and VO(II) ions adsorbed on SiO_2 and Al_2O_3 surface”
Rev.Roum.Phys., 27, 389 (1982)
4. S.Simon, Al.Nicula
„EPR on soda-borate glasses with NiO”
Studia UBB, Phys. 27, 50-54 (1982)
5. S.Simon, Al.Nicula
„Magnetic resonance on borate glasses with Gd_2O_3 and Eu_2O_3”
Studia UBB, Phys. 27, 59 (1982)
6. M.Peteanu, Al.Nicula
„EPR data corelated to magnetic measurement and optical spectroscopy of manganese ions in vitreous matrices”
St. Cerc. Fiz., 34(1), 15 (1982)

1983

1. O.Cozar, N.Grecu, I.Bratu, M.Coldea, V.Grecu
„ESR and magnetic susceptibility studies of some copper (II) p-benzoates’’
Studia UBB, Phys., 28, 33 (1983)
2. S.Simon, Al.Nicula
“EPR study of glasses and vitroceramics with gadolinium oxide”
Rev. Roum. Phys., 28, 1, 57 (1983).
3. O.Cozar, I.Ardelean, Gh.Ilonca
„Studii RPE si de susceptibilitate magnetica privind unele sticle din sistemul $x(CuOV_2O_5)(1-x)[2B_2O_3{\cdot}K_2O]$”
Rev. Chim. 34, nr.2, 121-125 (1983)
4. M.Peteanu, I.Ardelean, Al.Nicula
„EPR Investigation of Mn^{2+} ions in a $TeO_2{\cdot}PbO$ glass”
Rev. Roum. Phys. 28, 47-55 (1983)
5. I.Ardelean, O.Cozar, Gh.Ilonca
’’EPR and Magnetic Susceptibility Studies of $xCuO(1-x)[2B_2O_3{\cdot}PbO]$ Glasses’’
Rev. Roum. Phys. 28, nr.5, 451-457 (1983)

1984

1. O.Cozar, I.Ardelean
„RES a ionilor Cu^{2+} si V^{4+} în sticle fosfo-sodice”
Studia UBB, Phys. (2), 51-55 (1984)

2. O.Cozar, I.Ardelean
„Studii RES şi de susceptibilitate magnetică privind unele sticle din sistemul $x(CuO.V_2O_5)(1-x)[2B_2O_3.K_2O]$"
Rev. de Chimie 34(2), 121 (1983)
3. I.Ardelean, O.Cozar, Gh.Ilonca
„ESR and magnetic susceptibility studies of $xCuO(1-x).[2B_2O_3.PbO]$ glasses"
Rev.Roum.Phys., 28(5), 451 (1983)

1985

O.Cozar, I.Ardelean, L.Balatici,
„RES a ionilor Cu^{2+} si V^{4+} în sticle fosfo-sodice"
Studia UBB, Phys., 30, 51-55 (1985)

1986

1. I.Barbur, L. Stanescu
„ERS and thermal annealing studies of gamma defects in Na_2SeO_4"
StudiaUBB, Phys. 31, 41-44 (1986)
2. L.V.Giurgiu, Al.Nicula, S.V.Nistor
„EPR spin imaging by using dipolar fields"
Studia UBB, Phys. 31, 3 (1986).

1987

1. S. Simon, I. Barbur, I. Ardelean
„EPR on some superconducting oxide ceramics"
Studia UBB, Phys. 32, 96-99 (1987)
2. O.Cozar, I.Milea, I.Ardelean, T.Fiat, P.Simonfi
„EPR and diffuse reflectance studies on coloured quartz samples impurified with copper oxide"
Studia UBB, Phys., 32, 10 (1987)
3. S.Simon, V.Simon, Al.Nicula
„Magnetic resonance on borate glasses with high copper oxide content"
Studia UBB, Phys. 32, 55-62 (1987)

1988

1. I.Barbur, S. Simon, I. Ardelean, L. Stanescu, Gh. Cristea
„EPR study of intermediaite phase transition in ferroelastic $Pb_3(PO_4)_2$"
Studia UBB, Phys. 33, 1139-1143 (1988)
2. I.Barbur, S. Simon
„ESR evidence of structural phase transition in Na_2SeO_4"
Studia UBB, Phys. 33, 71-73 (1988)
3. O.Cozar, I.Ardelean, Gh.Cristea, Gh.Ilonca
„ESR Investigation of the Local Symmetry and Interaction Between Cu^{2+} and V^{4+} Ions in Potasium - Borate Glass"
Rev. Roum. Phys. 33 (7), 1125 (1988)
4. O.Cozar, R.Semeniuc, V.Znamirovschi, I.Haiduc
„ESR and IR studies of some oxovanadium dithiophosphonates"
Rev.Roum.Phys., 33, 1131 (1988)

5. E.Trif, D.Strugaru, I.Ivan, R.Rusu, G.Gheorghe
"Phase transition of the Y-type zeolites investigated by thermal analysis, XRD and RPE methods"
Studia UBB , Phys. 33, 79, 1988
6. A.Nicula, A.V.Pop, Al.Darabont, L.V.Giurgiu
"EPR investigation in the superconductor $GdBa_2Cu_3O_x$"
Studia UBB, Phys. 33, 71-73 (1988)

1989

1. O.Cozar, I.Ardelean, I.Bratu, Gh.Ilonca, S.Simon
„ESR, IR and magnetic susceptibility studies on $xV_2O_5(1-x)$ $[2B_2O_3.Li_2O]$ glasses"
Studia UBB, Phys. (1), 94 (1989)
2. O.Cozar, V. Znamirovschi, V.V. Grecu
„Studii RES asupra inetracțiunilor de schimb în complecşi metalici polinucleari"
St. Cerc.Fiz. 41, 777 (1989)
3. S.Simon, Gh.Ilonca, I.Barbur, I.Ardelean,
„EPR in Vitroceramics with Gadolinium Oxide"
Studia UBB, Phys. (2), 49-54 (1989)
4. A.Nicula, A.V.Pop, Al.Darabont, L.V.Giurgiu, I.Cosma
"Magnetic investigation as a fiunction of heat treatment in the Gd-Ba-Cu-O"
Studia UBB, Phys. 34, 70 (1989)
5. A.Nicula, A.V.Pop, Al.Darabont, L.V.Giurgiu,
"Gd^{3+} and Cu^{2+} EPR in the high-temperature superconductor$Y_{1-x}Gd_xBa_2Cu_3O_{7-\delta}$"
Studia UBB, Phys. 34, 70 (1989)

1990

M.Peteanu, I.Ardelean
„EPR Investigation of Fe^{3+} Ions in the $95TeO_2 \cdot 5PbO$ Glasses''
Studia UBB, Phys., 25, 79-84 (1990)

1991

A.V.Pop, Al.Nicula, L.V.Giurgiu, Al.Darabont
„The treatment in oxygene atmosphere and EPR absorbtion in $Y_{1-x}Gd_xBa$ CuO system"
Studia UBB, Phys., 34, 23 (1991)

1992

1. L.David, O.Cozar, G.Damian, V.Chis, A.Negoescu
„Crystal structure and Magnetic properties of two nitronyl nitroxide biradicals''
Studia UBB, Phys. 37, 69-81 (1992)
2. M.Peteanu, L.Cociu, I.Ardelean
„The influence of the Vitreos Matrix on the Cu^{2+} EPR Absorption Spectra''
Studia UBB, Phys., 37, 47-59 (1992)

1994

1. V.Chis, O.Cozar, G.Damian, L.David, C.Cosma, R.Semeniuc, T.Drăgoiu
„ESR Study of Free Radicals Obtained in Some Gamma-Irradiated Aminoacids"
Studia UBB, Phys. 39, 17 (1994)

2. I.Ardelean, O.Cozar, Gh.Ilonca, V.Simon, S.Filip
„EPR and Magnetic susceptibility studies of Bi_2O_3-PbO-Fe_2O_3 glasses"
Rom. Rep. Phys. 46 (2, 3), 235-242 (1994)
3. L.David, V.Chis, O.Cozar, R.Ssemeniuc, S.Negurici
„IR study of the coordination mode of Cu(II) ion in methazolamide compound"
Studia UBB, Phys. 39, 11-16 (1994)

1995

1. L.David, O.Cozar, I.Bratu, V.Chis, Gh.Bora
"IR, EPR and Mossbauer Investigation of Some Fe(III) Complexes with Antiinflammatory Drugs"
Studia UBB, Phys. 40, 25 (1995)
2. D. Maniu, I. Ardelean, O. Cozar
„EPR Study of $xV_2O_5(1-x)[3B_2O_3.K_2O]$ glasses"
Studia UBB, Phys. 40, 55 (1995)
3. V.Simon, I.Ardelean, O.Cozar, S.Simon, I.Milea, I.Lupşa, V.Mih, D.Becsa
„Some physical properties of irradiated and non-irradiate oxide glasses containing uranium"
Rom. Rep. Phys., 47, 7-8 (1995)
4. M.Peteanu, L.Cociu, I.Ardelean
„Paramagnetic centers induced by gamma irradiation in B_2O_3-GeO_2 glasses"
Studia UBB, Phys., 2, 3-8 (1995)
5. M.Peteanu, I.Ardelean, S.Filip, I.Todor, G.Salvan
„Electron paramagnetic resonance of Mn^{2+} ions in Bi_2O_3-GeO_2 glasses"
Studia UBB, Phys., 2, 39-15 (1995)
6. M.Peteanu, I.Ardelean, S.Filip, D.Alexandru
„EPR of Mn^{2+} in $70TeO_2$-$25B_2O_3$-5PbOglasses"
Rom. J. Phys.(1995)

1996

1. S. Filip. O. Cozar, V. Simon, I. Ardelean
„EPR and magnetic susceptibility studies of Cu^{2+} ions in Bi_2O_3.PbO glasses''
Studia UBB, Phys. 41, 25 (1996)
2. G.Damian, V.Znamirovschi, O.Cozar, M.Todică, V.Chis, L.David, R.Salomir
„Solvent effects towards the mobility of nitroxide radicals adsorbed on X and Y zeolites"
Studia UBB, Phys. 41, 49 (1996)
3. L.David, O.Cozar, L.Sumalean. R.Tetean, C.Craciun, N.Pop
„Structural studies of some Cu(II) complexes with thiazolylhydrazone"
Studia UBB, Phys. 41, 43 (1996)
4. M.Peteanu, I.Ardelean, S.Filip, D.Alexandru
„EPR of Mn^{2+} ions in $70TeO_2$-$25B_2O_3$-5PbO glasses''
Rom. J. Phys. 41, 593-601 (1996)
5. M.Peteanu, I.Ardelean, V.Simon, S.Filip, M.Flora
„EPR of Mn^{2+} ions in B_2O_3-SrO glasses"
Studia UBB, Phys. 41, 11-23 (1996)
6. M.Peteanu, I.Ardelean, V.Simon, S.Filip, G.Györffy
„EPR of Fe^{3+} ions in $70TeO_2 \cdot 25B_2O_3 \cdot 5PbO$ glasses"
Studia UBB, Phys. 41, 17-24 (1996)

1997

1. R.Micu-Semeniuc, O.Cozar, L.David, V.Chis, R.Semeniuc
"ESR study of some cooper(II)-1, 4-dihydrazinophtalazine compounds"
Rev.Roum.Chim., 42, 627-632 (1997)
2. V.Chis, G.Damian, L.David, O.Cozar, V.ZnamirovsciL.Kazirs-chi, D.Ristoiu
''Gamma Radiation effects on some biomolecules"
Studia UBB, Phys. 42, 39 (1997)
3. L.David, O.Cozar, V.Chis, D.Ristoiu, C.Bălan
„Spectroscopic and magnetic properties of the dimeric $[Cu(SO_4)\cdot$(1, 4-dihydrazinophtolazine)$\cdot H_2O]_2$ complex"
Studia UBB, Phys. 42, 49 (1997)
4. E.Forizs, O.Cozar, L.David, D.Ristoiu, C.Crăciun, C.Bălan
„Local structure investigations of some Cu(II)-theophylline complexes''
Studia UBB, Phys. 42, 31 (1997)
5. S.Simon, I.Ardelean, D. Eniu, V. Simon
„EPR study on radiotherapeeutic glasses"
Studia UBB, Phys. 42, 3-8 (1997)
6. I.Ardelean, M.Peteanu, V.Simon, F.Ciorcas
„EPR and magnetic susceptibility investigations of TeO_2-B_2O_3-SrO-Fe_2O_3 glasses"
Studia UBB, Phys. 42, 3-13 (1997)
7. I.Ardelean, M.Peteanu, V.Simon, F.Ciorcas
„EPR and magnetic susceptibility studies of Cu^{2+} ions in TeO_2-B_2O_3-SrO-Fe_2O_3 glasses"
Studia UBB, Phys. 42, 3-13 (1997)

1998

1. C. Craciun, C. Balan, C. Agut, D. Ristoiu, O. Cozar, L. David
„The metal-ligand bonding in some Cu(II)-complexes with ligands of biological relevance. Part I: Cu(II)-antiinflamatory drugs"
Studia UBB, Phys. 42, 41 (1998)
2. C. Balan, C. Craciun, D. Ristoiu, O. Cozar, L. David
„The metal-ligand bonding in some Cu(II)-complexes with ligands of biological relevance. Part II: Cu(II)-tranquilizing sedativ-hypnotic and myorelaxant agents"
Studia UBB, Phys. 42, 51 (1998)
3. O.Cozar, L.David, C.Crăciun
„ESR Study of some Cu(II)-theophylline complexes"
Roum.J.Phys. 43, 561-569 (1998)
4. I.Bratu, D.Maniu, I.Ardelean, O.Cozar
„IR and EPR investigations of the $xCuO(1-x)[3B_2O_3\cdot K_2O]$ glass structure"
Roum.J.Phys. 43, 361-366 (1998)
5. G. Damian, V. Miclaus, v. Znamirovschi, O. Cozar, V.Chiş, L.David, M. Todica, C. Paizs
„The dynamics of nitroxide radicals in chloroform and deuterated chloroform solutions absorbed on zeolites"
Progress in Catalisys, 137, 1-6 (1998)
6. I.Ardelean, S.Simon, M. Peteanu, V. Simon, F. Ciorcaş, C. Bob, S. Filip
„Valence states and magnetic interactions of manganese ions in Bi_2O_3-PbO and $Bi_2O_3PbOAs_2O_3$ glass matrices"
Rom. J. Phys. 43, 577-582 (1998)

7. M.Todică, S.Simon, I.Ardelean, V.Simon, E.Matei
„NMR and ESR study of local dynamics in polyisoprene-CCl_4 solutions"
Studia UBB, Phys. 43, 35-44 (1998)
8. I.Ardelean, M.Peteanu, R.Ciceo-Lucacel
„Cu^{2+} containing strontium borate glasses studied by electron paramagnetic resonance"
Studia UBB, Phys. 43, 3-13 (1998)
9. R.Ordean, R.Fekete, O.Pana, C.Filip, L.V.Giurgiu, K.Kessler, M.Mehring
„Change delocalization in quasi-one-dimensional molecular conductor KCP as seen by ESR"
Rom.J. Phys.43, 481 (1998)

1999

1. C. Crăciun, L. David, M. Rusu, O. Cozar, D. Ristoiu, I. Bratu
"IR and ESR Studies of $K_5[PVMo_2W_9O_{40}(H_2O)]\cdot 23H_2O$ Heteropolyoxometalate Complex''
Studia UBB, Phys. 44, 115 (1999)
2. C. Bălan, L. David, L. Ghizdavu, C. Crăciun, O. Cozar, D. Ristoiu
„IR, ESR and magnetic investigations of some transition metal complexes of γ-L-glutamyl derivatives"
Studia UBB, Phys. 44, 107 (1999)
3. O.Cozar, L.David, G.Damian, V.Chiş
„Structural and Dynamical Studies of Some Molecular Complexes of Biological Relevance"
Studia UBB, Phys. 44, 55-71 (1999)
4. R.F. Semeniuc, R.M. Semeniuc, I. Haiduc, O. Cozar
„Spectroscopic characterization of some chromium o-alkyldithiocarbonates"
Studia UBB, Chem., 44, 203-212 (1999)
5. L.David, O.Cozar, M. Armenean
„EPR study of some copper (II) complexes with dithiophosphonates as ligands"
Rom.Rep.Phys. 51, 757-762 (1999)
6. I.Ardelean, M.Peteanu, S.Simon, S.Filip, V.Simon, I.Todor, G.Salvan
„EPR and magnetic susceptibility studies of iron ions in $Bi_2O_3.GeO_2$ glass matrix"
Rom. Rep. Phys., 51, 56 (1999)
7. I.Ardelean, M.Peteanu, S.Filip, S.Simon, C.Bob, N.Muresan
„Structural investigation of some vitreous systems containing chromium by using EPR"
Rom. Rep. Phys., 51, 56 (1999)
8. I.Ardelean, M.Peteanu, V.Simon, F.Ciorcas, R.Ciceo Lucacel, S.Simon
„EPR and magnetic susceptibility investigations of iron containing$TeO_2.B_2O_3SrF_2$ and $TeO_2.B_2O_3$-SrO glasses"
Studia UBB, Phys.44, 3 (1999)
9. I.Ardelean, M.Peteanu, S.Simon, S.Filip, V.Simon, C.Bob, N.Muresan
„EPR investigation of some oxide vitreous systems containing chromium ions"
Rom. Rep. Phys. 51 (5-6), 505-510 (1999)
10. R.Ordean, C.Filip, L.V.Giurgiu, K.Kessler, M.Mehring, X.Filip, Al.Darabont
„Wath does ESR tell us about the magnetic exchange interaction in $(RE)Ba_2Cu_3O_{7-\delta}$"
Rom.Rep.Phys.51, 669 (1999)

2000

1. V.Chiş, Alina Buda, L.David, O.Cozar, A.Darabont, A.Căuş
„Structural Properties of the Free Radical Produced in a Gamma-Irradiated Single Crystal of Ammonium Tartrate"
Studia UBB, Phys. 45, 41-48 (2000)
2. R.M. Semeniuc, I. Haiduc, R. Semeniuc, O. Cozar
„Spectroscopic studies of some metallic bis-dithiophosphonates, $M(DTP)_2$, and of some adducts"
Studia UBB, Chem., 45, 185-197 (2000)
3. I.Ardelean, M.Peteanu, D.Maniu, Gh.Ilonca, V.Simon, V.Ioncu, P.Pascuta
„Structural and magnetic behaviour of iron ions in $3B_2O_3.K_2O$ glass matrix"
Studia UBB, Phys. 45, 9-19 (2000)
4. I.Barbur, L.David, I.Ardelean, A.Veres, G.Borodi
„Structural and EPR study on $Pb_2Mg_{1-x}Cu_xWO_6$ compound"
Studia UBB, Phys. 45, 29-32 (2000)
5. C.Craciun, L.David, O.Cozar, D.Rusu, M.Rusu, V.Chis
„Spectroscopic investigation of one multiuranium(IV) sanswich-tipe polyoxometalate complex"
Studia UBB, Phys. 45, 57-65 (2000))
6. I.Barbur, V.Chis, I.Batiu
„UV radiation effects on a new hydrazino-carvone compound. An ESR investigation."
StudiaUBB, Phys. 45, 91-97 (2000)

2001

1. Gh. Cristea L Stanescu, amd I. Ardelean
„Optical and E.P.R. study on solid solution of V_2O_5-MoO_3 Solid Solution"
Studia UBB, Phys. 46, 63 – 71, 2001
2. O.Cozar, L.David, C. Crăciun, V.Chiş
„X and W ESR studies of transition metal clusters encapsulated in sandwich-type polyoxometalates"
Studia UBB, Phys. 46, 176-182 (2001)
3. C. Crăciun, L.David, V.Chiş, O.Cozar
„EPR study of a trinuclear Mn^{2+} cluster encapsulated in one heteropolyanion"
Studia UBB, Phys. 46, 3-10 (2001)
4. S. Cavalu, G. Damian, M. Dansoreanu, S.Simon
"Correlaton times and magnetic interactions between tempyo spin label and blood proteins''
Studia UBB, Phys. 46, 1 (2001)
5. G. Damian, S. Cavalu, M. Dansoreanu, S.Simon, C.M. Lucaciu
„EPR investigation of non covalent spin labelled cytopchrome c and ovalbumin"
Studia UBB, Phys., 46, 465 (2001)
6. I.Ardelean, M.Peteanu, R.Ciceo-Lucacel, P.Pascuta, M.Flora
„EPR and magnetic susceptibility data on MnO-B_2O_3-As_2O_3 glasses"
Studia UBB, Phys. 46, 19-27 (2001)
7. M.Peteanu, C.Borsa, I.Ardelean
„EPR investigation of the Fe_2O_3-Bi_2O_3-PbO-As_2O_3 glass system"
Studia UBB, Phys. 46, 3-7 (2001)

8. Gh.Cristea, L.Stanescu, I.Ardelean
„Optical and ESR study on V_2O_5-MoO_3 solid solution"
Studia UBB, Phys. 46, 59-66 (2001)
9. I.Barbur, V.Chis
„ESR study of gmma-iradiated tetrabutilammoniumiodid"
Studia UBB, Phys.46, 9-12 (2001)
10. L.David, C. Crăciun, V.Chiş, R.Tetean
„Spectroscopic and magnetic investigation of one Cu(II) β-diketonate complex"
Studia UBB, Phys. 46 , 11-17 (2001)

2002

1. V. Chiş, A.L. Maniero, M. Brustolon, O.Cozar, L.David
„EPR and ENDOR Investigation an Gamma-Irradiated Single Crystal of L-Tyrosine-HCl"
Studia UBB, Phys. 47 (2002)
2. C.Crăciun, O. Cozar, L. David, V. Chiş
„Influence of the Amine-Type Ligands on the Local Symmetry in Co (II)- theophylline Complexes"
Studia UBB, Phys. 47 (2002)
3. I.Ardelean, M.Peteanu, N.Muresan
"EPR and magnetic susceptibility studies of $70TeO_2.25B_2O_3.5SrO$ glasses containing Cr^{3+} ions"
Studia UBB, Phys. 47 (2002).

Appendix 3

Scientific communications presented at international conferences

1961

I.Ursu, J.Turkevich
"Studiul proprietatilor catalitice si rezonanta magnetica a LiAl-H4"
Princeton Univ., Princeton, Colloque Ampere, Leipzig, 1961

1964

I.Ursu
''RES a sistemului Pt-C si activitatea sa catalitica''
Compte Rend. Congres XII Ampere, Bordeaux, 1963

1965

A.Calusaru, I.Barbur, I.Ursu
„Thermal annealing of paramagnetic defects induced by gamma irradiation $(NH_4)_2SO_4$ et $(ND_4)_2SO_4$ single crystals"
The Simposium "Chemical Effects of Nuclear Transformations", Viena, Proceedings, p.293-311, 1965

1967

A.Calusaru, I.Barbur, I.Ursu
„Recombination kinetics of radicals induced by gamma irradiation in single crystals of ammonium sulphate", 8p.
The second Tihany Simposium on Radiation Chemistry, Tihany, Ungaria, 1967.

1968

1. Gh. Cristea, A. Darabont
„ESR Spectrum of Mn^{2+} in $(NH_4)_2Cd(SO_4)_3$"
Procc. of the XV-th Colloque AMPERE on Mangetic Resonance and Radiofrequence Spectroscopy - Grenoble, France, 1968
2. Gh. Cristea, A. Darabont
„ESR Spectrum of Mn^{2+} in $(NH_4)_2Cd(SO_4)_{3\cdot n}H_2O$"
Procc. of the XV-th Colloque AMPERE Grenoble, France, 1968
3. Al.Nicula, S.I.Farcas, Al. Darabont
„ESR of NaCl and NaBr crystals doped with Ca^{2+} and Al^{3+}"
Procc. of the XV-th Colloque AMPERE Grenoble, France, 1968

1969

1. Al.Nicula, S.I.Farcas, Al.Darabont
„Double paramagnetic center in NaCl"
Tagung hochfrequenzspectroskopie der physikalischen gesellschaft in der D.D.R p.14-17 sept.1969, Karl-Marx-Universitat Leipzig

2. Al.Nicula, S.I.Farcas, Al.Darabont
„Orthorombic, axial and cubic paramagnetic centers in NaCl and NaBr"
Tagung hochfrequenzspectroskopie der physikalischen gesellschaft in der D.D.R p.14-17 sept.1969, Karl-Marx-Universitat Leipzig

1970

1. Gh. Cristea, H. J. Stapleton
„Concentration -Dependent Orbach relaxation Rates in Cerium Doped Lanthanum Magnesium Nitrate"
Procc. of the XVI-th Congresse AMPERE, Bucharest, Romania, 1970
2. Al.Darabont, S.V.Nistor
„ESR of NaCl single crystals doped with iron"
Procc. of the XVI-th Congresse AMPERE, Bucharest, Romania, 1970
3. Al.Darabont, S.V.Nistor, M.Peteanu
„The symmetry of paramagnetic and the type of irradiation"
Procc. of the XVI-th Congresse AMPERE, Bucharest, Romania, 1970
4. Al.Darabont, Al.Nicula, L.V.Giurgiu
„Temperature and irradiation influence on Cu^{2+} ESR spectrum in $K_2Zn(SO_4)_2$ $6H_2O$"
Procc. of the XVI-th Congresse AMPERE, Bucharest, Romania, 1970
5. S.V.Nistor, I.Ursu
„Theory of the ESR parameters for the O^- trapped-hole centers in doped NaCl crystals"
Procc. of the XVI-th Congresse AMPERE, Bucharest, Romania, 1970
6. Al.Darabont, Al.Nicula, M.Peteanu
„The symmetry of paramagnetic centers and the type of irradiation"
Procc. of the XVI-th Congresse AMPERE, Bucharest, Romania, 1970

1972

1. I.Barbur, A.Bodi, G.D.Popescu, V.Militaru
„ESR Study and Microwave Dielectric Measurements of Gamma Irradiation Ferroelectric Ammonium Hydrogen Sulphate"
Procc. of the XVII th Congress AMPERE, Turku, Finlanda, 1972.
2. V.Znamirovschi, O.Cozar, Al.Nicula
„ESR linewidth study of vanadyl ions in natural water and heavy water"
Procc. of the XVII th Congr. Ampere, Turku, Finlanda, 1972

1974

Al.Darabont, Al.Nicula, S.I.Farcas
„ESR of chromium doped $NH_4Al(SO_4)_2$ $12H_2O$"
XVIII-th Congresse AMPERE, Nottingam, 1974

1975

Al.Darabont, Al.Nicula, S.I.Farcas
„ESR forbidden transition of Fe^{3+} in ammonium alums"
Procc. of the II-nd specialized colloque AMPERE. Applications of resonance methods in solid state physics, Budapest, Ungaria, 1975

1976

1. Al.Darabont, Al.Nicula, S.I.Farcas
„Theoretical explanation of forbidden transitions of Fe^{3+} and Cr^{3+} in alums"
Procc. of XIX-th Congress Ampere, Heidelberg, 1976
2. Al.Darabont, P.Fitori, Al.Nicula, S.I.Farcas
„ESR study of vanadium ion in alums"
Procc. of XIX-th Congress Ampere, Heidelberg, 1976
3. O.Cozar, V.Znamirovschi
„EPR evidence for two cupric complexes in water-ethanol mixtures at 77K"
Abstract Congr. Ampere, Heidelberg, 1976

1978

1. O.Cozar, V.Znamirovschi, V.V.Morariu
„EPR behaviour of some Cu(II) complexes on Si_2 and Al_2O_3 surfaces"
Abstract Congr. Ampere, Tallin, 978
2. Al.Darabont, Al.Nicula, S.I.Farcas
„The electron paramagnetic resonance of the iron ion in K_3AlF_6"
Procc. of XX-th Congress Ampere, Tallin, 1978
3. E.Burzo, I.Ursu, V.M.Nazarov
„EPR study of neutron irradiated Fe_2O_3-B_2O_3-PbO glasses"
Procc. XXII-nd Congres Ampere, Zurich, 1984
4. L.V.Giurgiu, I.Ursu
„ESR spectroscopic investigation of Ta(V) doped AgCl"
Procc. XX-th Congres Ampere, Tallin, Estonia, 1978

1979

L.V.Giurgiu
„Platinum paramagnetic species investigated by EPR"
RAMIS Conference, Poznan, Poland, 1979

1981

S.Simon, Al.Nicula
''Magnetic resonance of broates glasses doped with paramagnetic ions''
Int. Conf. Amorphous System Investigated by Nuclear Methods, Balatonfured, Ungaria, 1981

1982

1. Lavinia Cociu, Al. Nicula
„EPR Study of the Defect Centers Produced by irradiation of the B_2O_3-Li_2O-Al_2O_3-RO system"
Procc. of the Int.Conf."Amorphous Semiconductors" Bucharest, Romania, 1982
2. M.Peteanu, Al.Nicula
„Fe^{2+}-Fe^{3+} interaction in borate glasses investigated by EPR"
Procc.Int.Conf."Amorphous semiconductors 1982, Bucharest, Romania
3. S.Simon, V.Simon, T.Iliescu, Al.Nicula
''Structural characterization of some oxide glasses containing molybdenum using optical and magnetic resonance spectroscopy''
Procc. of Int. Conf. on Amorphous Semiconductors, Bucharest, Romania, 1982

1983

1. S.Simon, A.Giurgiu, T.Petrisor, Al.Nicula
„Magnetic properties of barium titanate glasses with gadolinium"
Procc. of Int. Conf. on Magnetism of rare-earths and actinides, Bucharest, Romania, 1983
2. L.V.Giurgiu, I.Ursu, O.Pana, G.Nagy
„Solitons in one-dimensional KCP and the analysis of ESR linewidths"
Procc.RAMIS-Radio and microwave spectroscopy conference, Poznan, Poland, 1983
3. L.V.Giurgiu, I.Ursu, O.Pana, G.Nagy
„The analysis of EPR linewidth in KCP by coupled nuclear soin method"
Procc.RAMIS-Radio and microwave spectroscopy conference, Poznan, Poland, 1983
4. I.Ardelean, Gh.Ilonca, M.Peteanu
„EPR and magnetic susceptibility studies of $xMnO(1-x)[2B_2O_3{\cdot}K_2O]$ glasses"
Europhysics Conf.Abstracts.Soft Magnetic Materials 6, Eger Hungary, 1983, V.7E, Ed.S.Methfessel, 344-345

1984

1. I.Barbur, L.Stanescu
„ESR Study of Ferroelectric Lead-Orthovanadate"
Procc.of the XXII-nd Congress AMPERE, Zurich, Elvetia, 1984.
2. E. Trif, S. Petrişor, D. Strugaru, D. Vass
„EPR study of order-disorder aspecta in Y-type zeolites containing Fe^{3+} ions"
Procc. 22 Congres AMPERE, Zurich , Switzerland, 1984
3. I.Ursu, L.V.Giurgiu
„EPR spectra of a trigonally distorted $(HF6)^{3-}$ complex in irradiated Cs_2HfF_6 single crystals"
Procc. XXII-th Congress AMPERE, Zurich, Switzerland, 1984
4. E.Trif, M.Peteanu, Al.Nicula
„EPR of 3d ions in natrium-borate glasses"
Procc. XXII-th Congress AMPERE, Zurich, Switzerland, 1984

1985

1. O.Cozar, V.Znamirovschi
„EPR study of the interaction between transition metal ions adsorbed on SiO_2 and Al_2O_3 surfaces"
Abstracts of 7-th Specialized Colloque Ampere, Bucuresti, Romania, 1985
2. Al.Nicula, O.Cozar, I.Ardelean
„EPR and RMN studies of the microenvirounments of Cu^{2+} ions in B_2O_3-K_2O glasses"
Abstracts of 7-th Specialized Colloque Ampere, Bucuresti, Romania, 1985
3. O.Cozar, I.Ardelean
„The EPR study of local symmetry and interactions between copper and vanadium ions in soda-phosphate glasses''
Abstracts of 7-th Specialized Colloque Ampere, Bucuresti, Romania, 1985
4. S.Simon, V.Simon, Al.Nicula
"Magnetic resonance investigation of the transition from amorphous to crystalline state"
7-th Specialized Colloque AMPERE, Bucharest, Romania 1985
5. Al.Darabont, S.V.Nistor, M.Velter-Stefanescu
„ESR investigation of Cu^{3+} impurities in $(NH_4)AlF_5$ H_2O single crystals"
Procc. of the 7-th specialized colloque Ampere, Bucharest, Romania, 1985

6. L.V.Giurgiu
„A new model for fractionally charged soliton excitation in quasi-one-dimensional KCP"
RAMIS Conference, Poznan, Poland, 1985
7. L.V.Giurgiu, I.Ursu, O.Pana
„A model for fractionally charged soliton-like excitations in quasi-1D $K_2Pt(CN)_4Br_{0,3}$·3, $2H_2O$ complex"
Procc. RAMIS-Radio and microwave spectroscopy conference, Poznan, Poland, 1985
8. I.Ursu, L.V.Giurgiu, P.Fitori
„The geometry of the $W(CN)^{3-}_8$ molecular ion identified by EPR "
Procc. VII-thSpecialized Colloque AMPERE, Bucharest, Romania 1985
9. M.Peteanu, L.Cociu, Al.Nicula, E.Halmagean, Gh.Viisoreanu
"Structural defects detected in NTD-Silicon by using EPR"
Procc. of the7-th Specialized Colloque AMPERE, Bucharest, Romania, 1985
10. M.Peteanu, L.Cociu, Al.Nicula, E.Halmagean, Gh.Viisoreanu
"Structural defects detected in NTD-Silicon by using EPR"
7-th Specialized Colloque AMPERE, Bucharest, 1985

1988

1. S.Simon, V.Simon, I.Barbur
„Magnetic Resonance on Oxide Vitroceramics with Ferroelectric Crystallites"
The 6-th European Meeting on Ferroelectricity, Pozan (Polonia) 1988.
2. L.V.Giurgiu
„Hyperfine interaction investigated by EPR in molecular platinum complexes"
Procc. of the XXIV-th AMPERE Congress, Poznan, Poland, 1988
3. L.V.Giurgiu
„A credo for a spy: Magnetic exchange interaction in $Gd_xY_{1-x}Ba_2Cu_3O_{7-\delta}$ superconductors"
3-th General Conference of Balkan Physical Union, Cluj, Romania, 1988
4. L.V.Giurgiu, R.Ordean, O.Pana, R.Turcu
„A possible phase transition in intermediate ClO^-_4 doped polythiophene from EPR measurement"
Procc. XXIV-th CongressAMPERE, Poznan, Poland, B-106(1988)

1989

1. O.Cozar, I.Ardelean
„EPR and IR investigation of the local symmetry and interaction between vanadium ions in lithium-borate glasses"
In vol. "Abstracts of XIXth EUCMOS", Dresda, 1989
2. I.Bratu, O.Cozar, Gh.Bora, D.Breazu
„Structural studies on some Copper(II) compounds with antiinflamatory nesteroid ligands"
In vol. "Abstracts of XXVI Colloquium Spectroscopicum Internationale" Sofia, 1989
3. A.Pop, Al.Nicula, Al.Darabont, L.V.Giurgiu
„Magnetic investigation in superconducting and nonsuperconducting system $Y_{1-x}Gd_xBa_2Cu_3O_{7-\delta}$"
Procc.RAMIS-Radio and microwave spectroscopy conference, Poznan, Poland, 1989

1990

1. O.Cozar, I.Ardelean, Gh.Ilonca, S.Simon, I.Barbur, I.Bratu
„The valence states and interactions between chromium ions in lithium-borate glasses"
Procc. of the 25-th Congress AMPERE , Stuttgart, 1990
2. I.Barbur, S.Simon, I.Ardelean, Gh.Cristea
„EPR evidence for an intermediate premartensitic transition in $Pb_3(PO_4)_2$"
Procc. of the 25-th Congress AMPERE , Stuttgart 1990.
3. V.Ioncu, Gh.Cristea, I.Barbur, E.Tataru, S.Simon
„Nuclear quadrupol resonance spectrometer"
Procc. of the 25-th Congress AMPERE , Stuttgart, 1990.
4. O.Cozar, I.Bratu, I.Ardelean, S.Simon, V.Znamirovschi
„EPR of copper (II) complexes with indomethacinum and ibuprophenum ligands"
Ext.Abstr.Congr. Ampere, Stuttgart, 1990
5. S.Simon, O. Cozar, I.Barbur, V.Simon, I.Ardelean, Gh. Ilonca
„The partial cristallization effect on the EPR spectra from Bi-Sr-Ca-Gd-Cu-O vitrieous matrices"
Ext.Abstr. Congr. Ampere, Stuttgart, 1990
6. S.Simon, O.Cozar, I.Barbur, V.Simon, I.Ardelean, Gh.Ilonca, V.Ioncu,
„The Crystallization Effect on the EPR Spectra From Bi-Sr-Ca-Cd-Cu-O Vitreous Matrices"
Ext.Abstr. Congr. AMPERE , Stuttgart 1990, p. 82-83
7. Al.Nicula, A.Pop, L.V.Giurgiu, Al.Darabont, I.Cosma
„Magnetic properties investigated by EPR and static susceptibility in the superconducting system $Y_{1-x}Gd_xBa_2Cu_3O_{7-\delta}$"
Procc.XXV-th Congress AMPERE, Stuttgard, Germany, 1990

1991

1. O.Cozar, I.Ardelean, S.Simon, L.David
„ESR investigation of some potassium-borate glasses with manganesse and vanadium ions"
Procc.of "1st General Conference of the Balkan Physical Union", Thessaloniki, 1991
2. S.Simon, O.Cozar, I.Ardelean, V.Simon, E.Burzo,
„The local order from glasses and their thermal history"
1st General Conference of the Balkan Physican Union, 1991, Thessaloniki, Greece, Proc. vol. II

1992

1. O.Cozar, C.Cosma, V.Znamirovschi, L.David, G.Damian, V.Chis
„EPR investigation of DL-Lysine-^{15}N and DL-Ornithine-^{15}N copper (II) complexes"
Ext.Abstr. of 26-th Congress Ampere , Athens, Greece, 1992
2. C.Cosma, O.Cozar, L.Dărăban, T.Fiat
„ESR Study on gamma irradiated foodstuffs"
Ext. Abstr. of 26-th Congress Ampere, Athens, Greece, 1992
3. O.Cozar, I.Ardelean, S.Simon, V.Simon, V.Mih
„EPR of vanadium and manganesse ions in soda-phosphate glasses"
Ext. Abstr. of 26-th Congress Ampere, Athens, Greece, 1992

4. O.Cozar, V.Znamirovschi, L.David, E.Trif
„Adsorbtion Study of Some Cu(II) Amino-Acid Compleses on SiO_2 and Al_2O_3 by EPR Method"
Abstr. of 6-th Int.Symposium on Mag.Res. in Colloid and Interface Science, Firenze, 1992
5. E.Trif, D.Strugaru, I.Ivan, O.Cozar
„EPR Study of Cu(II) Location and Reasctivity in Erionite „
Abstr. of 6-th Int.Symposium on Mag.Res. in Colloid and Interface Science, Firenze, 1992
6. V.Znamirovschi, O.Cozar, C.Cosma, D.Strugaru
„EPR Study of Some Metallic Cations Adsorbed on Silica and Alumina Surfaces''
Abstr. of 6-th Int.Symposium on Mag.Res. in Colloid and Interface Science, Firenze, 1992
7. E.Trif, D.Strugaru, O.Cozar, V.Cristea
„XRD and EPR Study of Cr-exchanged ZSM-5 zeolite"
Int. Conf. On defects in insulating materials.Singapore, Schloss- Nordkirchen, Germany, 1992
8. A.Pop, L.V.Giurgiu, Al.Darabont, F.Balibanu
„Crystal field effects in the EPR of Gd^{3+} in superconducting $Y_{0,95}Gd_{0,05}Ba_2Cu_3O_{7-\delta}$"
Procc.XXVI-th Congress AMPERE, Athens, Greece, 1992
9. A.Pop, L.V.Giurgiu, Al.Darabont
„Measurement of the magnetic fields at the surface of by $Y_{1-x}Gd_xBa_2Cu_3O_{7-\delta}$ means of free radical ESR"
Procc.XXVI-th Congress AMPERE, Athens, Greece, 1992
10. L.Cociu, E.Halmagean, M.Peteanu, G.Popescu
„Irradiation induced defects in passivating glass"
Int.Conf. on defects in insulating materials, Schloss Nordkirchen, RFG, 1992
11. Lavinia Cociu, E. Halmagean, M. Peteanu and G. Popescu
„Irradiation induced defects in passivating glasess"
Procc. of the International Conference on Defects in Insulating Materials, 1992

1993

1. I.Barbur, I.Ardelean, O.Cozar
„EPR and antiferroelectric effects in Pb_2MgWO_6"
AMPERE Summer Institute on Advenced Techniques in Experimental Magnetic Resonance, Portorož, Slovenia, 1993.
2. O.Cozar, I.Ardelean, I.Barbur, V.Mih
„The local symmetry and interaction between V^{4+} and Mn^{2+} in soda phosphate glasses"
AMPERE Summer Institute on Advenced Techniques in Experimental Magnetic Resonance, Portorož, Slovenia, 1993.

1994

1. L. David, V. Chis, V. Znamirovschi, O. Cozar
„ESR Study of Some Solvent Effects on Cu(II)-Aspirinate Complex"
Abstract of European ESR Meeting on Recent Advances and Applications to Organic and Bioorganic Materials, Paris, 1994
2. L. David, V. Chis, V. Znamirovschi, O.Cozar
„ESR Study of Some Cooper (II) -1.4 Dihydrasinophtalasine Complexes"
Abstract of European ESR Meeting on Recent Advances and Applications to Organic and Bioorganic Materials, Paris, 1994

3. Lavinia Cociu, D. Cristescu, E. Halmagean, M. Ilie, A. Pantelica, M. Salagean
„Ion-Exchange Effects in BK7 - Type Glass"
Advanced Materials in Optics, Electro-Optics and Communications Technologies, P. Vincenzini editor, Tecna Publishers, Faenza-RA, Italy, 1994
4. S.Simon, A.van der Pol, E.J.Reijerse, E. de Boer
"Paramagnetic species in some amorphous aluminium-borates catalysts"
11-th Speciallized Colloque Ampee, Menton(Nice), France, 1994

1995

1. O.Cozar, I.Bratu, J.P.Huvenne, P.Legrand
„IR and EPR Structural Investigation of some Cu(II)-Complexes with Antiinflammatory Drugs"
Spectroscopy of Biological Molecules, (Edited by J.C.Merlin, S.Turrel, J.P.Huvenne, Kluwer Academic Publishers), Boston, London, 1995
2. O.Cozar, L.David, V.Chis, E.Foris, G.Damian, I.Bratu
„Local structure analysis Cu(II)-diazepam complexes by ESR spectroscopy"
Abst. of XXIX Colloquium Spectroscopicum Internationale, Leipzig, 1995
3. S.Simon, J.M.P. van Moorsel, A.P.M.Kentgens, E. de Boer
"Low coordinated surface species in gadolinium doped amorphous and crystalline alumina"
VII Int.Symp. on Magn.Res. in Collloid and Interface Science, Madrid, Spain, 1995

1996

1. I.Ardelean, I.Barbur, G.Borodi, A.Veres, I.Cosma
„Structural, electric and magnetic studies on $Pb_2Mg_{1-x}Mn_xWO_6$-type compounds"
15th General Conference of the Condensed Matter Division (European Physical Society), Baveno-Stresa, Italy, 1996.
2. I.Ardelean, I.Barbur, A.Veres, G.Borodi, V.Timar
„Fe substitution effects on structural and electric properties of $Pb_2Mg_{1-x}Fe_xWO_6$ antiferroelectric compounds"
3rd General Conference of the Balkan Physical Union, Cluj-Napoca, Romania, 1997
3. L. David, V. Chis, O. Cozar, E. Forisz, C. Crãciun
„ESR Study of some solvent effects on Cu(II)-oxazepam complexes"
Abstr. of the 2nd Inter. Confer. of the Polish EPR Association, Warsaw, 1996
4. O.Pana, C.Kessler, C.Filip, L.V.Giurgiu, I.Ursu, M.Mehring
„Delocalization of solitins in KCP as seen byESR"
Procc.XVIII-th Congress AMPERE, Canterbury, England, 1996
5. C.Kessler, C.Filip, L.V.Giurgiu, M.Mehring, P.Castelaz, Al. Darabont
„ESR investigation of the exchange interactoin between Gd^{3+} and conduction electrons system in $Gd_{1-x}Y_xBa_2Cu_3O_{7-\delta}$ oriented powders"
Procc.XVIII-th Congress AMPERE, Canterbury, England, 1996
6. S.Simon, Gh.Borodi, T.Farcas
"Oriented crystalline layers on the surface of bismuth superconducting glass ceramics"
IUCr. XVII Congr. and Gen. Assembly, Seattle, USA, 1996

1998

1. L.David, O.Cozar, E.Forizs, D.Ristoiu, I.Bratu, C.Craciun
„Local structure analysis of some Cu(II) theophiline complexes"
Ext. Abstr.of 29th AMPERE-13th ISMAR Int. Conference, Berlin, 1998

2. O.Cozar, L.David, E.Forizs, V.Chis, R.Teteanu, M.Todica„ESR studies of some Cu(II)-oxazepam complexes"
Ext.Abstr. at the 29th AMPERE-13th ISMAR Int. Conference, Berlin, 1998,
3. O.Cozar, I.Ardelean, V.Simion, L.David, N.Vedean, V.Mih
„EPR studies of Cu^{2+} and V^{4+} ions in leed-phosphate glasses"
Ext. Abstr. at the 29th AMPERE-13th ISMAR Int. Conference, Berlin, 1998
4. O.Cozar, I.Ardelean, V.Simion, L.David, V.Mih, N.Vedean
„The local structure and interactions between V^{4+} ions in soda-phosphate glasses. An EPR study."
Ext.Abstr. at the 29th AMPERE- 13th ISMAR Int. Conference, Berlin, 1998, vol.II
5. O.Cozar, L.David, G.Damian, C.Balan, R.Roca, M. Armenean
„EPR Study of the complexes of Cr(III) an Cu(II) with some nucleotides"
17-th Turkish Physics Conference, Alanya, 1998 Abstr. of Conf.
6. L. Daraban, Lavinia Cociu, V. Znamirovschi, C. Cosma, G. Borodi, T. Fiat, La. Daraban
„The study of some physical control methods of precious and semiprecious stones"
31st International Symposium on Archaeometry, Budapest, Hungary, 1998
7. C.Kessler, C.Filip, L.V.Giurgiu, M.Mehring, Al.Darabont, R.Ordean
„The exchange coupling between RE-4f electrons and the carriers in HTSC as revealed by ESR"
Procc.ISMAR-AMPERE Conference, Berlin, Germany, 1998
8. M.Peteanu, O.Cozar, I.Ardelean, V.Simion, F.Ciorcas, S.Lupsor
„Structural and magnetic priperties of $CuO\text{-}TeO_2\text{-}B_2O_3\text{-}SrO$ glasses"
Abs.of 7-th European magnetic materials and application Conference, Zaragoza, Spain, 1998
9. M.Peteanu, I.Ardelean, V.Simion, F.Ciorcas, S.Filip, I.Tudor
„EPR studies of $Fe_2O_3\text{-}Bi_2O_3\text{-}GeO_2$ glasses"
Abs.of 7-th European magnetic materials and application Conference, Zaragoza, Spain, 1998

1999

1. Lavinia Cociu, C. Cosma
„Electron Paramagnetic Resonance Spectroscopy as a tool to study radiation damage in Glasses"
Book of Abstracts, Colloquium Spectroscopicum Internationale XXXI, 1999, Ankara, Turkey
2. Lavinia Cociu, M. Peteanu
„EPR and optical Study of the Nature of Chromium Complexes in Glasses"
Book of Abstracts, Colloquium Spectroscopicum Internationale XXXI, 1999, Ankara, Turkey
3. L.V.Giurgiu
„Spin relaxation investigated by EPR in the molecular conductor $Rb_2Pt(CN)_4(FHF)_{0,4}$"
12-th Specialized Colloque AMPERE Pisa, Italy, 1999
4. S.Simon, A.P.M.Kentgens, D.Iuga, M.Pop, E. de Boer
"Porous lanthanum alumino-borates investigated by magnetic resonance"
Annual Meeting of the Am. Ceram. Society, Indianapolis, USA, 1999

5. S.Simon, A.P.M.Kentgens, D.Iuga, M.Pop, E. de Boer
"Surface species on porous aluminates"
Int. Conf. on Spectroscopy of Transition Metal Ions on Surfaces and Defects Sites in Solids, Nieuwport, Belgia, 1999

2000

1. E. de Boer, A.P.M.Kentgens, S.Simon
''Magnetic resonance on lanthanum-borates and aluminum-borates"
Procc.of BSAT-II, Cairo 2000
2. L.V.Giurgiu
„Multi-frequency ESR study of the quasi-one-dimensional conductor $Rb_2Pt(CN)_4(FHF)_{0,4}$"
30-th AMPERECongress, Lisbon, Portugal, 2000

2001

1. I. Ardelean, V Simon, O.Cozar, Gh. Ilonca, C. Craciun, S. Filip, C. Cefan
''EPR and magnetic interaction of V^{4+} ions in strontium borate oxide glasses"
Procc.XIX Int. Congress on Glasses, Extended Abstracts, Edinburgh, Scotland, 2001, vol. 2
2. S.Simon
„Local order investigation on paramagnetic doped bismuth-borate glasses"
Procc.XIX Int. Congress on Glasses, 2001, Edinburgh, Scotland, vol. 2
3. L.V.Giurgiu
„A guided tour through magnetic exchange interaction in Gd-doped YbaCuO superconductors"
19-th RAMIS Conference, Poznan, Poland, 2001

2002

I.Ardelean, O.Cozar, L.David, I.Barbur
"The distribution mode of V^{4+} ions in B_2O_3-SrO glasses"
Procc. of the XXXI Congr. AMPERE, Poznan, 2002

Appendix 4

Ph. D. Thesis based on results obtained in EPR Laboratory

1. Sergiu V. Nistor – "Studiul imperfectiunilor locale in cristale ionice prin rezonanta electronica de spin", *Conducator stiintific: Acad. Prof. Dr. I. Ursu,1969*

2. Gheorghe Cristea – "Studiul fenomenului de "bottleneck" in relaxarea spin-retea a ionilor Nd3+ si Ge3+ in LMN la temperaturi joase", *Conducator stiintific: Acad. Prof. Dr. I. Ursu, 1971*

3. Ioan Barbur – "Studiul prin rezonanta electronica de spin a defectelor paramagnetice induse prin iradiere in compusi cu azot si sulf", *Conducator stiintific: Acad. Prof. Dr. I. Ursu, 1972*

4. Sorin Farcas – "Defecte paramagnetice prodese prin iradiere si impurificare cu cationi in cristale ionice", *Conducator stiintific: Prof. Al. Nicula,1976*

5. Onuc Cozar – "Structura moleculara si dinamica de absorbtie a unor complecsi de Cu(II) determinate prin RES", *Conducator stiintific: Prof. Dr. Doc. V. Mercea, 1979*

6. Ioan Ardelean – "Studiul unor proprietati magnetice, electrice si radiospectroscopice ale sticlelor semiconductoare din sistemul $Fe_2O_3.B_2O_3.PbO$*", Conducator stiintific: Prof. Dr. Doc. I. Pop,1979*

7. Mihai Alexandru Peteanu – "Transformari de faza in sisteme vitoase dopate cu fier si mangan*", Conducator stiintific: Prof. Dr. Al. Nicula,1984*

8. Dorina Strugaru – "Studii structurale si spectroscopice asupra zeolitilor sintetici impurificati cu nichel", *Conducator stiintific: Acad. Prof. Dr. I. Ursu,1984*

9. Simion Simon – "Rezonanta magnetica pe materiale oxidice vitroase si partial cristalizate ce contin elemente din grupa 3d si pamanturi rare", *Coducator stiintific: Prof. Dr. Al. Nicula,1986*

10. Alexandru Darabont – "Cresterea monocristalelor si studiul proprietatilor fizice ale acestora", *Conducator stiintific: Prof. Dr. Al. Nicula, 1987*

11. Aurel V. Pop – "Studiul proprietatilor magnetice si electrice ale compusilor oxidici supraconductori cu T_c inalte", *Conducator stiintific: Prof. Dr. Al. Nicula, I.Cosma, 1992*

12. Leontin David – "Corelari magnetostructurale in compusi moleculari", *Conducator stiintific: Prof. Dr. O. Cozar ,1995*

13. Grigore Damian – "Studii de structura si dinamica moleculara a unor compusi absorbiti pe materiale poroase", *Conducator stiintific: Prof. Dr. O. Cozar, 1997*

14. Vasile Chis – "Studii de structura si dinamica asupra unor radicali liberi si molecule de interes biologic", *Conducator stiintific: Prof. Dr. O. Cozar,1998*

15. Liviu Giurgiu – "Rezonanta electronica de spin a ionilor paramagnetici 4f si 5d"*, Conducator stiintific: Acad. Prof. Dr. I. Ursu, 2001*

16. Simona Cavalu – "Studii de spectroscopie RES si Raman ale unor proteine hemice si nehemice", *Conducator stiintific: Prof. Dr. S. Simon, 2001*

17. Aurel Pasca – "Studiul efectelor fototermice in faza condensata", *Conducator stiintific: Prof. Dr. S. Simon, 2001*

18. Cora Craciun – "Investigatii prin metode spectroscopice si magnetice ale unor polioxometalati cu ioni tranzitionali si actinide", *Conducator stiintific: Prof. Dr. O. Cozar, 2002*

STUDIA UNIVERSITATIS BABEŞ-BOLYAI, PHYSICA, XLVIII, SPECIAL ISSUE, 2003

EPR OF Cr^{3+} IONS IN SOME BORATE VITREOUS SYSTEMS

M. PETEANU, N. MURESAN, RALUCA CICEO-LUCACEL and I. ARDELEAN

Faculty of Physics, Babes-Bolyai University, 3400 Cluj-Napoca

ABSTRACT. Several peculiar aspects of the microstructural details of the vitreous matrix in the impurity ions neighbourhood, their distribution on structural units and valence states, and also the type and strength of interactions involving them, were revealed by means of EPR in series of borate glasses containing chromium ions, as being strongly dependent on the matrix composition and the doping level of the sample.

Introduction

The local order in diamagnetic vitreous matrices may be revealed by the 3d paramagnetic ions used as probes in EPR experiments. It is well known that electron paramagnetic resonance (EPR) supply valuable information about the local site symmetry, the fine structure parameters of the EPR absorption spectra being very sensitive to local structure. Chromium ions have often been used to investigate vitreous materials structure by means of EPR. Data have been reported for a great variety of glasses where Cr^{3+} species were detected as isolated in strongly distorted octahedral symmetric sites subjected to strong ligand field effects, or associated in exchange coupled pairs, depending on the Cr_2O_3 content of the glass. Cr^{5+} species have also been detected in some oxide vitreous materials.

There is a great variety of vitreous systems for which Cr^{3+} EPR spectra were reported. In phosphate glasses of complex composition Zacharov et al. [1] detected Cr^{3+} ion EPR resonances with anisotropic g factors having the values $g_{\perp} = 1.78$ and $g_{||} = 5.0$. The EPR spectrum and the optical absorptions of Cr^{3+} ions were studied as a function of Cr_2O_3 content in another phosphate system by Landry et al. [2]. They evidenced that the EPR spectrum gradually changes with increasing Cr_2O_3 concentration from an initial low-field absorption assigned to isolated, octahedrally coordinated Cr^{3+} ions, to one at high field with a $g \approx 2.0$ attributed to exchange coupled pairs of Cr^{3+} ions, which are individually six-fold coordinated. The antiferromagnetic nature of the coupling was elucidated by Fournier et al. [3].

In sodium borate glasses studied by Loveridge et al. [4] only a $g \approx 2.0$ resonance was observed, the shape of which is dependent on the alkali content. The absence of higher g resonances was interpreted as proving a zero field-splitting of the observed chromium center considerably smaller in borate than in phosphate glasses [5].

In chalcogenide glasses chromium impurity atoms may exist in various valence states according to the EPR and magnetic susceptibility data reported by Chepeleva et al. [6]. Besides being incorporated into the glass network Cr^{3+} ions may exist in microcrystalline inclusions, where phase transitions of the Cr^{3+} spin system may occur. Absorptions at $g = 1.98$ were detected for the Cr^{5+} ionic species, being

characterized by anisotropic, asymmetric and very narrow signals [6]. The $g \approx 1.98$ absorptions caused by Cr^{5+} ions were also detected in soda-lime-silicate glass fibres [7] and other oxide glasses containing chromium ions [8-10].

Cr^{3+} ions were used as local probes in fluoride glasses [11-14] because they adopt octahedral coordination in a fluoride medium, and the network is built up from corner-shared octahedra. Dance et al. [12] studied the EPR spectrum of Cr^{3+} ions in a fluoro-aluminate glass and considered the large absorption centered at g = 1.98 as caused by exchange within the pair of Cr^{3+} ions. The X-band Cr^{3+} EPR spectrum exhibits two broad resonances at g = 5.0 and g =1.97 as reported for chromium fluoride glasses studied by Legein et al. [14]. The g = 5.0 resonance was attributed to isolated Cr^{3+} ions in strongly distorted sites characterized by $\Delta > h\nu$ values, Δ being the zero field splitting between the two Kramer doublets. The g = 1.97 resonance attributed to isolated Cr^{3+} ions, was related to weakly distorted sites characterized by $\Delta < h\nu$. The resonance at g = 2.0 generally observed in fluoride glasses was assigned to Cr^{3+} ions pairs [2, 11, 12, 15]. From the frequency dependence of the spectra studied in [14] it was proved that Cr^{3+} ions are characterized by a continuous fine structure parameter distribution in the range 0.06-0.55 cm^{-1}, which was taken into account for simulations of these spectra according to Czjzek's model [16].

Cr^{3+} ion alkali-zinc-borosulfate glasses were investigated by Rao et al. [15]. The EPR spectra exhibit an intense resonance line centered at g = 1.99 and two less intense resonance lines at g = 4.93 to 4.97 and g = 5.26. The low-field spectra resonance lines were attributed to isolated Cr^{3+} ions. From the EPR and optical data it was concluded an octahedral site symmetry around Cr^{3+} ions, and a predominantly covalent character of the bond. The chemical bonds character was also thoroughly studied by Fuxi et al. [11, 17, 18] and Duffy et al. [19] in dependence on matrix composition.

Our studies concerning oxide vitreous systems containing Cr_2O_3 are based on data obtained by performing various experimental techniques, namely EPR, magnetic susceptibility measurements, IR spectroscopy, and X-ray diffraction analysis. Matter of investigation were binary borate glasses: B_2O_3-PbO [20], B_2O_3-Li_2O [21]; ternary boro-tellurite ones: TeO_2-B2O3-PbO [22, 23], TeO_2-B_2O_3-SrF_2 [24]; and also special glasses, based on nonconventional network-formers, heavy metal oxides: Bi_2O_3-PbO [25], Bi_2O_3-GeO_2 [26]. The paper synthetises our most representative theoretical and experimental results, concerning chromium containing borate systems.

Experimental procedure

Details on samples preparation are given in papers [20-24]. Generally, glasses were prepared by using reagent grade purity starting materials mixed in suitable proportion to achieve the desired doping level. Melting was performed in sintered corundum crucibles, using an electric furnace. Quenching was realized in air, at room temperature, by pouring the melt on stainless steel plate. Samples structure was tested by X-ray analysis selecting the composition range for which the diffraction pattern is typical for vitreous compounds and do not reveal any crystalline phase.

The EPR measurements were realized at room temperature, in X frequency band (9.4 GHz) and 100 kHz field modulation, with a JEOL-type equipment.

Theoretical approach

Most of the above mentioned papers assign the low-field resonance absorptions of Cr^{3+} ($3d^3$; $^4F_{3/2}$) ions in glasses to isolated ions subjected to a strong orthorhombic crystal field arising from a slightly distorted octahedral environment. The $^4F_{3/2}$ state splitting in strong crystalline field of rhombic symmetry may be obtained by using the spin Hamiltonian

$$\mathcal{H} = g\beta HS + D\left[S_z^2 - \frac{1}{3}S(S+1)\right] + E(S_x^2 - S_y^2) \quad , \tag{1}$$

where β is the Bohr magneton, H the magnetic field, S the effective electron spin and the parameters D and E represent the axial and the rhombic distortion of the octahedron, respectively. Cr^{3+} ions have a d^3 (L = 3, S = 3/2) electron configuration (where L is orbital moment). Their interaction with the crystalline field is strong and is the principal term determining the energy levels. Since the spin-orbit interaction and the crystalline field distortion act on the singlet orbital, the Zeeman term will split the two Kramers doublets and the energy levels will depend on the magnetic field and consequently on D and E. Several transitions may occur between the doublet levels for each direction of the magnetic field. According to Wickman et al. [28] the spin Hamiltonian (equation 1 may be written as

$$\mathcal{H} = S_z^2 - \frac{1}{3}S(S+1) + \lambda(S_x^2 - S_y^2) + g\beta HS = \mathcal{H}_o + g\beta HS \tag{2}$$

introducing the parameter λ = E/D with distinct values within $0 \le \lambda \le 1/3$. Only positive values of λ are taken into account.

In zero magnetic field, the crystalline field term, after diagonalization, introduces the ground state splitting into two Kramers doublets

$$\psi_i(\pm) = a_i\left|\pm 3/2\right\rangle + b_i\left|\mp 1/2\right\rangle \ , \quad i = 1; 2 \tag{3}$$

corresponding to the energy levels (in units of D)

$$\varepsilon_i = (-1)^{i-1}\left[3\lambda^2 + 1\right]^{1/2} \ , \quad i = 1; 2 \ . \tag{4}$$

The coefficients a_i and b_i

$$a_i = \left(\frac{\varepsilon_i + 1}{2\varepsilon_i}\right)^{1/2} \quad , \quad b_i = \left(\frac{\varepsilon_i - 1}{2\varepsilon_i}\right)^{1/2} \tag{5}$$

are functions of the parameter λ according to equation 4.

The principal values of the effective g tensor result as

$$\begin{aligned} g_i(x) &= 4\left[3^{1/2}a_i b_i + b_i^2\right], \\ g_i(y) &= 4(-1)^{i-1}\left[3^{1/2}a_i b_i - b_i^2\right], \\ g_i(z) &= 4(-1)^{i-1}\left[3a_i^2 - b_i^2\right] \end{aligned} \tag{6}$$

and according to (4) and (5) one obtains the g_{eff} values dependence on the relative crystalline field parameter λ for the two doublets:

$$g_1(x) = 2\left[\frac{3\lambda - 1}{\sqrt{3\lambda^2 + 1}} + 1\right] \quad , \quad g_2(x) = 2\left[-\frac{3\lambda - 1}{\sqrt{3\lambda^2 + 1}} + 1\right],$$

$$g_1(y) = 2\left[\frac{3\lambda + 1}{\sqrt{3\lambda^2 + 1}} - 1\right] \quad , \quad g_2(y) = 2\left[\frac{3\lambda + 1}{\sqrt{3\lambda^2 + 1}} + 1\right], \qquad (7)$$

$$g_1(z) = 2\left[\frac{2}{\sqrt{3\lambda^2 + 1}} + 1\right] \quad , \quad g_2(z) = 2\left[\frac{2}{\sqrt{3\lambda^2 + 1}} - 1\right].$$

According to equation (7) one may represent the g_{eff} variation as a function of λ, for the two doublets, and obtain diagrams which allow to determine the values of λ characterizing the Cr^{3+} ions vicinity for any value of experimentally detected g (Fig. 1). For $\lambda = 0$ corresponding to a pure axial field, one obtains $g_1(x) = g_1(y) = 0$, $g_1(z) = 6$ (forbidden transitions), and $g_2(x) = g_2(y) = 4$, $g_2(z) = 2$ resulting in absorptions characterized by $g_{||} = 4$ and $g\perp = 2$ values. For $\lambda = 1/3$, corresponding to a pure rhombic field one obtains $g_1(x) = 2$, $g_1(y) = 1.46$, $g_1(z) = 5.46$ and $g_2(x) = 2$, $g_2(y) = 5.46$, $g_2(z) = 1.46$. Consequently for Cr^{3+} ions in rhombic vicinities the resonance absorptions occur at 5.46, 2 and 1.46 values of g_{eff}.

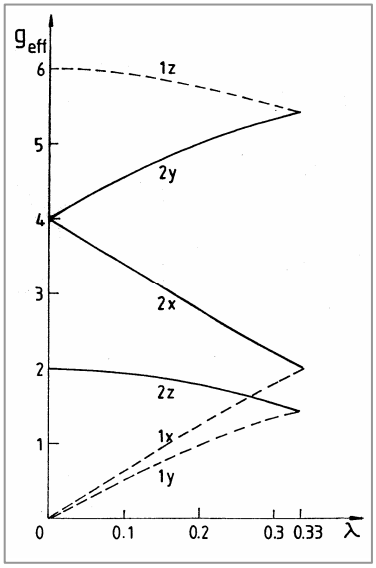

Fig. 1. The g_{eff} values dependence on the relative crystal field parameter $\lambda = E/D$.

Because of the crystalline field parameters distribution in glasses the absorption lines are generally broadened and often appear as a superposition of more contributions. In other materials, as silicalites [30] or aluminas [10], where the structural units are better defined, the absorption lines are sharper and therefore easier to be localized on both spectra and diagrams. Such diagrams were used by Trif et al. [29] to identify the sites involving Cr^{3+} in molecular sieves (zeolites).

Results and discussion

The vitreous systems $xCr_2O_3 \cdot (100\text{-}x)[3B_2O_3 \cdot PbO]$ was studied within $0 < x \leq 35$ mol %. The recorded EPR spectra strongly depend on the chromium content of the sample (Fig. 2). At low impurifying level ($x < 3$ mol %) the absorption is due to isolated Cr^{3+} ions in coordination with oxygen atoms, in sites of orthorhombic

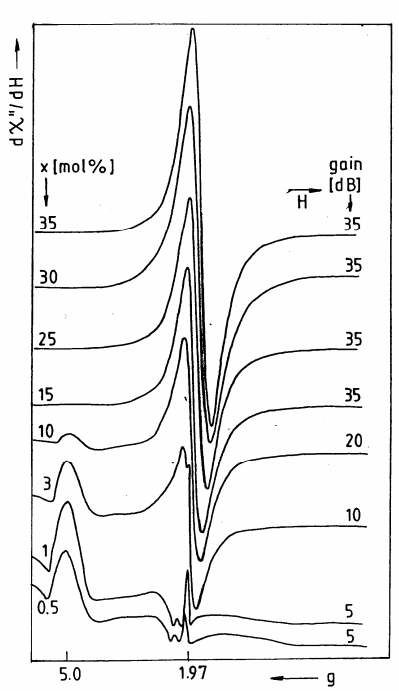

Fig. 2. nEPR absorption spectra of Cr^{3+} ions in glasses of the system $xCr_2O_3(100-x)[3B_2O_3{\cdot}PbO]$.

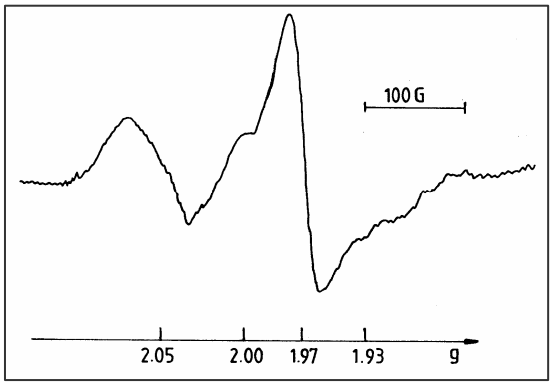

Fig. 3. The high-field signals detailed for the EPR spectrum of the $0.5Cr_2O_3{\cdot}99.5[3B_2O_3{\cdot}PbO]$ sample.

symmetry, giving rise to EPR signals with g_{eff} = 5.0 and 2.05 (Figs. 2 and 3). These values may be found on the $g_2(y)$ and $g_2(x)$ curves (Fig. 1) corresponding to the lowest doublet (2). Due to its peculiarities, especially the short ranged width ($\Delta H_{1.97} \cong 67.01$ G) the signal at g_{eff} = 1.97 was attributed to Cr^{5+} species in accord with reported data [2, 7-9]. The local order in the Cr^{3+} ions neighbourhood is affected by the progressive increasing of the Cr_2O_3 content of the matrix, fact evidenced by the decreasing of the intensity of signals corresponding to isolated Cr^{3+} ions in orthorhombic sites, up to their extinction, for x > 10 mol % when the lattice disorder is accomplished. In compensation, the broad signal at g_{eff} = 1.98 rises with increasing chromium concentration and overlaps the Cr^{5+} ions absorption line (g_{eff} = 1.97). Its parameters concentration dependence is given in Fig. 4. Up to x = 20 mol % the line-width increases linearly (Fig. 4 a) but its evolution does not satisfy the Kittel and Abrahams relation [31] based on dipolar interaction, being concordant with the Moon relation [32] developed in terms of magnetically coupled clusters of ions. Even for concentrations where the dipole-dipole interactions act as principal mechanism of line broadening, there are also super-exchange interactions involving the Cr^{3+} ions. For x > 20 mol % exchange interactions are prevalent and the signal narrows. A correct interpretation of the line-parameters evolution (Fig. 4) has to take into account the X-ray diffraction analysis results which evidenced, for x > 20 mol % microcrystalline precipitates of

Cr_2O_3 in the studied glasses [20]. The added oxide assimilation into the glass matrix becomes more difficult within the high concentration range. A decreased contribution of Cr^{3+} ions to the clustered formations, together to their even intenser magnetic coupling with narrowing effects on the EPR line, result in the increasing stop of the line intensity estimated as $I_{1.98} = I(\Delta H_{1.98})^2$ where I denotes the line-amplitude.

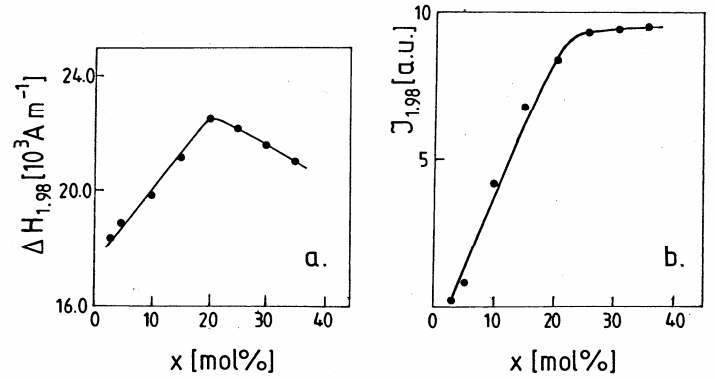

Fig. 4. Concentration dependence of the line-width (a) and intensity (b) corresponding to the $g_{eff} = 1.98$ absorption line in the Cr^{3+} ions spectrum for glasses of the $xCr_2O_3(100-x)[3B_2O_3{\cdot}PbO]$ system.

The system $xCr_2O_3{\cdot}(100-x)[2B_2O_3{\cdot}Li_2O]$ did not show any crystalline phase in the concentration range $0.5 \leq x \leq 20$ mol % according to X-ray diffraction and IR analysis [21]. The EPR absorption spectra show the same features like the previously presented system, even the narrow signal ($\Delta H_{1.97} = 45$ G) ascribed to Cr^{5+} ions (Fig. 5). The low-field signal, corresponding to Cr^{3+} ions in orthorhombic sites subjected to strong crystalline filed effects, decreases in intensity when the chromium content of the sample rises and also show a slight change of the g_{eff} value from 5.103 to 4.877 revealing a change in the site symmetry to a more axial configuration. At about x = 3 mol % the signal due to associated ions also appears, showing the dipolar broadening up to 10 mol % Cr_2O_3 balanced by the exchange narrowing for higher concentration.

The structural evolution of the two systems when increasing the Cr_2O_3 content within $0 \leq x \leq 20$ mol %, as revealed by the EPR details, is different. The low-field signal remains detectable in the spectrum of glasses with Li_2O within a broader concentration range than in the case of the PbO containing one (Figs. 2 and 5). On the other hand, the exchange narrowing takes place at about 10 mol % at the high field signal of Li_2O containing system and only for $x > 20$ mol % in glasses with PbO (Fig. 4 a). The matrix appears to be less structurally diversified when increasing the impurifying level in the Cr_2O_3-B_2O_3-Li_2O system case, the local ordering preserves within a broader composition range, the magnetic ordering takes place at a lower doping level and imposes as narrowing mechanism. In contrast to this, the Cr_2O_3-B_2O_3-PbO matrix appears more diversified structurally, the short range order in the Cr^{3+} ion vicinity is compromised at lower impurity concentration, the magnetic ordering takes place at higher doping level.

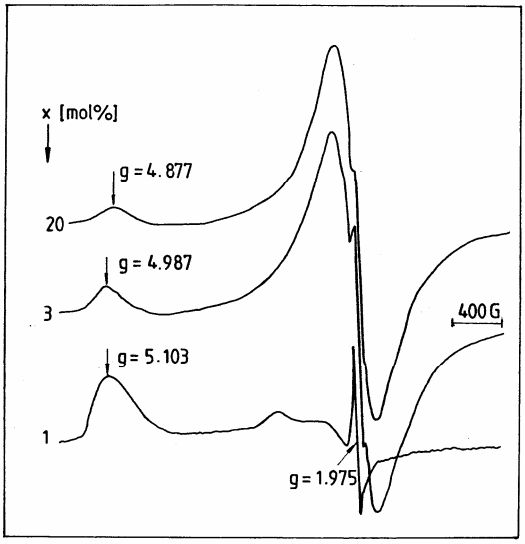

Fig. 5. EPR absorption spectra due to Cr^{3+} ions in glasses of the system $xCr_2O_3(100-x)[3B_2O_3{\cdot}Li_2O]$.

By passing to more complicated compositions, ternary boro-tellurite systems were studied, namely TeO_2-B_2O_3-PbO, TeO_2-B_2O_3-SrF_2 and TeO_2-B_2O_3-SrO impurified with Cr_2O_3 by means of a controlled doping process. None of the ternary boro-tellurite glasses contains Cr^{5+} ionic species but only Cr^{3+} ions, as revealed by means of EPR and magnetic susceptibility measurements [22-24]. The spectrum principally consist in absorptions at $g_{eff} \approx 4.8$ and $g_{eff} \approx 1.97$ corresponding to isolated Cr^{3+} ions in orthorhombic sites subjected to strong ligand field effects, respectively to those associated by means of magnetic (dipolar and/or exchange type) interactions. For all the investigated compositions the low-field signal remains unchanged as shape and intensity within the hole concentration range. According to its origin (distorted vicinities subjected to strong crystal-field effects) this signal proves the structural stability of the matrix in receiving Cr^{3+} ions in a wide concentration range. Because TeO_2 is a major component, the lattice is more compact and the strong crystal field configurations structurally favoured [33].

The system $xCr_2O_3{\cdot}(100-x)[70TeO_2{\cdot}25B_2O_3{\cdot}5PbO]$ was studied for $1 \leq x \leq 20$ mol %. The low-field signal (Fig. 6) shows a superposition of contributions: the line centered at $g \approx 4.8$ corresponding to isolated Cr^{3+} ions in strong crystal field of orthorhombic symmetry, and a broadener one approximated by the dotted line in Fig. 6, centered at $g_{eff} \approx 4.0$ and corresponding to preponderant axial vicinities. The signal is not sensitive to concentration. The $g_{eff} = 1.97$ one depends strongly on the impurifying level. The intensity $I_{1.97}$ increase within $1 \leq x \leq 20$ mol %. The line-width has a more nuanced evolution: up to x = 3 mol % the signal broadens dipolarly and may be associated to isolated Cr^{3+} ions in less distorted octahedral sites; within $3 \leq x \leq 10$ mol % the even intenser magnetic coupling of ions acts as narrowing mechanism of the line; due to structural changes and increased disorder the exchange interactions become weaker for x > 10 mol % and the line broadens again (Fig. 7).

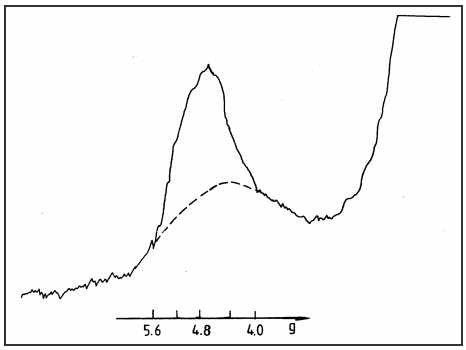

Fig. 6. Low-field absorption signal corresponding to the sample $1Cr_2O_3 \cdot 99[70TeO_2 \cdot 25B_2O_3 \cdot 5PbO]$.

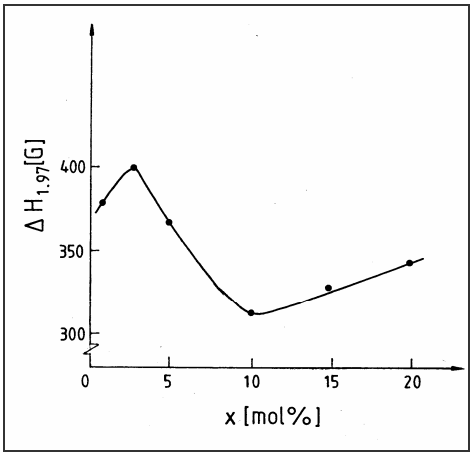

Fig. 7. Concentration dependence of the line-width of the $g_{eff} = 1.97$ signal in the EPR spectrum of $xCr_2O_3 \cdot (100\text{-}x)[70TeO_2 \cdot 25B_2O_3 \cdot 5PbO]$ glasses.

The system $xCr_2O_3 \cdot (100\text{-}x)[70TeO_2 \cdot 25B_2O_3\ 5SrF_2]$ was studied for $0 \leq x \leq 20$ mol %. For $x < 1$ mol % the spectrum presents both low-field ($g_{eff} = 4.8$ and 4.0) and high field ($g_{eff} = 2.05$; $\Delta H_{2.05} \cong 440$ G) signals showing the g tensor anisotropy, associated to isolated Cr^{3+} ions in sites of orthorhombic symmetry subjected to strong ligand field effects. For $x > 1$ mol % the signal due to associated ions at $g_{eff} = 1.97$ partially overlaps the $g_{eff} = 2.05$ one. This signal, associated to ions in weak crystal field neighbourhood shows a progressive increasing with concentration. The exchange narrowing imposes from the very beginning of the concentration dependence of the line-width (Fig. 8), and is stopped for $x > 10$ mol % due to structural disorder effects in the matrix.

Contrarily to the TeO_2-B_2O_3-PbO glass matrix, previously discussed, where the line narrowing accedes for $x > 3$ mol % at $g = 1.97$ lines, for TeO_2-B_2O_3-SrF_2 glasses this occur at lower impurity level ($x > 1$ mol %) and lines at $g_{eff} = 1.97$ are generally narrower. On the other hand the magnetic susceptibility measurements revealed for glasses with PbO [23] considerably higher values of the magnetic coupling than those corresponding to glasses with SrF_2 [42]. Surprises once again the contradiction of a stronger magnetic coupling but less efficient as narrowing mechanism in balancing the line broadening, in the case of the system with PbO comparatively to that containing SrF_2 (or Li_2O in the case of binary glasses previously presented). This particular behaviour is due to the special properties of PbO, its ambiguous network-former/network-modifier character, and especially its strong stabilizer properties. Consequently the vitreous matrix becomes more diversified structurally, and more vulnerable at increasing Cr_2O_3 amounts in its composition up to the total structural disorder. Besides the homogeneous line broadening due to dipol-dipol interactions, the inhomogeneous one due to larger crystal field parameters distribution also acts as more pronounced in PbO containing matrices.

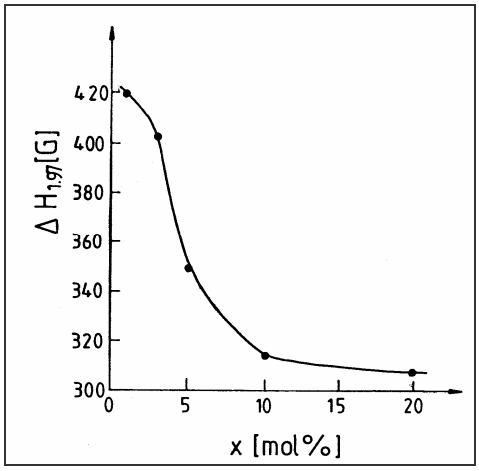

Fig. 8. Concentration dependence of the g_{eff} = 1.97 signal line-width for glasses of the system $xCr_2O_3 \cdot (100\text{-}x)[70TeO_2 \cdot 25B_2O_3 \cdot 5SrF_2]$.

When changing SF_2 to SrO as network-modifier in the boro-tellurite matrix the Cr^{3+} ions distribution is almost the same on different structural units, fact revealed by the concentration dependence of the EPR spectra structure. The response of the weak crystal field configurations is more sensitive to the Cr_2O_3 increasing amount. The exchange narrowing of the line due to associated ions (g_{eff} = 1.97) occurs for x > 1 mol % but is more accentuated than in the case of SrF_2 containing glasses, within the whole concentration range. The magnetic coupling is stronger in SrO based glasses. In the boro-tellurite series of composition taken into account SrO appears to be less active as network-modifier as compared with SrF_2 or PbO, so the matrix is less structurally affected during the doping process, and magnetic order of chromium ions in weak crystal field configurations is supported by the Cr_2O_3 content increasing.

Conclusions

Several binary and ternary borate glasses containing chromium impurity ions were investigated by means of EPR.

The valence state of chromium ions entering the matrix as paramagnetic species, depends on the matrix composition. Both Cr^{3+} and Cr^{5+} valence states were detected in B_2O_3-PbO and B_2O_3-Li_2O matrices. Only Cr^{3+} ions were identified in the studied boro-tellurite systems.

The EPR spectrum of Cr^{3+} paramagnetic ions show absorption lines due to isolated ions in orthorhombic sites subjected to strong ligand field effects, having low-field and high-field components due to the g tensor anisotropy, and absorptions due to associated ions in weak crystal-field vicinities. The ions distribution on all these structural units and their reciprocal weight at different doping levels depend on the matrix composition. The low-field signals due to ions connected into the network in coordination with oxygen atoms gave us information about the structural stability of the vitreous matrix when increasing the impurity content. The high-field signal due to associated ions gave information on both the interactions involving impurity ions and the role of the network-modifier component in the structural evolution of the investigated material when increasing the Cr_2O_3 content of samples.

REFERENCES

V.K.Zakharov, D.M.Yudin, Sov. Phys. Solid State 7, 1267 (1965)

R.J.Landry, J.T.Fournier, C.G.Young, J. Chem. Phys. 46, 1235 (1967)

J.T.Fournier, R.J.Landry, R.H.Bartam, J. Chem. Phys. 55, 2522 (1971)

D.Loveridge, S.Parke, Phys. Chem. Glasses 12, 19 (1971)

J.Wong, C.A.Angell, "Glass Structure by Spectroscopy", Marcel Dekker Inc., New York 1967, p. 65

J.V.Chepeleva, E.R.Zhilinskaya, V.V.Lazukin, A.P.Cernov, Physica Status Solidi (b) 73, 65 (1976)

R.Brückner, N.Sammet, H.Stockhorst, J. Non-Cryst. Solids 40, 273 (1980)

J.Wong, C.A.Angell, Appl. Spectrosc. Revs. 4(2), 155 (1971)

N.S.Garifyanov, Sov. Phys. Solid State 4, 1975 (1963)

A.Simon, A. Van Der Pool, E.J.Reijerse, A.P.M.Ketgens, G.J.M.P. Van Morsel, E.De Boer, J. Chem. Soc. Faraday Trans. 91(10), 1519 (1995)

G.Fuxi, D.He, L.Huiming, J. Non-Cryst. Solids 52, 135 (1982)

J.M.Dance, J.J.Videau, J.Portier. J. Non-Cryst. Solids 86, 88 (1986)

E.H.Harris, Phys. Chem. Glasses 28, 196 (1987)

C.Legein, J.Y.Bouzare, J.Emery, C.Jacoboni. J. Phys. Cond. Matter. 7, 3853 (1995)

A.Shriniwasa Rao, J.Lakshmana Rao, J.S.V.Laksman, Solid State Commun. 85(6), 529 (1993)

G.Czjzek, J.Fink, F.Götz, H.Schmidt, C.M.D.Coey, J.P.Rebauillat, A.Lineard, Phys. Rev. B 23, 2513 (1981)

J.Fuxi, D.He, L.Huiming, J. Non-Cryst. Solids 52, 143 (1982)

J.Fuxi, L.Huiming, J. Non-Cryst. Solids 80, 20 (1986)

J.A.Duffy, M.D. Ingram, J. Am. Chem. Soc. 93, 6448 (1971)

I.Ardelean, Gh.Ilonca, M.Peteanu, D.Barbos, E.Indrea, J. Mater. Sci. 17, 1988 (1982)

O.Cozar, I.Ardelean, I.Bratu, Gh.Ilonca, S.Simon, Solid State Commun. 86, 569 (1993)

I.Ardelean, M.Peteanu, V.Simon, S.Filip, N.Muresan, Studia Univ. Babes-Bolyai, Physica XLI (2), 3 (1996)

M.Peteanu, V.Simon, N.Muresan, I.Ardelean, S.Filip, J.Mat. Sci. Technol. 13, 374 (1997)

I.Ardelean, M.Peteanu, V.Ioncu, N.Muresan, Mod. Phys. Lett. B 15 (22), 941 (2001)

I.Ardelean, O.Cozar, V.Simon, S.Filip, J. Magn. Magn. Mat. 157/158 165 (1996)

I.Ardelean, M.Peteanu, V.Simon, C.Bob, S.Filip, J. Mat. Sci. 33, 357 (1998)

I.Ardelean, M.Peteanu, S.Simon, S.Filip, V.Simon, C.Bob, N.Muresan, Rom. Rep. Phys. 51(5-6), 5005 (1999)

H.H.Wickman, M.P.Klein, D.A.Shirley, J. Chem. Phys. 42, 2113 (1965)

E.Trif, Al.Nicula, Studia Univ. Babes-Bolyai, Physica 2, 23 (1974)

J.S.T.Mambrin, H.O.Pastore, C.U.Davanzo, E.J.S.Vichi, O.Nakamura, H.Vargas, Chem. Matter. 5, 166 (1993)

C.Kittel, E.Abrahams, Phys. Rev. 90, 238 (1953)

D.W.Moon, J.M.Aitken, R.K.Crone, G.S.Cieloszky, Phys. Chem. Glasses 16, 91 (1975)

G.Sperlich, P.Urban, Phys. Status Solidi (b) 61, 475 (1974).

STUDIA UNIVERSITATIS BABEŞ-BOLYAI, PHYSICA, XLVIII, SPECIAL ISSUE, 2003

NITROXIDE SPIN LABELS IN EPR INVESTIGATIONS

G. DAMIAN

"Babeş-Bolyai" University, Department of Physics, RO-3400 Cluj-Napoca, Romania; e-mail: dgrig@phys.ubbcluj.ro

ABSTRACT. Synthesized forty years ago, spin labels (nitroxide radicals) represent chemically stable paramagnetic molecules used as the molecular probes for testing structural properties and molecular mobility of different physical, chemical and biological systems, by electron paramagnetic resonance (EPR). The physical basis for nearly all EPR applications is the anisotropy of the nitroxide signal and the sensitivity of the EPR spectra to various relaxation pathways. The interaction between an electron of a spin label and an external magnetic field depends on their relative orientations. The splitting and the center of EPR spectra of an oriented sample are used to determine the orientation of labeled domains. The width of the signal is proportional to the orientational disorder, which is used to measure conformational heterogeneity of environment. The applications of the nitroxide spin labels at interface processes are discussed in this rewievs.

Keywords: spin label, EPR, zeolites, proteins, pH

1. Introduction

There are a number of stable free radicals called spin labels (nitroxide radicals), chemically stable paramagnetic molecules which can be used as the molecular probes for testing structural properties and molecular mobility of different physical, chemical and biological systems. First synthesized forty years ago [1], nitroxides now play crucial roles in materials science [2, 4], chemistry [5] and life science [6]. These molecular species can be attached by covalent or noncovalent bonds to particular sites in molecular systems and produce EPR spectra, which provide information on changes in the chemical and physical characteristics in the neighborhood of the site. The characteristic structural feature of all nitroxide radicals is the NO group with the nitrogen attached to two alkyl substituents (that are part of a ring structure with six- member ring piperidine derivative or a five-member ring pyrroxamide derivative). The main spin density of the unpaired electron is located on the π* molecular orbital of the NO –bond. The powder pattern therefore also how a splitting due to the hyperfine tensor of the ^{14}N nucleus. Therefore, electron paramagnetic resonance (EPR) which uses the properties of magnetic dipole transitions in electron spin and electron-nuclear coupled spin systems and related phenomena and is a powerful tool for probing the electronic properties of both ordered and disordered solid state materials, chemical complexes and biological materials.

The main requirements of spin labels for testing structural properties and molecular mobility of different physical, chemical and biological systems, can be summarized as [7]:

- the sensitivity in environments to "report" changes in the system of interest
- the physical properties of labeled molecules must be either unique or distinct from the properties of the system under investigation
- the studied system must be remaining unchanged or to suffer little perturbations in its structure and function as result of the incorporation of the spin labels molecules.

Beside the their great applicability as the molecular probes (spin labels) for testing structural properties and molecular mobility of different systems due to their large stability, the ability of the nitroxide radicals to scavenge radicals finds uses ranging from the very applied, as U.V. stabilizers in plastics, to very theoretical, as probes for organic reaction mechanisms [8, 11] which attests to the scope of the utility of these unusual species.

2. Structural characteristics

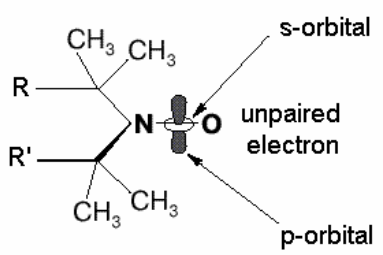

Fig.1. General structure of nitroxide spin labels

The spin labels, are nitroxide derivatives containing an unpaired electron in the 2pπ orbital of the N─O bond (Figure 1). The R and R' fragments forms five- or six-membered rings, obtaining differents labeled molecular paramagnetic species These species are remarkably stable due to the presence of four methyl groups on neighboring carbon atoms.

The electronic configuration of the paramagnetic center presents four main characteristics [12]: (i) the nitrogen and oxygen atoms are sp^2 hybridized and carbon atoms sp^3 (ii) the σ-skeleton include two σ (sp^2-sp^3) between nitrogen and carbon and only one bond σ (sp^2-sp^2) between nitrogen and oxygen, (iii) the oxygen atom has two sp^2 orbitals chemical inactives each of them occupied by two coupled electrons, localized in the plan of the N─O bond, (iv) the unhybridized $2p_z$ orbitals from nitrogen and oxygen participate to forms the π-bonded state and π*-antibonded state (Figure 2).

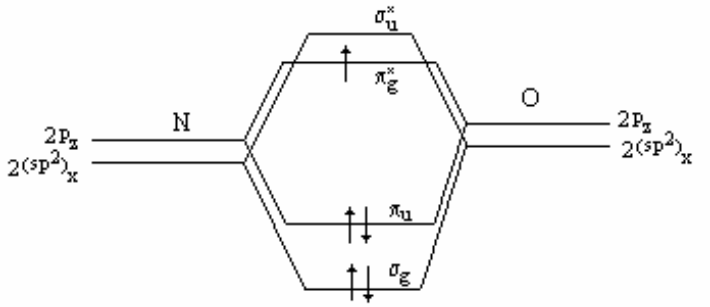

Fig.2. Energetical diagram of the N─O bond

3. Basic features of the EPR spectra

A free electron has a spin angular momentum S which, in a given direction (usually is the z direction), can only assume two values, $M_S = \frac{1}{2}$ and $M_S = -\frac{1}{2}$ in $\hbar = \frac{h}{2\pi}$ unit (where h is Planck's constant). An electron carries a magnetic moment μ_s which is collinear and antiparallel to the spin itself and given by the expression:

$$\mu_S = -g\,\mu_B S \tag{1}$$

with μ_B denoting the Bohr magneton (intrinsic unit of electron magnetic moment) and *g* denoting the spectroscopic splitting factor (relates contribution of spin and orbital motion of the electron to its total angular momentum).

The energy *(*E) of a magnetic dipole (μ) in a static magnetic field H, is given by equation:

$$E = -\mu \cdot H \tag{2}$$

Thus, the energy levels from Equations (3.1) and (3.2) are

$$E = \pm\frac{1}{2} g\,\mu_B H \tag{3}$$

resulting in an energy gap which increases linearly with the magnetic field (figure 3):

$$\Delta E = g\,\mu\,H \tag{4}$$

An oscillating magnetic field can flip the electrons from one energy level to the other if its own energy, defined by the oscillating frequency ν, equals the energy gap. Hence, for resonance between the oscillating field (microwave) and the electron spin, the condition in equation (5) has to be satisfied:

$$h\nu = g\,\mu\,H \tag{5}$$

The resonance condition can also be obtained by considering a spinning electron moving in an orbit around a nucleus placed in a magnetic field. From classical mechanics, the rate of change of the magnetic moment is proportional to the torque produced by the interaction of the moment and the magnetic field and given by their vector product:

$$\frac{d\mu}{dt} = \mu \times \gamma\,H \tag{6}$$

where γ is a magnetogyric ratio (ratio of magnetic and inertia moments) characteristic of a given electron:

$$\gamma = \frac{g\,\mu_B}{\hbar} \tag{7}$$

The torque will force the magnetic dipole (μ) to process around the static field at a defined frequency, the Larmor frequency, ω_L, given by:

$$\omega_L = \gamma H \tag{8}$$

Electrons orbiting around a nucleus experience a small local field produced by the nuclear magnetic moment. This field enhances or counteracts the external field depending on the orientation of the nuclear dipole. This interaction between the nucleus and the electron is known as hyperfine interaction. Similar to electron spin, nuclear spin (I) is also quantized to 2I+1 levels. Since the selection rule for spin transitions dictates that the total spin quantum number can only change by 1, the hyperfine interactions lead to 2I+1 transitions. In the case of nitroxide labels, it is the nitrogen nucleus which interacts with the unpaired electron. For N the nuclear spin number m_I is 1, so that three electron transitions are observed (Figure 3). The resonance condition of Equation (3.5) is thus modified to include hyperfine interactions, a:

$$h\nu = g\mu H + m_I a \qquad (9)$$

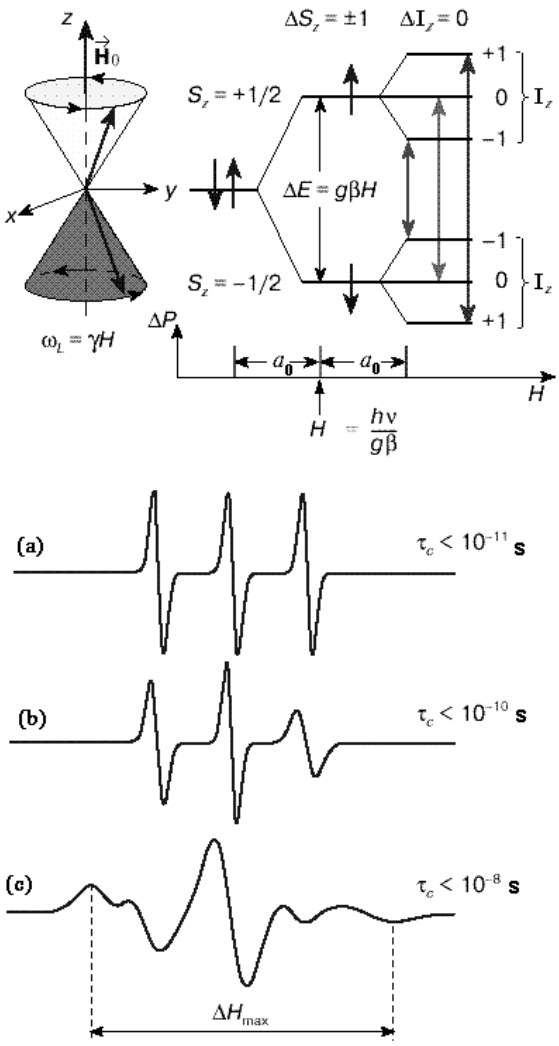

Fig.3. Zeeman and hyperfine interactions of unpaired electrons with nitrogen nuclear spin

The hyperfine interaction between an electron and the nucleus has both an isotropic and anisotropic (dipolar) component.

The magnitude of the isotropic splitting, a_0, is proportional to the electron spin density on the nucleus. Since the unpaired electron is located between the oxygen and nitrogen, increasing the polarity of the medium decreases the oxygen's attraction and increases the electron density on the nitrogen. Thus, a_0 is a sensitive measure of the spin environment. The pπ orbital of an unpaired electron is asymmetric, making the dipolar interactions of the electron and nucleus orientation dependent. Such, the asymmetry of the Zeeman and hyperfine interactions defines EPR sensitivity to orientation and to rotational motion (Figure 3 cases (a), (b) and (c)).

The extent of microwave absorption, which defines the intensity of the EPR signal, is proportional to the difference in spin populations, N, between the upper and lower energy states. The ratio of the two populations is determined by the Boltzmann distribution:

$$\frac{N_{+\frac{1}{2}}}{N_{-\frac{1}{2}}} = \exp(-\frac{\Delta E}{kT}) \tag{10}$$

This relation shown that the difference in spin populations is increased by either increasing the magnetic field H or reducing the temperature T. Such, the activation energy of the spin labels, can be calculated from represantion of the correlation times vs.1/T.

The difference between the levels decreases with absorption and an efficient relaxation pathway has to exist to restore the Boltzmann equilibrium. Relaxation pathways include the dipolar spin–spin relaxation – sharing of energy between electrons or nuclei – and spin–lattice relaxation – sharing vibrational modes with the lattice. They are characterized by relaxation times T_2 and T_1, respectively. Relaxation times are defined as the time interval between initial perturbation and when the deviation from equilibrium decays to 1/e of its initial value. The relaxation rates are additive and their sum defines the width (at half-height) of the resonance signal, Γ:

$$\Gamma = \frac{1}{\gamma}\left(\frac{1}{T_2} + \frac{1}{T_1}\right) \tag{11}$$

Faster relaxation (shorter T_1 or T_2) results in broader line widths. For paramagnetic ions, the strong coupling of spins to lattice (short T_1) produces broad lines. Lowering the temperature weakens lattice coupling (increases T_1) and is commonly used to observe resonance of transition metal ions. The coupling of free radicals (including spin labels) to the lattice is weak, therefore spin–spin relaxation is more efficient and the line width is determined by T_2 because the EPR signal shape, varies with concentration (Figure 4). It illustrates that the linewidths of the resonant transitions are not infinitely small and can be altered by the environment. At low concentrations, each line has a width because of the heterogeneous broadening, i.e. unresolved structure of the small hyperfine constants and the homogeneous broadening, Γ_0:

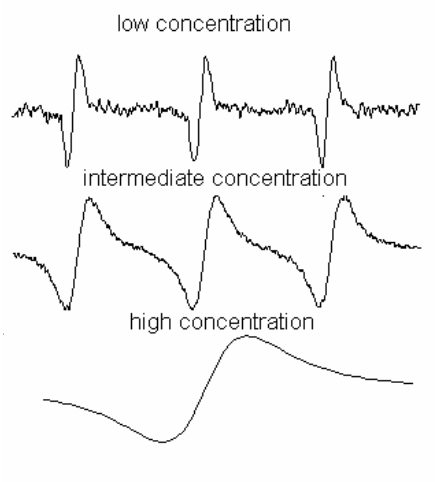

Fig.4. EPR signal shape, as function of the spin label concentration

$$\Gamma_0 = \frac{1}{\gamma} \cdot \frac{1}{T_2} \tag{12}$$

which is caused by a limited lifetime T_2 (spin-spin relaxation time) of a radical at a particular spin state. The full width half maximum, Γ, is $3^{1/2}/2 = 0.866$ times greater than the measured distance between maximum and minimum of the experimentally detective derivative of absorption. This lifetime can be affected by the dipole-dipole (and exchange) interaction with other

radicals. If another unpaired electron is at a distance *r*, the magnitude of its field at the spin can take any value between $\pm 2\frac{\mu_B}{r^3}$, depending on orientation. Due to the fast rotation of both radicals, the interaction averages this field to zero except for a very short period of time during collision after which the radical can end up at random configuration of its nuclear spins. Result of such randomization is equivalent to the jumping from one spectral position to another. For nitroxyl radical, such as TEMPO, with three equivalent spectral lines (S = 1), only 2/3 of such collisions result in a shift. Because of that, the width will increase only at 2/3 of the rate of collision. There exist three situations of the exchange spin-spin interactions:

- slow exchange-when the spin labels concentrations is low,

$$\Gamma = \Gamma_0 + \frac{2}{3} k \frac{C}{\gamma} \tag{13}$$

where k is the collision rate constant and C is radicals concentration

- intermediate exchange- With further increase of the concentration, the broadening will be accompanied by a measurable decrease in separation between the peaks, ΔB:

$$\left(a_N^2 - \Delta B^2\right)^{\frac{1}{2}} = \frac{2}{3} k \frac{C}{\gamma} \tag{14}$$

where a_N is the hyperfine constant on nitrogen (separation between lines)

- fast exchange-when the concentration is high, the overall width of now a single-line spectrum, starts decreasing:

$$\Gamma = \Gamma_0 + a_N^2 \cdot \frac{\gamma}{k \cdot C} \tag{15}$$

The lineshape of an EPR spectrum depends, among exchange interactions, on the orientation of the paramagnetic center with respect to the applied magnetic field (Figure 3). In a powder, or a frozen aqueous solution, the paramagnetic centers will be fixed with a random distribution of orientations, and in the case of anisotropic g- and hyperfine interactions this will lead to a broadened EPR spectrum, since all orientations contribute equally. In the liquid state, however, the paramagnetic centers are not fixed but undergo rotational fluctuation. In the case of fast rotation, the anisotropic interactions are thereby averaged to zero, giving rise to sharp EPR lines. If the velocity of the rotational motion decreases, the EPR spectrum will approach that of the powder spectrum. Therefore, a rotational correlation time for a paramagnetic molecule can also be determined by EPR using semiempirical formula [16].

For isotropic motion in the rapid tumbling limit, the spectra will be isotropic with the averages of the principal components of the g-values and hyperfine splitting factor, a^N. The rate of the isotropic motion determines the relative widths of resonances and the width, ΔH_m, of an individual (hyperfine) line, in the first approximation can be written as a function of the z component of the nitrogen nuclear spin number (m = -1, 0, 1) [14, 15]:

$$\Delta H_m = A + B \cdot m + C \cdot m^2 \tag{16}$$

where the A coefficient includes other contributions than motion. The terms B and C are functions related to the rotational correlational time (τ) and can be defined as a function of peak to peak line width of the central line, ΔH_0 [G], and the amplitudes of the m-th line I_m [13]:

$$B = \frac{1}{2}\Delta H_0\left(\sqrt{\frac{I_0}{I_1}} - \sqrt{\frac{I_0}{I_{-1}}}\right) = 0.103\,\omega_e[\Delta g \Delta a^N + 3(\delta g)(\delta a^N)]\tau_B[1 + \frac{3}{4}(1+\omega_e^2\tau_B^2)^{-1}] \quad (17)$$

$$C = \frac{1}{2}\Delta H_0\left(\sqrt{\frac{I_0}{I_1}} + \sqrt{\frac{I_0}{I_{-1}}} - 2\right) = 1.181\cdot 10^6[(\Delta a^N)^2 + 3(\delta a^N)^2]\tau_c[1 - \frac{3}{8}(1+\omega_c^2\tau_c^2)^{-1} - \frac{1}{8}(1+\omega_e^2\tau_c^2)^{-1}] \quad (18)$$

in which

$$\Delta a^N = a_{zz}^N - \frac{1}{2}(a_{xx}^N + a_{yy}^N), \delta a^N = \frac{1}{2}(a_{xx}^N - a_{yy}^N) \quad (19)$$

$$\Delta g = g_{zz} - \frac{1}{2}(g_{xx} - g_{yy}), \delta g = \frac{1}{2}(g_{xx} - g_{yy}) \quad (20)$$

and $\omega_N = 8.8\cdot 10^{-6} <a^N>$, a^N is the isotropic hyperfine splitting and ω_e the EPR spectrometer frequency in angular units.

In range from $5\cdot 10^{-11}$ to 10^{-9} s (motion in the rapid tumbling limit) and magnetic field above 3300 G, Δg and Δa^N vanish, and the correlation times τ_B and τ_C are directly related to the B and C coefficients by the following simple relations [16]:

$$\tau_B = \tau_z = K_1 \cdot B \quad (21)$$

$$\tau_C = \tau_{x,y} = K_2 \cdot C \quad (22)$$

where $K_1 = 1.27\cdot 10^{-9}$ and $K_2 = 1.19\cdot 10^{-9}$. The average correlation times is:

$$\tau = (\tau_B \cdot \tau_C)^{\frac{1}{2}} \quad (23)$$

The slow motion of spin probe, lead to a broadening of the EPR lines. In this case, the rotational correlation time, τ, is larger than 10^{-9} s, and thus, the relation (8) is not applicable.

The isotropic nitrogen hyperfine splitting changes to a powder like spectrum, with the peak-to-peak distance between the external peaks of the spectrum ($2 \cdot a'_{zz}(N)$) depending on the magnitude of the rotational correlation time, τ. Another lineshape theory for slow isotropic Brownian rotational diffusion of spin-labeled proteins has been developed by J. Freed [17]. Thus, the correlation time can be evaluated from the ratio of the observed splitting between the derivative extrema a'_{zz} and principal value a_{zz}, determinated from rigid matrix spectrum [16,18]:

$$\tau = \alpha\left(1 - \frac{a'_{zz}}{a_{zz}}\right)^{\beta} \quad (24)$$

The α and β parameters depend on the kind of the diffusion process. where a and b are empirical constants, which are tabulated in e.g. Poole and Farach, 1987 [16]. For small spin probe, the intermediate jump diffusion is preferable [16].

4. Applications of Spin Labels in EPR Study at Interfaces

The main application of the nitroxide spin label in the EPR investigation, is molecular study at liquid-solid interfaces, which give valuable informations on the structure and dynamics of molecular interactions occurring in colloid systems. Two aspects can be taken in consideration: (i) liquid-inorganic surface support and (ii) liquid-organic surface support (biological systems).

4.1. Porous surfaces

The adsorption of spin labels on inorganic support was studied using nitroxide radicals and hydrophilic (NaY zeolites and SiO_2-Merck), hydrophobic (HY zeolies and SiO_2-Arcc) and neutral (Al_2O_3 neutral) porous materials [19]. The behaviors of spin labels are depending on the nature and hydroaffinity of surfaces, solvent nature and degree of hydration giving rise specific line shape of the EPR signal.

For hydrophilic surfaces (Figure 5), the mobility of molecules decrease monotonicaly with decreasing of number of water molecules (Figure 6).

In case of hydrophobic surfaces (Figure 7), due to the hydrophobic forces, the molecular mobility are strongly depended on the first layer of water molecules on the surface. Thus, the molecular mobility (Figure 8) is suddenly changed when only one water layer is remains. [20]. Also, in the first layer of the hydrophobic surfaces the concentration of the paramagnetic centers increase and as result, spin-spin interactions are involved in dynamically processes [21]. The motion of the nitroxide radicals on porous surfaces is determinated by the existence of the strength of acidic sites, too. This effect was evidentiated using organic solutions with nitroxidic radicals and adsorbed on the inorganic supports with different strength and concentrations of the acidic sites [22, 25]. The spin label molecules forms adsorption complexes with the Lewis acidity possessing zeolite cations and thereby the spin density distribution at the nitroxide group of the molecule changes. This was directly detected by electron spin resonance spectroscopy via the nitrogen hyperfine coupling constants of the probe molecule. It was found a linear dependence of the nitrogen spin density at the π-orbital of the nitroxide group on the electronegativity of the zeolite cations [26].

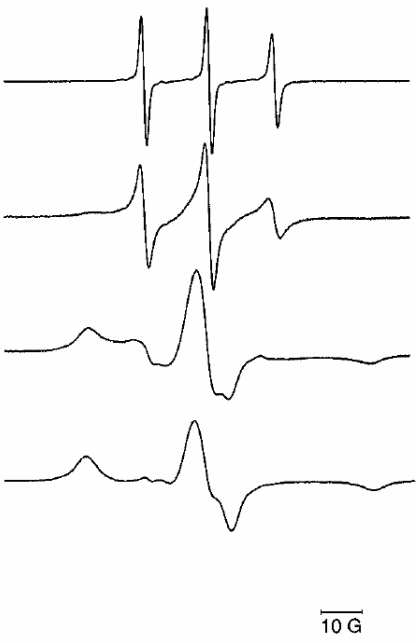

Fig. 5. EPR spectra of adsorbed Tempo-spin label on hydrophilic SiO_2 at different degree of dehydrations

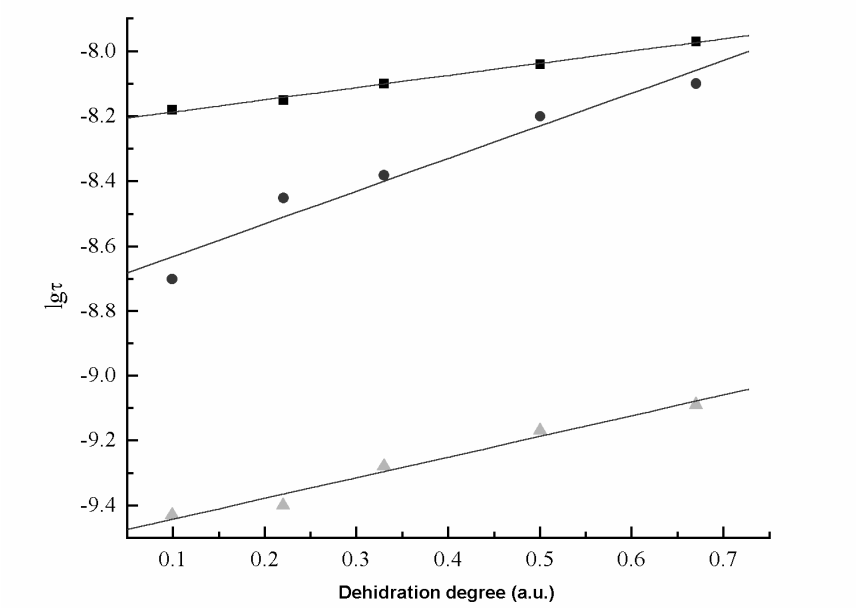

Fig. 6. Correlation times vs dehydration degree of some spin labels on hydrophilic surfaces (Tempyo-■, Acetamide-Tempo-●, oxo-Tempo-▲)

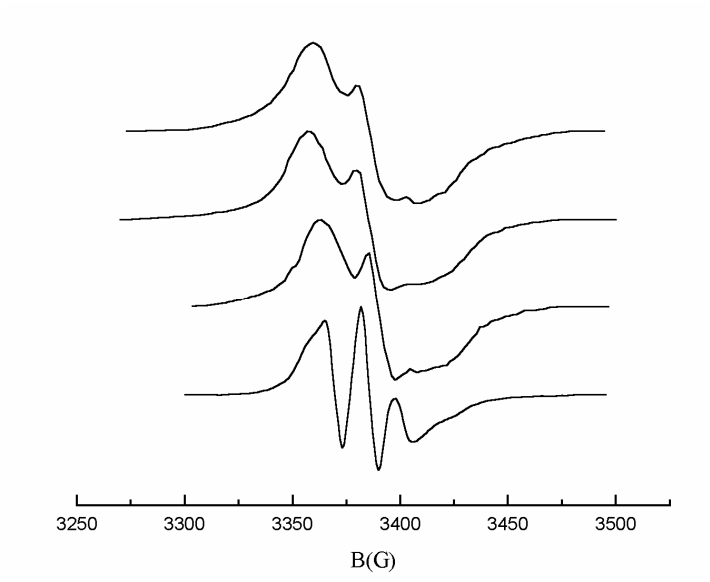

Fig. 7. EPR spectra of adsorbed Tempo-spin label on hydrophobic SiO_2 at different degree of dehydrations

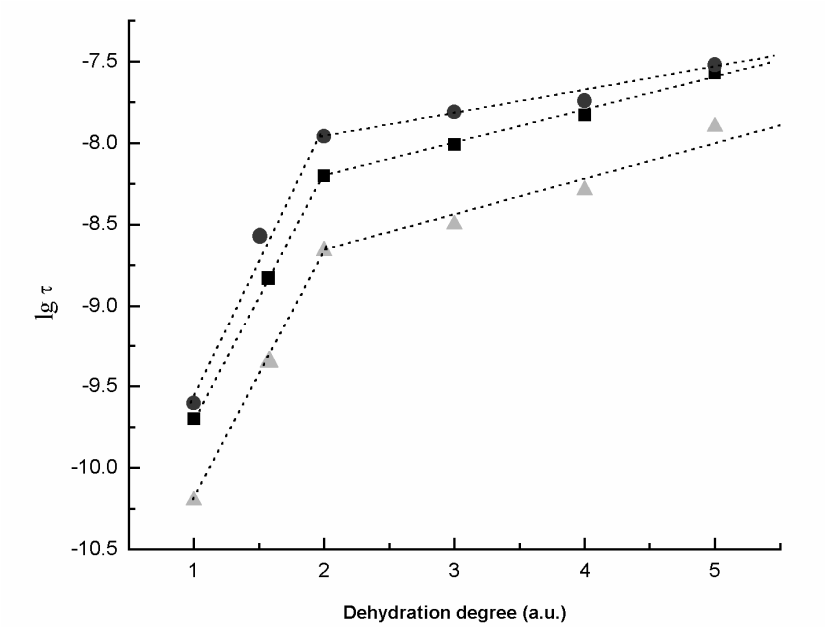

Fig. 8. Correlation times vs dehydration degree of some spin labels on hydrophobic surfaces (Tempyo-■, Acetamide-Tempo-●, oxo-Tempo-▲)

4.2. Biological systems

The use of EPR to study biological systems has been greatly facilitated by the spin labeling technique, in which a stable nitroxide free radical (spin label) is introduced as a molecular probe that conveys information about the structure and motional dynamics at its site of attachment. Nitroxide spin labels are useful in solving biochemical problems, because they are small probes that may not perturb the conformation of the target macromolecule, and because molecular biological approaches readily introduce nitroxides at points of interest in proteins. The EPR of nitroxide spin labeled biological molecules have been extensively used in the last decades for the study of their interactions, mobility and microenvironment in biological systems. Use of EPR for investigating biomolecules could also be ascribed to: (1) the influence of the local environment and dynamics of the spin-labeled site on the EPR spectral lineshape; (2) the ease of site-directed spin labeling (SDSL); (3) the absence of size constraints (which is a major limitation in NMR-based approaches to study macromolecular structure); (4) the low molecular volume of the spin [27]. The study of molecular processes at liquid-organic surface supports was made using nitroxide radicals and new nicotinic acid derivatives spin label, as molecular probes, and organic polymers[28] (i.e. human blood plasma, bovine serum albumin and multilamelar liposomes) [29, 30]. When the rate of probe migration is slow on the EPR time scale (~$5 \cdot 10^6$ s^{-1}) and the concentration of probe in the two media is sufficiently high, two distinct subspectra contribute to the observed spectrum. If the

rates of probe rotation in the two media are quite different, it is possible to obtain spectra in which resonances due to the probe in two environments are distinguishable (Figure 9). For instance, the EPR spectra of nitroxide spin label in BSA molecules, consist of two spectral parts; the major part marked with arrows, (Figure 9-subspectrum I) has a line shape resembling the powder spectrum of the rigid matrix (strong lyophilized sample) and is typical for slow isotropic rotational motion, and the minor part of the spin label spectrum (marked with an asterisk) is typical for faster isotropic rotational fluctuations (Figure 9-subspectrum II) [31]. The minor parts (marked with an asterisk) have a rotational correlation time of $\tau_f = 4.5 \cdot 10^{-9}$ s, which must be regarded as fast rotation and indicate that these spin label are located in flexible protein chains, probably at the surface of the protein. The major parts of the spectra have correlation times of $1.4 \cdot 10^{-8}$ s typical for slow rotation and show that The spin labels are located in non-flexible, e.g. folded, parts of the protein.

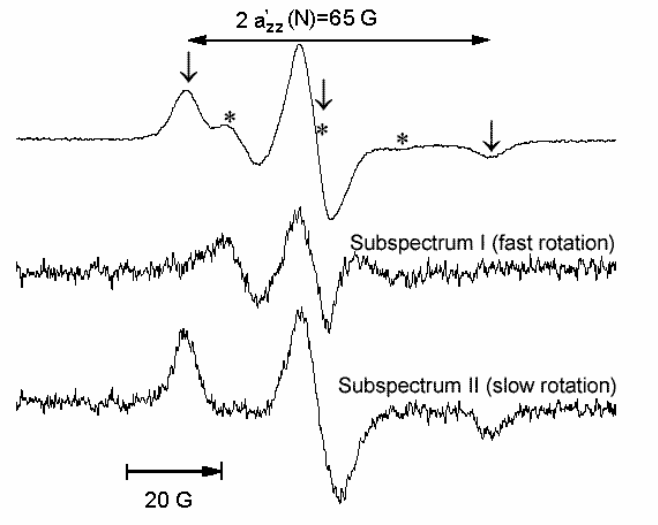

Fig. 9. Integral and partially EPR spectrum of Tempyo spin label at high concentration BSA

Quantitation of the relative intensities of the two components, by using either spectral subtraction or spectral simulation via the exchange-coupled two-component Bloch equations, yields information on the stoichiometry and specificity of the lipid-protein interaction. Quantification by integration of the spectrum yielded ~20 % of the spin label with fast motion and ~80 % with slow motion. By subtracting the minor part, Figure 9-subspectrul I, from the original spectrum, Figure 9-upper spectrum, only the major part remains (Figure 9-subspectrum II). This spectrum implies an almost rigid attachment of the spin label to the globular protein. The same behaviors, vas observed for haemoglobin at different pH [32]. In Figure 10 are plotted the average of the correlation time for differents values of the pH. As shown in figure, the pH influences the rotational correlation time. In acid pH range, the NH_2 groups of the label molecule as well as those of the aminoacids residues are protonated. The

fact that τ shows greater values in this range followed by a significant decrease in the basic pH range, indicate a low mobility of spin label in acid environment while an increasing of mobility can be noticed in basic pH range. A minimum mobility can be observed around the isoelectric point of both proteins (for BSA pH_i = 4.8, and for BH, pH_i=6.8). From the pH dependence of correlation time (involving the mobility of the label as well), we assume that in acid environment, the mobility of spin label molecules are reduced due to formation of the hydrogen bonds between NH_2 group of spin label and side chains of neighboring amino acids. One can correlate this observation with the fact that serum albumin undergoes reversible isomerization in the pH range 2.7-7 from expanded form characterized by 35% α-helix content, to normal form characterised by 55% α-helix content accompanied by a decrease in β-sheet. It is well known that β-sheet conformation favours the formation of hydrogen bonding.

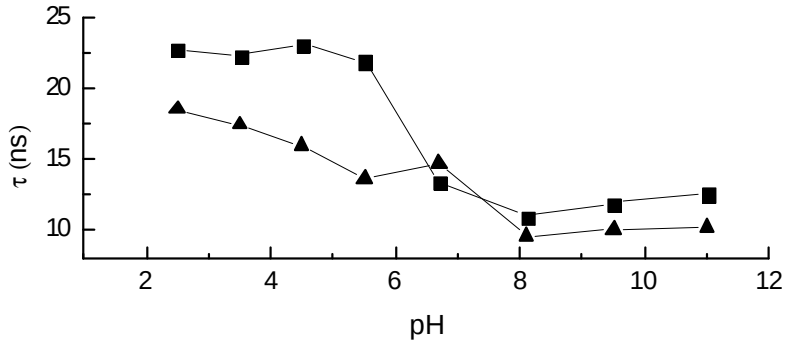

Fig. 10. Correlation times (τ) as a function of pH for Tempyo spin label in lyophilized bovine serum albumin (■) and bovine haemoglobin (▲).

The property of losing EPR signal of nitroxide spin labels as a result of exposure to reducing agents, can be exploited because the kinetics of the nitroxides disappearance provides useful biochemical and biophysical information about the antioxidant property of biological systems.

5. Conclusions

The diverse applications of EPR spectroscopy to study molecular processes at interfaces, where other methods have proven unsuccessful, will ensure its continued use in examining structure–function relationships. Such, EPR spectroscopy is a useful tool to further our understanding even when high-resolution structures are available, since it facilitates studies of internal motions and dynamics of molecules in solution or in the different processes, including heterogeneous catalysis.

Technical advances in EPR spectroscopy, which include new probes with specific labeled sites (SLS) and higher magnetic fields, increase in absolute sensitivity, spectral dispersion and diversity of applications. Lastly, the development of powerful computational simulations makes EPR user-friendly and increases the number of EPR practitioners outside of the community of spectroscopists.

REFERENCES

[1] Rosantev, E.G. *Free Nitroxyl Radicals*, Plenum Press, New York 1970

[2] Matsuda, K.; Iwamura, H. *Curr. Opin. in Solid State & Mat. Sci.*, 2, 446-450, 1997.

[3] Nakatsuji, S.; Anzai, H. *J. Mater. Chem.* 7(11), 2161-2174, 1997.

[4] Gatteschi, D. *Curr. Opin. in Solid State & Mat. Sci*, 1, 192-198, 1995

[5] Aurich, H.G. in *Nitrones, Nitronates and Nitroxides* Patai, A. (Ed) 313, 1989

[6] Mitchell, J.B.; Samanuni, A. *Biochem.* 29, 2802-2807, 1990

[7] Berliner, L.J., *Spin Labeling, Theory and Application*, Adademic Press, New York, NY, 1976.

[8] Bottle, S.E.; Busfield, W.K.; Jenkins, I.D.; Thang, S.; Rizzardo, E.; Solomon, D.H. *Eur. Polym. J.* 25, 671-676, 1989.

[9] Adam, W.; Bottle, S.E.; Finzel, R.L.; Kamel, T.; Peters, E.M.; Peters K.; von Schnering, H.G. *J. Org. Chem.* 52, 982-988, 1992.

[10] Beckwith, A.L.J.; Bowry, V.W.; Ingold, K.U. *J.Am.Chem.Soc.* 115, 4983-4992, 1992.

[11] Bowry, V.W.; Ingold, K.U. *Ibid*. 114, 4992-4996, 1992

[12] Damian, G., Miclauş, V., *Radicali Nitroxidici*, Ed. EFES, Cluj-Napoca, 2001

[13]] C.P.Poole Jr., and H.A. Farach, in *Theory of Magnetic Resonance*, (John Wiley & Sons, New York, NY, 1987), pp 319-321.

[14} A. Redfield, '*The Theory of Relaxation Processes'*, *Adv. Magn. Reson*., 1, (1965)1.

[15] S.A.Goldman, G.V.Bruno, C.F.Polnaszek, and J.H.Freed, *J.Chem. Phys*., 56, (1972) 716.

[16] S.Schreier, C.F.Polnaszek, I.C.P. Smith, *Biochimica et Biophysica Acta*, 515 (1978) 375.

[17] J.S. Hwang, R. P. Mason, L.-P. Hwang, and J. H. Freed, *J.Phys.Chem*. 79 (1975), 489.

[18] Morrisett, J.D. in *Spin Labelling – Theory and application*, Berliner J. Ed., Acad.Press, (1975) pp. 273-331

[19] G.Damian, O.Cozar, V.Miclaus, Cs.Paizs, V.Znamirovschi, V.Chis, L.David*, Colloids and Surfaces A: Physicochemical and Engineering Aspects* 137(1998)1.

[20] G.Damian, O.Cozar, V.Miclaus, Cs.Paizs, M.Todica, V.Chis, *Balkan.Phys.Lett*. 5(1997) 289.

[21] G.Damian, V.Znamirovschi, O.Cozar, M.Todica ,V.Chis, L.David, R.Salomir, *Studia UBB, Physica*, XLI, 1(1996)49

[22] G.Damian, V.Miclaus, V.Znamirovschi, O.Cozar, N.Dulamita, V.Chis, L.David*, Progress in Catalysis*, vol.7, 2(1998)61.

[23]. M.Todica, O.Cozar, G.Damian, L.David, *J.Mol. Structure*, 482-483(1999)355

[24] G.Damian, O.Cozar, M.Todica, L.David, D.Ristoiu *J. of Mol. Stucture* , 482-483 (1999) 287-289

[25] C.Cimpoiu, V. Miclaus, G. Damian, *Journal of Liquid chromatography & Related Technologies (in press)*

[26] Gutjahr, M.; Pöppl, A.; Böhlmann, W.; Böttcher, R*., Colloids and Surfaces A: Physico-chemical and Engineering Aspects* 189 (2001) 93-101

[27] R.Biswas, H. Kuhne, G.W.Brudvig, V.Gopalan, *Science Progress* (2001), 84 (1), 45–68

[28] V.Miclaus, G.Damian, C.M.Lucaciu, *Studia Universitatis Babes-Bolyai, Physica*, XLVII, 1 (2002) (in press)

[29] S.Cavalu, S.Simon, G.Damian, M.Dânşoreanu, C.M.Lucaciu, *Studia Universitatis Babes-Bolyai, Physica, XLVI, 1, 68(2001)*

[30] G.Damian, S.Cavalu, M.Dânşoreanu, C.M.Lucaciu, *Studia Universitatis Babes-Bolyai, Physica, Special Issue, 465(2001)*

[31] G.Damian, *Studia Universitatis Babes-Bolyai, Physica, XLVII, 2, 2002 (in press)*

[32] S.Cavalu, G.Damian, M.Danşoreanu, *Biophysical Chemistry* (in press)

STUDIA UNIVERSITATIS BABEŞ-BOLYAI, PHYSICA, XLVIII, SPECIAL ISSUE, 2003

THE FINE STRUCTURE OF THE EPR SPECTRA OF THE CHROMIUM IONS IN NON-CRYSTALLINE SOLIDS

LAVINIA COCIU

Faculty of Physics, "Babes-Bolyai" University, 3400 Cluj-Napoca, Romania

ABSTRACT. The features of the fine structure of the EPR spectra of the chromium ions in non-crystalline solids are discussed. The EPR spectra of Cr^{3+} ion in polycrystalline materials and the shift of the spectral features in terms of the *E/D* values are analysed. The computer simulation of some experimental EPR spectra of borate glasses reveals the presence of chromium in its tri- (d^3) and penta- (d^1) valence states ; the found Hamiltonian parameters of Cr^{3+} ions are *g=1.98, D*=0.216 cm^{-1} and *E/D* = 0.330. For Cr^{5+} ions, the symmetry of the $\tilde{g}$ -tensor changes from cubic (*g=1.978)* to axial ($g_x = g_y = 1.98$; $g_z = 1.93$), when the Na_2O content in glasses increases.

Introduction

The investigation of the local environment symmetry and crystal field parameters of the impurity paramagnetic ions in the disordered crystals and glasses are the current topics of solid state physics. The sensitivity of both the spin Hamiltonian parameters and chromium EPR spectra to the coordination of the ions, was used in order to study the various materials physical properties [1-3]. The compositional dependence of the valence state of Cr ions in glasses is not well understood [4]. In the present paper, we report the results of our EPR investigation of some oxide glasses containing chromium and the computer simulation of the experimental spectra recorded in the X band ($h\nu_o = 0.32$ cm^{-1}) of the microwave field.

Theoretical aspects

The EPR spectra of Cr^{3+} ions ($3d^3$, $^4F_{3/2}$) in orthorhombic crystalline field are described by the spin Hamiltonian including Zeeman and fine structure terms [5] with the same principal axis system (x,y,z):

$$\mathrm{H}_s = \beta[g_x S_x B_x + g_y S_y B_y + g_z S_z B_z] + D[S_z^2 - \frac{1}{3}S(S+1)] + E(S_x^2 - S_y^2)\,, \qquad (1)$$

where $g_x \equiv g_{xx}$, $g_y \equiv g_{yy}$, $g_z \equiv g_{zz}$ and $D = 3/2D_{zz}$, $E = (D_{xx} - D_{yy})/2$. For an d^3 ion, the $\tilde{g}$ -tensor is very nearly isotropic even in highly distorted crystal fields [6]. An orientation-dependent, anisotropic EPR line in non-single-crystal substances such as polycrystalline or amorphous solids, is generally characterised by an asymmetric powder pattern [7-10] which represents the envelope of the properly weighted spectral lines from the corresponding single crystals at all possible orientations. In the first-order of the perturbation theory, under the assumption of δ-line shape, an anisotropic $M \rightarrow M$ - 1 fine-structure transition in a polycrystalline samples gives rise to an asymmetric absorption powder pattern consisting of three features (two step shoulders and one divergence peak) [11] at the magnetic fields values

$$B_x^M = \frac{h\nu_0}{g_x\beta} + (2M-1)\frac{1}{2}\frac{D-3E}{g_x\beta}, \quad (2)$$

$$B_y^M = \frac{h\nu_0}{g_y\beta} + (2M-1)\frac{1}{2}\frac{D+3E}{g_y\beta}, \quad (3)$$

$$B_z^M = \frac{h\nu_0}{g_z\beta} - (2M-1)\frac{D}{g_z\beta}, \quad (4)$$

where ν_o is the microwave constant frequency. If the $\tilde{D}$ tensor has an axial symmetry, $E = 0$ and there is a divergence peak at $B_x^M = B_y^M$ and a shoulder at B_z^M. When $M = 1/2$, $2M - 1 = 0$ and $1/2 \rightarrow -1/2$ transition is not influenced by the polycrystalline aspect of the sample. We simulated the derivative EPR spectrum (Fig. 1) which illustrates this case; the simulation parameters are shown in the figure caption.

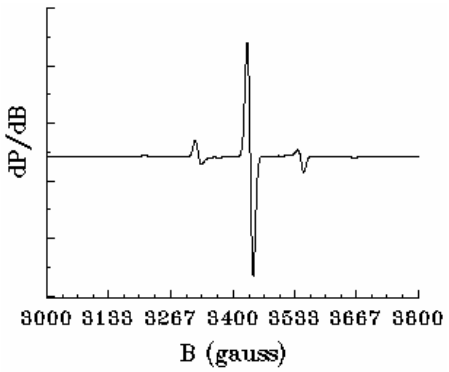

Fig. 1 Simulated EPR spectrum of Cr^{3+} ion. ν_o =9.5095 GHz; g =1.978; E = 0 D =0.0105 cm^{-1}; Gaussian line shape with 10 gauss peak to peak width.

Second-order perturbation theory is often used to study the effects of the crystalline field symmetry on the magnetic induction values at which the central $1/2 \rightarrow -1/2$ transition appears. We have taken over the formal identity between the fine-structure ($\vec{S} \cdot \tilde{D} \cdot \vec{S}$) term in the EPR Hamiltonian and the NMR quadrupolar interaction ($\vec{I} \cdot \tilde{Q} \cdot \vec{I}$) which was stressed in the review article of Taylor, Baugher and Kriz [8] and found the relation

$$D = \frac{2}{5}\sqrt{3h\nu_0 g\beta\Delta B} \quad (5)$$

between *D* coefficient and the splitting ΔB of the central $1/2 \rightarrow -1/2$ transition, assuming a negligible $\tilde{g}$ -tensor anisotropy. We simulated the EPR powder spectrum (Fig. 2) of the Cr^{3+} ion in a polycrystalline alum, using the found H_S parameter values when we studied the line-shape of the chromium doped $(NH)_4Ga(SO_4)_2 \cdot 12H_2O$ single crystal [12]. The splitting of the $1/2 \rightarrow -1/2$ line is evident in Fig 2. Sometimes, in the EPR literature, the $g_{eff} = h\nu_o / \beta B$ value is used in order to localise the spectral feature occurring at the *B* field when the microwave frequency is maintained at constant ν_o value. In Fig. 2, the shoulder at *B* ~ 2200 gauss has g_{eff} ~3.0; in the case

of a greater *D* value the spectrum should be spread over a wider field range and the lower field shoulder would have $g_{eff} > 3$. A distinction has to be made between this case ($D < h\nu_o$) and another situation which leads to greater g_{eff} values at an EPR line of Cr^{3+} spectrum. In the case of an axial ligand field at Cr^{3+} sites and $D > h\nu_o$, a single resonance transition is observed and the angular dependence of the spectrum $B_r = h\nu_o / \beta g(\theta)$ is determined by the equation [13]:

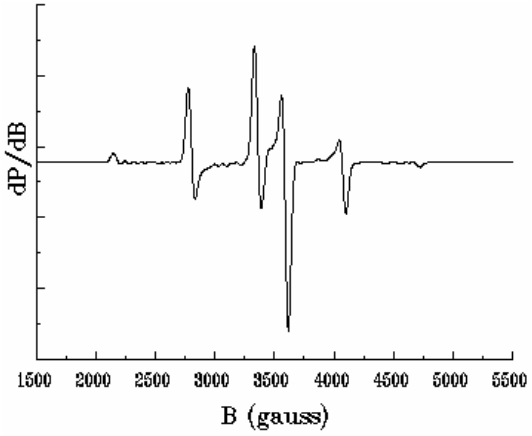

Fig. 2. Simulated EPR spectrum of Cr^{3+} ion. ν_o =9.5095 GHz ; g =1.978; E = 0 D =0.060 cm^{-1}; Gaussian line shape with 40 gauss peak to peak width.

$$g^2(\theta) = g_{\parallel}^2 \cos^2\theta + 4g_{\perp}^2 \sin^2\theta\,, \tag{6}$$

where θ is the angle between the static magnetic field vector and the z-axis of the $\tilde{g}$ -tensor coordinate system. The resonance field $B_r(\theta = 0^o)$ value corresponds to the $g_{\parallel}$ component. The $B_r(\theta = 90^o) = B_{\perp}$ corresponds to the $2g_{\perp}$ value and this feature is referred to the "g_{eff} = 4 resonance" for a $S = 3/2$ ion.

In the case of the rhombic symmetry of the $\tilde{D}$ tensor with $0 \le E < D < h\nu_o$, the powder pattern of the $1/2 \rightarrow -1/2$ transition depends on the E/D value which is a measure of the rhombicity of the crystalline field at the Cr^{3+} site. Again, using the information in paper [8] as well as the first pointed by Burns [14] similitude between the NMR and EPR notations, we calculated the expressions for the $1/2 \rightarrow -1/2$ resonance component fields. For E/D *< 1/9*, there are five features at the fields:

$$B_{1,\,\text{shoulder}} = B_0 - \frac{4}{3}\left(1 + 3\frac{E}{D}\right)\frac{D}{g\beta}\frac{D}{h\nu_0}\,, \tag{7}$$

$$B_{2,\,\text{divergence}} = B_0 - \frac{4}{3}\left(1 - 3\frac{E}{D}\right)\frac{D}{g\beta}\frac{D}{h\nu_0}\,, \tag{8}$$

$$B_{3,\,\text{shoulder}} = B_0 + 3\frac{E^2}{D^2}\frac{D}{g\beta}\frac{D}{h\nu_0}\,, \tag{9}$$

$$B_{4,\,\text{divergence}} = B_0 + \frac{3}{4}\left(1-\frac{E}{D}\right)^2 \frac{D}{g\beta}\frac{D}{h\nu_0}, \tag{10}$$

$$B_{5,\,\text{shoulder}} = B_0 + \frac{3}{4}\left(1+\frac{E}{D}\right)^2 \frac{D}{g\beta}\frac{D}{h\nu_0}. \tag{11}$$

If $E/D > 1/9$, between $B_{3,\,\text{shoulder}}$ and $B_{4,\,\text{divergence}}$ there exists one more divergence at

$$B_{6,\,divergence} = B_0 + \frac{2}{3}\left(1-9\frac{E^2}{D^2}\right)\frac{D}{g\beta}\frac{D}{h\nu_0}, \tag{12}$$

where $B_o = h\nu_o / g\beta$. A resonance line may be broadened by a number of causes; in consequence, not all the features (2)-(4) and (7)-(11) are resolved in spectrum. An experimental powder EPR spectrum must be computer simulated. We have simulated the EPR powder spectrum of Cr^{3+} ions in rhombic crystalline fields with $D = 0.06$ cm^{-1} and a variable E/D ratio. The simulated spectra are shown in the Figure 3. The chosen line width is not too large, so it can be watched the shift of the resolved spectral features when E/D value increases from 0.050 to 0.330.

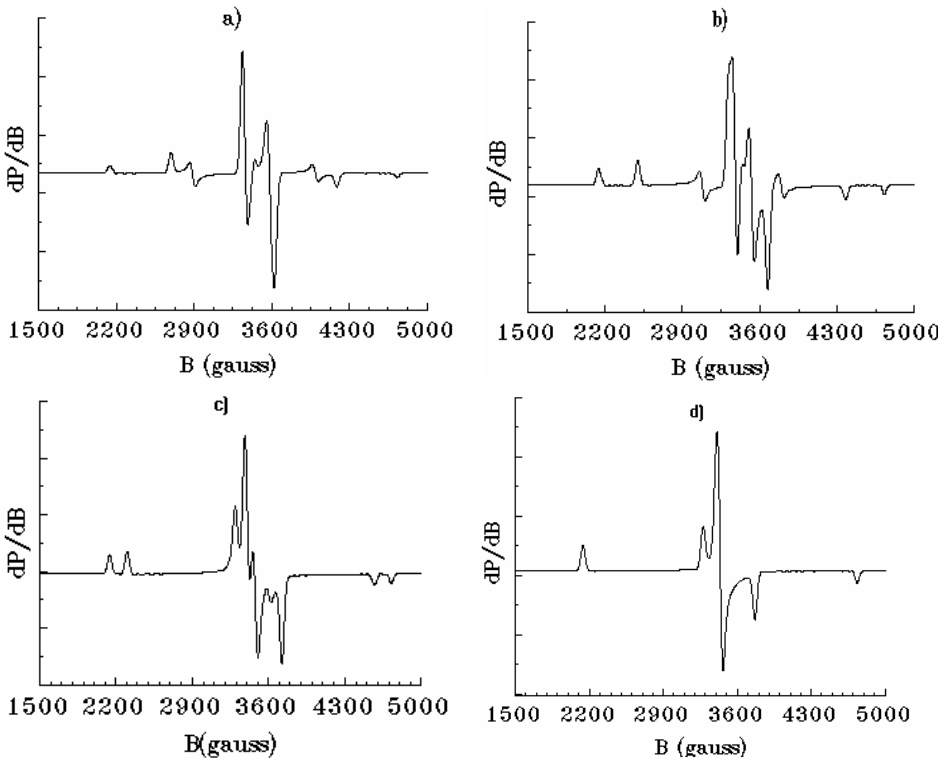

Fig. 3. Computer simulated EPR spectra of Cr^{3+} ion. ν_o = 9.5095 GHz; g = 1.978; D = 0.060 cm^{-1}; E/D values are: a) 0.05; b) 0.15; c) 0.25 and d) 0.330. Gaussian line shape.

Experimental results

The nominal composition of the undoped glasses was $xNa_2O(100\text{-}x)\ B_2O_3$ with x between 5 and 40 mole %. For every fixed x, in 10 g of B_2O_3-Na_2O glass sample, Cr_2O_3 was added in 0.30 weight percentage. The row materials H_3BO_3, Na_2CO_3 , Cr_2O_3 were of analytical grade. Batch materials of the first glass system were maintained in sintered corundum crucibles at 1200 ^oC in an electric furnace with air atmosphere, for 0.5 hour.

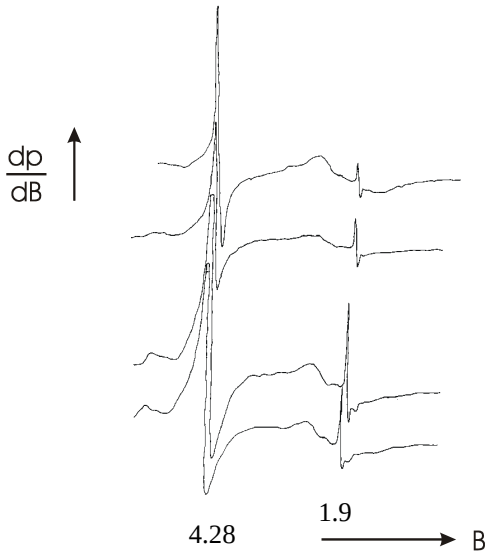

Fig. 4. Experimental EPR spectra of Cr_2O_3 doped $xNa_2O(1\text{-}x)B_2O_3$, with x = 5 mol% (F_1); 20 mol% (F_4); 30 mol% (F_6); 35 mol% (F_7). ν_o = 9.38 GHz.

The EPR measurements, at room temperature, were carried out on a JEOL spectrometer (JES-3B) operating in X-band microwave frequency. The magnetic field was calibrated by means of a proton resonance probe.

Figure 4 shows several typical experimental EPR spectra of chromium doped bulk glasses; all of them, even of the undoped sample, have a g_{eff} = 4.28 line characteristic to Fe^{3+} ions in glasses [15]; its presence is due to the used crucibles. The shoulder at low field and the other lines (at g_{eff} around 1.9) are due to the isolated chromium ions.

Computer simulation of the experimental spectra

In most cases, the computer simulation is the only way to extract reliably spin Hamiltonian parameters from paramagnetic centres EPR spectra. Figure 5 shows one of the simulated spectra of the chromium ions in the lowest Na_2O content investigated glasses. Fig 5 is a superposition of two EPR spectra: one of them from Cr^{5+} ions with an isotropic g =1.978, and the other from Cr^{3+} ions coexisting in the glasses. The simulated fine structure of Cr^{3+} ions is shown in Fig. 6; we note the shoulder at ~ 8000 gauss. The experimental spectra were recorded until about 5000 gauss, so the high field shoulder is absent. The H_s parameters of simulated spectra are given in the figure captions. The same Cr^{3+} ion spectrum with axial D = 0.216 cm^{-1} coefficient and E/D = 0.330 was taken as a component of the Fig. 7 spectrum which is characteristic to the higher Na_2O content samples. The second component in Fig. 7 is the simulated Cr^{5+} spectrum shown in Fig. 8; as it can be seen in figure, the $\tilde{g}$ -tensor has an axial symmetry.

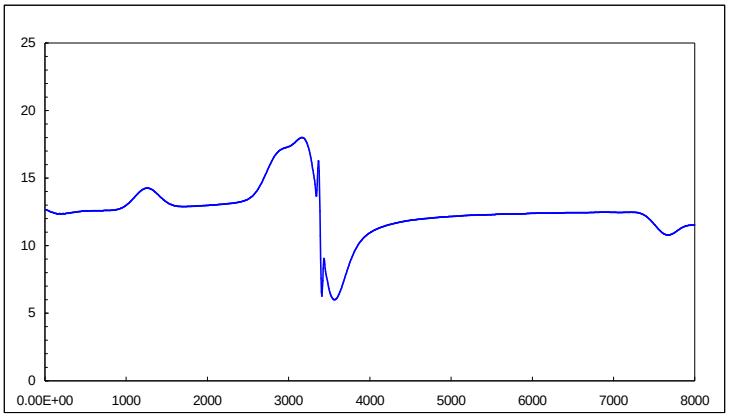

Fig. 5 Calculated EPR spectrum as a superposition of two components: 1. 60 % EPR spectrum of Cr^{3+} ion, shown in Fig. 6; 2. 40 % EPR spectrum of Cr^{5+} ion with isotropic g = 1.978 and Gaussian line shape; peak to peak line width is 30 gauss; ν_o = 9.381 GHz.

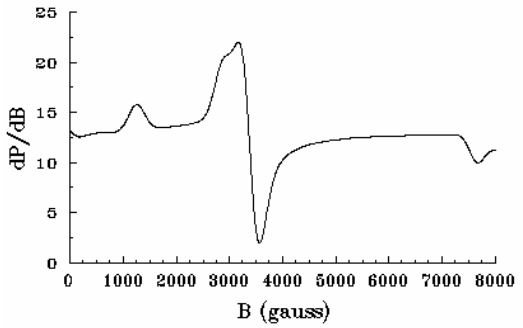

Fig. 6 Simulated EPR spectrum of Cr^{3+} ion at ν_o = 9.381 GHz. g = 1.98; D = 0.216 cm^{-1} and E/D = 0.330 ; Gaussian line shape; peak to peak line width is 300 gauss.

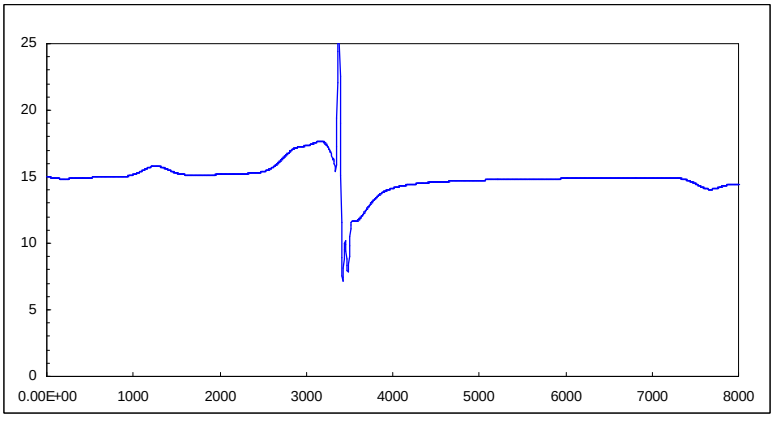

Fig. 7 Calculated EPR spectrum as a superposition of two components: 1. 30 % EPR spectrum of Cr^{3+} ion, shown in Fig. 6; 2. 70 % EPR spectrum of Cr^{5+} ion shown in Fig. 8.

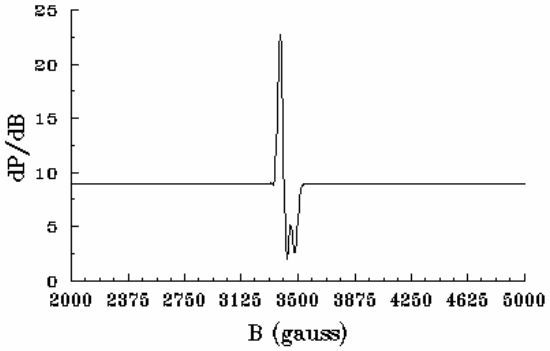

Fig. 8 Simulated EPR spectrum of Cr^{5+} ion at ν_o = 9.381 GHz.
$g_x = g_y = 1.98$; $g_z = 1.93$; Gaussian line shape; peak to peak line width is 30 gauss.

Discussions

Above, we have presented only two calculated EPR spectra of the chromium ions in investigated borate glasses. In order to explain the experimental results, on the basis of our findings [16] from optical absorption spectra, we suppose the isolated Cr^{3+} ions in intermediate crystalline field positions, with *D* and *E* values ranging from site to site because of the vitreous matrix disorder.

Octahedrally coordinated Cr^{3+} ions shows zero field splitting values [6] less or greater than X-band Zeeman splitting. The line positions in the EPR spectra are sensitive to *D* and *E* parameters, resulting a variety of spectral shapes. In the papers [15], [17], [18] the low field shoulder in the Cr^{3+} EPR spectra is reported with g_{eff} values ranging between 4 and 6. The authors of reference [19] found in a 77K recorded EPR spectrum of a 0.4 wt % Cr_2O_3 doped B_2O_3-Na_2O glass sample, two shoulder at $g_{eff} \approx 3.7$ and 5.2. Paul and Upreti [20] do not report any EPR line with $g_{eff} > 2$, but they found optical transitions from $^4A_2$ ground state to ^2E and $^2T_1$ excited states of the ^2G term of Cr^{3+} ion in octahedral coordination, which are characteristic to stronger crystalline fields. Optical studies of the distributions of the ligand field sites occupied by the dopant Cr^{3+} ions in inorganic glasses, pointed out the existence of statistical distributions [21] with the largest width for borate glasses; such a large Gaussian distribution requires more weak-field sites for chromium dopants than in silicate glasses. The symmetry lowering distortions of the octahedra have weaker strength.

In the simulated spectra we have incorporated the distribution of H_S parameters via the σ_i component values of an angular dependent line width function

$$\sigma = \left(\sigma_x^2 l_x^2 + \sigma_y^2 l_y^2 + \sigma_z^2 l_z^2 \right)^{1/2}, \tag{13}$$

where l_x, l_y and l_z are the component of the $\vec{l}(\sin\theta\cos\phi, \sin\theta\sin\phi, \cos\theta)$ unit vector in the direction of the magnetic field.

Spin Hamiltonian of Cr^{5+} ion ($3d^1$, $^2D_{3/2}$) includes only Zeeman term; the anisotropy of the $\tilde{g}$-tensor depends on the sample compositions. Pentavalent chromium ions in glasses have precursors in chromate complexes $(CrO_4)^{2-}$. In the low Na_2O content glasses, Cr^{5+} ions have tetrahedral surroundings. Large amount of network modifier results in more disorder and axial, or rhombic, or even lower symmetry of the $\tilde{g}$-tensor.

Conclusion

We have measured and analysed the X-band EPR spectra of chromium dopant ions in some borate glasses. The computer simulation of experimental spectra revealed both octahedrally coordinated Cr^{3+} ions and tetrahedrally coordinated Cr^{5+} ions; their relative weight depends on the Na_2O content in glasses.

REFERENCES

1. I. Ursu, La resonance paramagnétique, Dunod. Paris, 1968.
2. R. P. Bonomo, A. J. D. Bilio and F. Riggi, Chem. Phys., 151, 323 (1991).
3. J. R. Pilbrow, Transition Ion Electron Paramagnetic Resonance, Clarendon Press, Oxford, 1990, ch. 5.
4. T. Murata, M. Torisaka, H.Takebe, M. Morinaga, J. Non-Cryst. Solids, 220, 139 (1997).
5. A. Abragam, B. Bleaney, Electronic Paramagnetic Resonance of Transition Ions, Clarendon Press - Oxford, 1970.
6. B. R. McGarvey, in "Transition Metal Chemistry", vol. 3, ed. R. L. Carlin, Dekker, New York, 1966, p. 89.
7. P. C. Taylor, P. J. Bray, J. Magn. Res. 2, 305 (1970).
8. P. C. Taylor, J. F. Baugher and H. M. Kriz, Chem. Revs., 75, 203 (1975).
9. Al. Nicula, Rezonanßa magnetic¾, Ed. didactic¾ ¿i pedagogic¾, Bucure¿ti, 1980.
10. J. Kliava, EPR Spektroskopia neuporiadoćenâh tverdâh tel, Ed. Zinatne, Riga, 1988.
11. S. Lee and S-Z Tang, Phys. Rev. B, 2761 (1985).
12. Lavinia Cociu, Gh. Cristea, Studia Univ. Cluj-Napoca 1, 73 (1971).
13. F. E. Mabbs and D. Collison, Electron Paramagnetic Resonance of Transition Metal Compounds, Elsevier, London, 1992, p. 582.
14. G. Burns, J. Appl. Phys., 32, 2048 (1961).
15. D. L. Griscom, Electron Spin Resonance, in Glass Science and Technology, vol. 4B, D. R. Uhlmann and N. J. Kreidl eds., Academic Press, Boston, 1990, p. 151.
16. Lavinia Cociu, M. Peteanu, EPR and Optical Study of the Nature of Chromium Complexes in Glasses, Book of Abstracts, Colloquium Spectroscopicum Internationale XXXI, September 5-10, 1999, Ankara, Turkey, p. 343
17. M. S. Brückner, M. Sammet and H. Stockhorst, J. Non-Cryst. Solids, 40, 273 (1980).
18. X. F. Liu, J. M. Parker, E.A. Harris and C. Topacli, Spectroscopic and Structural Behaviour of Cr^{3+} in Transparent Gahnite Glass - Ceramics, in Physics of noncrystalline solids, L. D. Pye, W. C. La Course and H. J. Stevens eds., p. 642.
19. R. S. Abdrahmanov, T. A. Ivanova, Fiz. khim. stekla, 3, 562 (1977).
20. A. Paul, G. C. Upreti, J. Mater. Sci., 10, 1149 (1975).
21. M. Yamaga, B. Henderson and K. P. O☎ Donnel, Phys. Rev., B44, 4853 (1991).

STUDIA UNIVERSITATIS BABEŞ-BOLYAI, PHYSICA, XLVIII, SPECIAL ISSUE, 2003

EPR OF PARAMAGNETIC IONS IN SOME COMPLEX PEROVSKITE COMPOUNDS

I. BARBUR, I. ARDELEAN

Faculty of Physics, Babes-Bolyai University, 3400 Cluj-Napoca, Romania

ABSTRACT. EPR measurements of Mn^{2+}, Fe^{3+}, Cu^{2+} and V^{4+} ions in complex perovskite compounds Pb_2MgWO_6 are reported. By Mn, Fe or Cu partial substitution for Mg a small ordering of cations is changed and this fact is reflected in shape and widths of the EPR lines.

1. Introduction

It is well known that a large number of $Pb_2B'B"O_6$ compounds containing divalent or trivalent ions as B' ions (Mg, Mn, Fe) and W, Nb, Mo as B" ions belong to complex perovskite-type compounds. An ordered distribution of the B' and B" ions occurs when a large difference exists in either charges or ionic radii [1]. Almost all complex perovskite families have destorted unit cells and high dielectric constant. The anomalies in dielectric constant are due to the ferroelectric or antiferroelectric transitions.

Lead mangnesium tungstate, Pb_2MgWO_6 (thereafter PMW) belongs to complex perovskite-type compounds with general formula $A^{2+}B_{0.5}^{2+}B_{0.5}^{6+}O_3$ in which ordered distribution of Mg^{2+} and W^{6+} ions is most probably to the existence of a large difference in charges and ionic radii of these ions. PMW and its solid solutions has been the subject of X-ray [2], electrical [3] and optical [4] studies, since its discovery by Smolenskii et al. [5]. At 38^{o}C the PMW undergoes a phase transition from the rhombic paralelectric to the tetragonal antiferroelectric state with a well defined suprastructure.

In previous papers [6-9] we have reported the influence of Mg and W substitution by Mn, Fe, Cu and respectively V ions on structure, electrical and magnetical properties in Pb_2MgWO_6.

In this contribution we present EPR data of Mn, Fe, V, Cu and V ions substitutions in PMW.

It is well known that electron paramagnetic resonance is a powerful tool in studying the detailed atomic arrangament around a paramagnetic impurity ion [10].

2. Experimental

All the polycrystalline samples of Pb_2MgWO_6: (Mn, Fe, Cu, V) were prepared by reacting stoichiometric proportions of PbO, $Mg(NO_3)_2{\cdot}6H_2O$, $MnCO_3$, Fe_2O_3, CuO, WO_3 species using high purity grade chemicals. The mixtures were calcinated at 700^{o}C for 4 hours and sintered at 1000^{o}C for 2 hours. All the samples were prepared in air atmosphere.

EPR spectra were recorded using a JEOL JES-3B modified X-band spectrometer. The instrument setting were: microwave frequency 9500 MHz, modulation frequency 100 kHz, field scan 200 G, time constant 1 second, cavity TE_{102}, sensitivity $3 \cdot 10^{11}$ spins/Gauss and microwave power 10 mV. The field homogeneity in the volume of the sample was $1.1 \cdot 10^{-6}$ %.

The calibration of magnetic field for g factor and hyperfine splitting values was performed by using NMR signals of protons (NMR magnetometers type MJ 110R).

3. Results and discussion

a) EPR of Mn^{2+} ions in $Pb_2Mg_{1-x}Mn_xWO_6$ (PMMnW)

In order to study the influence of Mg substitution by Mn on the structural, electric and magnetic properties in Pb_2MgWO_6, X-ray diffraction, dielectric permitivity, EPR and magnetic susceptibility measurements on $Pb_2Mg_{1-x}Mn_xWO_6$ compounds (x = 0; 0.01; 0.05; 0.1; 0.3 and 0.5) were performed [7].

Dielectric anomaly at T_c (38^oC) related to an antiferroelectric phase transition in PMW was observed in the variation of dielectric permitivity ε versus temperature T. The Curie temperature increases linearly with Mn contents and this behaviour appears to be a common property for complex perovskites which involve a ferroelectric or antiferroelectric transition.

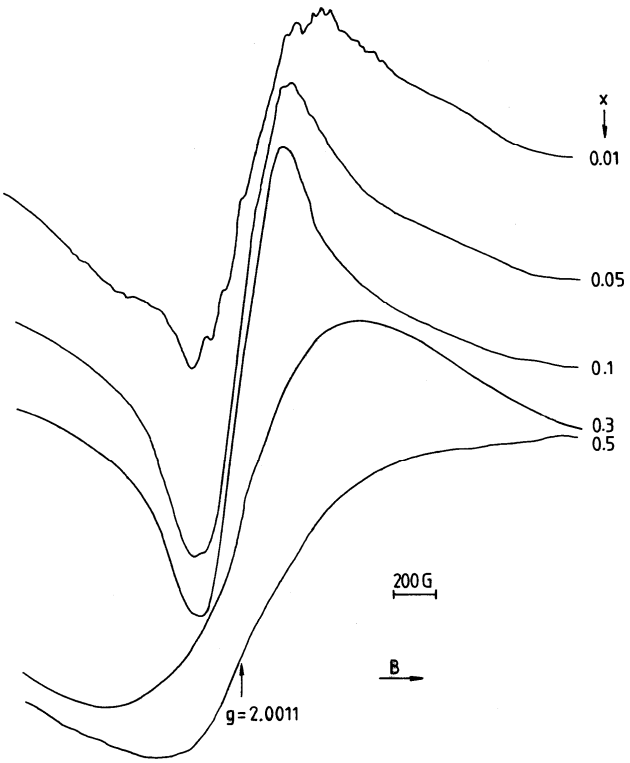

Fig. 1. EPR spectra of Mn^{2+} in $Pb_2Mg_{1-x}Mn_xWO_6$.

EPR spectra of all PMMnW samples consist of a single line corresponding to g ≅ 2.0 which is due to the Mn^{2+} ions (Fig. 1).

For x = 0.01 a not so well resolved sextet is observed, corresponding to the hyperfine interactions (I = 5/2). EPR line-width ΔH depends on x (Fig. 2). Up to x = 0.1, ΔH remains constant (~400 Gs) and than increases to 1500 G for x = 0.5. This behaviour suggets dipolar interactions between Mn^{2+} ions, which up to x = 0.1 are constants and then the intensity of the dipolar interactions increases probable due to the increase of Mn^{2+} ions concentrations.

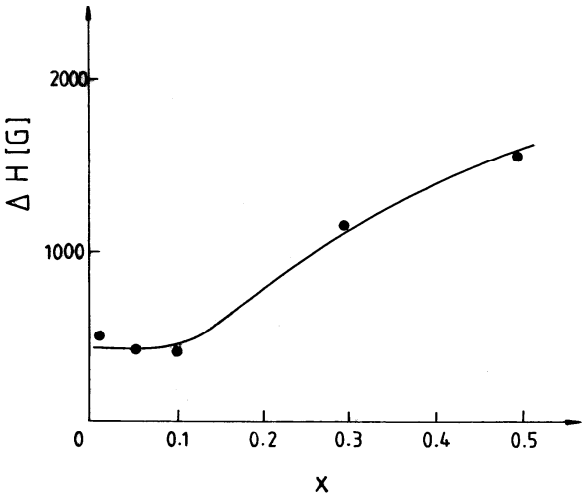

Fig. 2. The composition dependence of the EPR line-width of Mn^{2+} in $Pb_2Mg_{1-x}Mn_xWO_6$.

No EPR absorption line was detected at g ≅ 4.3 which correspond to isolated Mn^{2+} ions, or at g = 1.4 which is due to W^{5+} ions.

Presence of Mn^{2+} ions in $Pb_2Mg_{1-x}Mn_xWO_6$ is confirmed also by magnetic susceptibility measurements [7].

b) EPR of Fe^{3+} ions in $Pb_2Mg_{1-x}Fe_xWO_6$ (PMFW)

EPR spectra of PMFW samples consist of a single intense line centered at g = 2.0 corresponding to Fe^{3+} ions (Fig. 3). For x = 0.1 a small line is observed at g ≈ 4.3 which is charactersitic for isolated Fe^{3+} ions. No EPR line was detected at g = 1.4 corresponding to W^{5+} ions. The line-width of the EPR spectra depends on x (Fig. 4). Up to x = 0.1, ΔH increase with increasing of x. This broadening of the line suggest dipolar interactions between Fe^{3+} ions for x ≤ 0.1. For higher Fe^{3+} ions concentrations, this broadening is balanced by narrowing mechanisms and, therefore, ΔH increasing is stopped. This suggests that the some of the iron ions, for x > 0.1 are involved in superexchange magnetic interactions, result confirmed by the magnetic susceptibility data [9].

c) EPR of Cu^{2+} ions in $Pb_2Mg_{1-x}Cu_xWO_6$ (PMCW)

The EPR spectrum of PMCW is shown in Fig. 5. This spectrum is due to the Cu^{2+} ions and reflects the change of the local symmetry around the Cu^{2+} ions by its concentration increasing [11].

For x = 0.1 the shape of EPR spectrum is rhombic (g_1 = 2.527, g_2 = 2.178, g_3 = 2.051). This suggests one rhombic octahedral symmetry around the Cu^{2+} ion with d_z^2 orbital as ground state. This situation is due to the substitution of the Mg^{2+} ion by Cu^{2+} in the Oxy planes and to the difference in the ionic radii of these ions.

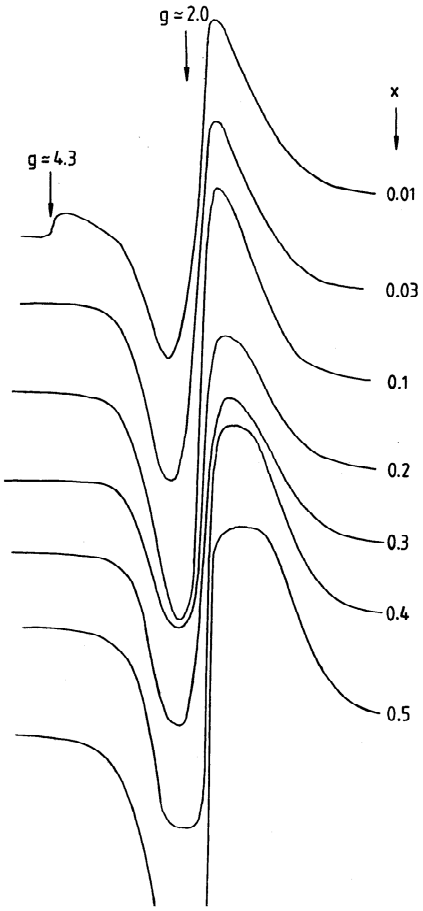

Fig. 3. EPR spectra of Fe^{3+} in $Pb_2Mg_{1-x}Fe_xWO_6$.

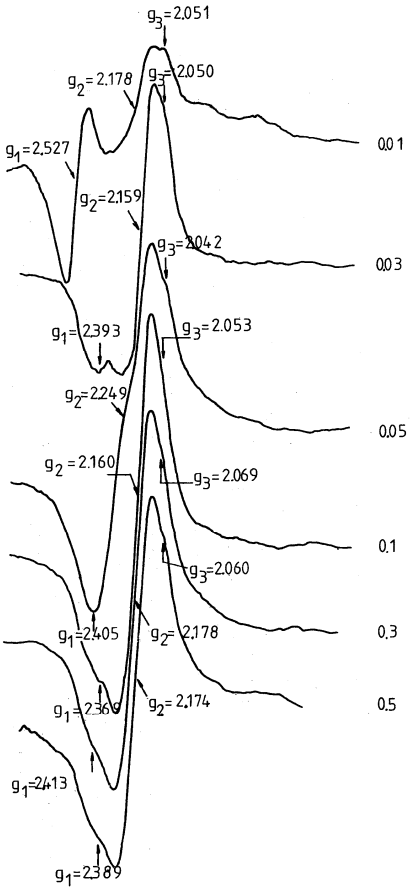

Fig. 5. EPR spectra of Cu^{2+} in $Pb_2Mg_{1-x}Cu_xWO_6$.

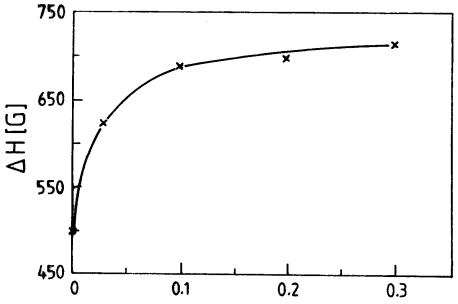

Fig. 4. The composition dependence of the EPR line-width of Fe^{3+} in $Pb_2Mg_{1-x}Fe_xWO_6$.

The proximity of Cu^{2+} ions from (Oxy) planes changes the local symmetry to one elongated octahedral with $d_{x^2-y^2}$ orbital ground state. This appears very clearly from x = 0.3 concentration spectrum where the g_2 signal, becomes the strongest.

At x = 0.05 the signal is very broad ($\Delta B_{pp} \approx$ 550 G) with some features at g_1 = 2.405, g_2 = 2.249, g_3 = 2.042 and suggests the existence of dipolar interaction between the Cu^{2+} ions. Up to x = 0.5 the rhombic shape of the spectrum (g_1 = 2.380, g_2 = 2.165, g_3 = 2.060) remains unmodified by x increasing.

d) EPR of V^{4+} ions in $Pb_2MgW_{1-x}V_xO_6$ (PMWV)

EPR spectra of PMWV samples consist of a single line centered at g = 2.007 (Fig. 6). This spectrum is due ti the V^{4+} ions but presence of V^{5+} ions is not excluded. The shape and intensity of this line depend on x [11]. For x = 0.1 the tendency of resolving of hiperfine interactions is observed. The line-width of the EPR spectra depend on x (Fig. 7). Up to x = 0.3 ΔH increase with x increasing and than ΔH decrease for $0.3 \leq x \leq 0.4$. This behaviour suggests dipolar interactions between V^{4+} ions for $x < 0.3$ and magnetic superexchange for $x \geq 0.3$. No EPR line was detected at g = 1.4 corresponding to W^{5+} ions.

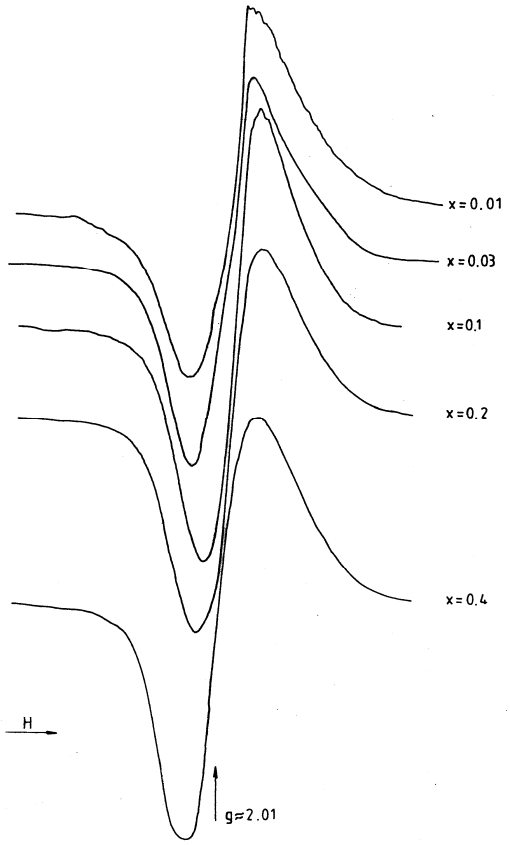

Fig. 6. EPR spectra of V^{4+} in $Pb_2MgW_{1-x}V_xO_6$.

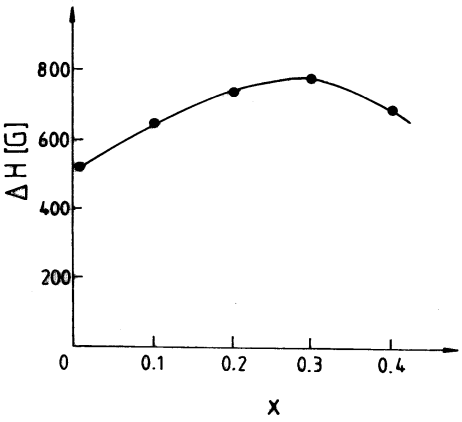

Fig. 7. The composition dependence of the EPR line-width of V^{4+} ions in $Pb_2MgW_{1-x}V_xO_6$.

4. Conclusions

As was mentioned above, $PbMg_{1/2}W_{1/2}O_3$, belongs to lead-based complex perovskite compounds of Pb(B',B")O_3-type showing long range B site ordering of the cations. In the family of $Pb^{2+}(B'_{1/2}B''_{1/2})O_3$ perovskites there is an average B site valence of +4 in the superstructure which gives rise to the so-called stoichiometric

ordering. This ordering can be modified by compositional variation. By Mn, Fe or Cu substitution for Mg and V for W, a small ordering is changed and therefore the EPR spectra of Mn^{2+}, Fe^{3+}, Cu^{2+} and V^{4+} reflect this effect. It is interesting to notice, that additional of Fe, PMFW, decreases the Curie temperatuyre up to $-75^{o}C$ which is transition temperature for disordered perovskite compound $Pb(Fe_{1/2}W_{1/2})O_3$.

In case of V substitution for W the decreases of the dielectric constant at T with a addition of V is probably due to the crystallite size decreases. A possible crystallite-size (or grain-size) dependence of the dielectric constant for PMWV is suggested by similar behaviour reported on lead-containing perovskite ceramics [13].

REFERENCES

1. F.S.Galasso, Perovskites and High-T_c superconductors, Gordon and Breach, New York, 1990
2. A.I.Zaslavskii and M.F.Bryzhina, Soviet Phys. Crystallogr. 7, 709 (1962)
3. N.N.Krainik and A.I.Agranovskaia, Fiz. Tverd. Tela 2, 70 (1960)
4. L.S.Kamzina et al., Izv. Akad. Nauk SSSR, Ser. Fiz. 39, 813 (1975)
5. G.A.Smolenskii and A.I.Agranovskaia, Soviet Phys. Solid State, 2, 990 (1959)
6. I.Barbur, I.Ardelean, Gh.Borodi, A.Veres, V.Timar, Ferroelectric Lett. 23, 69 (1997)
7. I.Ardelean, I.Barbur, A.Veres, Gh.Borodi, I.Cosma, J. Mat. Sci. Lett. 16, 1735 (1997)
8. I.Barbur, I.Ardelean, Phase Transitions, 74, 367 (2001)
9. I.Ardelean, I.Babur, A.Veres, G.Borodi, V.Timar, Balkan. Phys. Lett. 5, 892-895 (1997)
10. I.Ursu, Resonance Paramagnetique Electronique, Dunod, Paris, 1968
11. I.Barbur, L.David, I.Ardelean, A.Veres, G.Borodi, Studia, Univ. Babes-Bolyai, Physica, 45, 27 (2000)
12. I.Barbur, I.Ardelean, G.Borodi, A.Veres, V.Timar, Ferroelectrics Lett., 23, 69 (1997)
13. S.L.Swartz, T.R.Shrout, W.A.Schulze, L.E.Cross, J. Am. Ceram. Soc. 67, 311 (1984).

STUDIA UNIVERSITATIS BABEŞ-BOLYAI, PHYSICA, XLVIII, SPECIAL ISSUE, 2003

APPLICATION OF EMR TO PLATINUM MOLECULAR COMPLEXES

L.M. GIURGIU

National Institute for Research&Development of Isotopic and Molecular Technologies P.O. Box 700, 3400 Cluj-Napoca, Romania

ABSTRACT. An analysis of the EMR experiments on the quasi-one-dimensional conductors and cyanide complexes based on platinum ions is given. The different hyperfine interaction parameters involved will be discussed. I will point at those highlights as charge delocalization and spin density distributions wich are emerged from the discussion of the EMR data.

1. Introduction

I wish to focus on the molecular complexes based on platinum ions which are of particular interest either for their unusual electronic properties in the solid state or due to the unstable oxidation states of the metal ion.The attention will be devoted to the quasi-one-dimensional (Q1D) platinum conductors and the low spin Pt – tetracyanide complexes in dilute and izolated form.

The highly unisotropic spectral features of the Q1D compounds have attracted considerable interest in order to understand the solid state interaction which are present in these materials [1].The early studies of the spectral properties have suggested the prospect of novel electrical properties which could fullfil the criteria for 1D high temperature excitonic superconductor [2]. In terms of their electrical conductivity, the normal molecular solids have been viewed as insulators with conductivities typically below $10^{-7}\ \Omega^{-1}\ cm^{-1}$. The observation of conductivities in the range of $10^{+2} – 10^{+5}\ \Omega^{-1}\ cm^{-1}$ for several members of the Q1D molecular solids in therefore quite remarkable and deserving of interest, both from scientific and potentially a technological viewpoint. Moreover, for many of these materials the conductivity actually increases with decreasing temperature in a manner characteristic of metallic substances, in contrast to the usual thermally activated (semiconductor-like) conductivity behaviour found for molecular solids.

The electronic structure and spectroscopic properties of transition metal cyanide complexes have been much investigated [3]. Molecular Pt-cyanide complexes are of particular interest since the Pt-ion has a low spin and exhibit several interesting properties. These complexes are diamagnetic but can be made paramagnetic by irradiating them with X - rays or γ - rays. The Pt – ions in the irradiated complexes may show unusual and unstable oxidation states [4]. The energy levels and the electronic ground states are sensitive to the site symmetry and complexes having different site symmetries can be studied by incorporating them in alkali halides [5]. Here, the positive ion vacancies created for charge compensation could change the site symmetry at the Pt – ion.

Electron Magnetic Resonance (EMR) spectroscopy offers the opportunity to study the magnetic interactions and to obtain more information about the spin dynamics in platinum molecular complexes (PtMC) [6,7,8]. The main goal of this article is to introduce the non-expert in the field of EMR to the achievements of EMR in PtMC, i.e. to what kind of information EMR can suply on the magnetic interactions in these complexes. I will concentrate on the questions

(i) can EMR provide informations about the charge or spin delocalization in Q1D Pt conductors

(ii) is the platinum hyperfine interaction influenced by the delocalization

(iii) are there spin densities transferred to the ligands in molecular Pt – cyanide complexes?

I will demonstrate in the following that the analysis of the EMR parameters: g - factor, hyperfine and superhyperfine tensor elements has revealed detailed informations on the electron system in these molecular complexes.

2. Physical properties of platinum molecular complexes

The outstanding features associated with the Q1D – platinum conductors are anisotropic physical properties, the most noteworthy of which is the 1D- metallic conductivity along the metal chain axis. This takes place via electron delocalization along the overlapped d_{z^2} orbitals as depicted in Fig.1. The genesis of such systems requires that some important conditions must be met [9], which are realized in the following two classes:

(i) The "integral – valence" compounds are generally square planar metal complexes of the d^8 metal ions (Pt^{2+}) which assume a columnar stacking arrangement in the solid state as to produce a linear chain of metal atoms along one direction in the crystal. Coordination ligands which promote these interaction are limited mainly to Cl^-, CN^- and $(C_2O_4)^{2-}$

A good example may be found in the compound $Pt(NH_3)_4PtCl_4$, known as Magnus Green Salt (MGS). The Pt – Pt separation ($d_{||}$) in the corresponding chains is 3.25 Å. Although significantly larger than the separation in Pt metal itself (2.78 Å), this is apparently sufficiently short to permit appreciable overlap of $5d_{z^2}$ orbitals.

It is well established that MGS is an excelent example of an extrinsic 1D semiconductor in which small amounts of Pt^{4+} complexes in the solutions used to prepare this material lead to the incorporation of Pt^{3+} - like defects which can be identified by there EMR spectrum in the solid state [10-14]. These defects which appear to be delocalized over several Pt sites but effectively bound to the vecinity of the interstitial charge compensating anions, form energy states close to the top of the filled $5d_{z^2}$ orbitals of the Pt^{2+} ions. Electrons thermally excited into these states produce holes in the d_{z^2} band which serve as the charge carriers for electrical conduction.

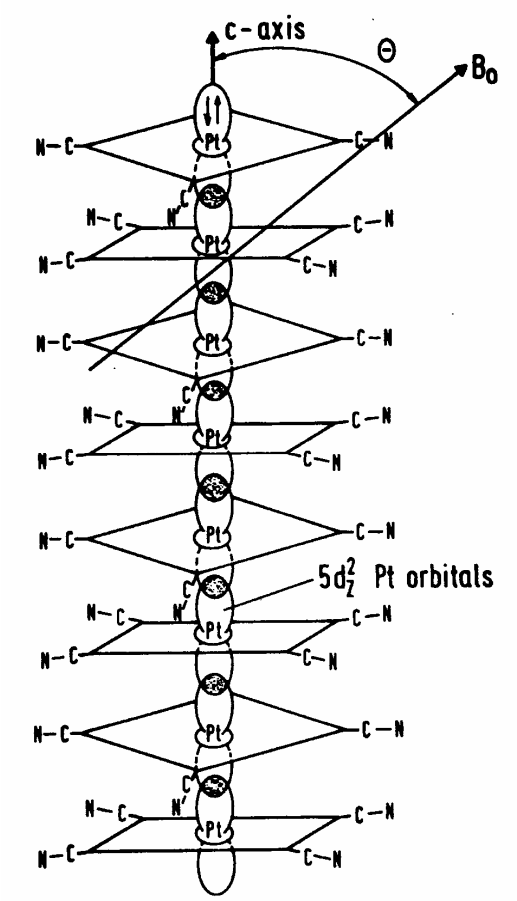

Figure 1. Diagram of overlapped Pt - d_{z^2} orbitals which result in a metal chain formation

(ii) The "non-integral" valence compounds or mixed valency planar compounds, are obtained by partial oxidation of the $[Pt(CN)_4]^{2-}$ complexes. The prototype of these Q1D – conductors is $K_2Pt(CN)_4B_{10.3} \cdot 3.2\ H_2O$, KCP(Br). The crystal structure consists of a columnar stacked array of planar $Pt(CN)_4$ units to form a chain of Pt atoms with a very short $d_{\|}$ separation, $d_{\|} = 2.894$ Å.

Overlap of the 5 d_{z^2} Pt orbitals (see Fig.1) leads to a Q1D valence band which is completely filled. Partial oxidation of the Pt ions from Pt^{2+} to $Pt^{2.3+}$, due to the presence of 0.3 Br per Pt, results in a partial depletion of this band which is completely characterized by an occupation number of 0.3 holes per Pt atom. The ^{195}Pt Mössbauer experiments suggest that all the Pt atoms are chemically equivalent and consequently the fractional valence charge is delocalized [15]. Yet, within the framework of the structural disorder model a delocalization of the electron states of about 10 lattice sites was estimated [16].

The EMR investigation of KCP(Br) have revealed the presence of the bound d_{z^2} - like hole states associated with a d_{z^2} - like valence band [14,17,18].

Concerning the molecular Pt - cyanide complexes, I would like to mention that the alkali halides are the most fancied host crystals for incorporating these complexes in dilute and isolated form for EMR studies [4,5]. This is possible due to the good matching of the symmetry and size of the Pt – cyanide complexes with those of one or the other alkali halide lattices. The unit cell dimensions of the alkali halides used in our investigations are 0.563 nm (NaCl) and 0.629 nm (KCl). The EMR parameters of the Pt – complexes showed systematic variations which could be discussed in terms of changes in the nature of binding in relation to the charge state of the Pt – ion and the host lattice spacings.

The mechanism for the formation of paramagnetic Pt-cyanide complexes could be understood on the following basis.

The Pt – tetracyanide complex $[Pt(CN)_4]^{2-}$ having a square planar coordination is diamagnetic and corresponds to Pt^{2+} ion with a d^8 configuration. It could substitutionally replace $[MCl_4]^{3-}$ (M = Na, K) unit in the crystal. The coordination of Pt^{2+} now becomes sixfold with $2Cl^-$ ions present on either site of the plane of $4CN^-$ ions. Now the molecular Pt^{2+} complex could be represented as $[\ Pt\ (CN)_4Cl_2]^{4-}$. Since the valence state of the Pt ion (+2) is different from that alkali ion (+1), in order to maintain the charge neutrality of the crystal a cation vacancy $\oplus$ occupying nearest neighbour or next nearest neighbour position will be created. This leads to a molecular complex of the form $\{\ [\ Pt(\ CN\ )_4Cl_2]^{4-} + \oplus\ \}$.

The γ - rays irradiation of the doped crystals creates secondary electrons which are captured by the Pt - tetracyanide complexes and the result can be represented by the following equation:

$$\left\{\left[Pt\ (CN)_4\ Cl_2\right]^{4-} + \oplus\right\} \xrightarrow{\gamma-\text{irradiation}} \left\{\left[Pt\ (CN)_4\ Cl_2\right]^{3-} + 2\oplus\right\} \quad (1)$$

Here, the two positive ion vacancies associated with the complex for charge compensation could be situated, for example along the [1 0 0] direction [12]. This leads to a molecular complex with C_{4v} or D_{4h} symmetry corresponding to d^7 configuration (Pt^{3+} ion). Fig. 2 shows the model of the $[\ Pt(\ CN)_4\ Cl_2\ ]^{3-}$ molecular complex.

The possible d – orbital energy level schemes in $[\ Pt(\ CN)_4\ Cl_2\ ]^{3-}$ complex, displayed in Fig.3, can be predicted by considering symmetry arguments. In a six – coordinate octahedral field, the five independent d – orbitals split into a lower energy triplet, t_{2g}, and a higher – energy doublet, e_g where the doublet is composed of the d_{z^2} and $d_{x^2-y^2}$ orbitals whose electron density is directed at the ligands; therefore, the doublet is destabilized by electron repulsion relative to the triplet. The three possibilities that result as the tetragonal field increases are shown as cases A, B and C (Fig.3.) Case C gives the correct energy - level ordering for the $[\ Pt(\ CN)_4\ Cl_2\ ]^{3-}$ molecular complex [4,12].

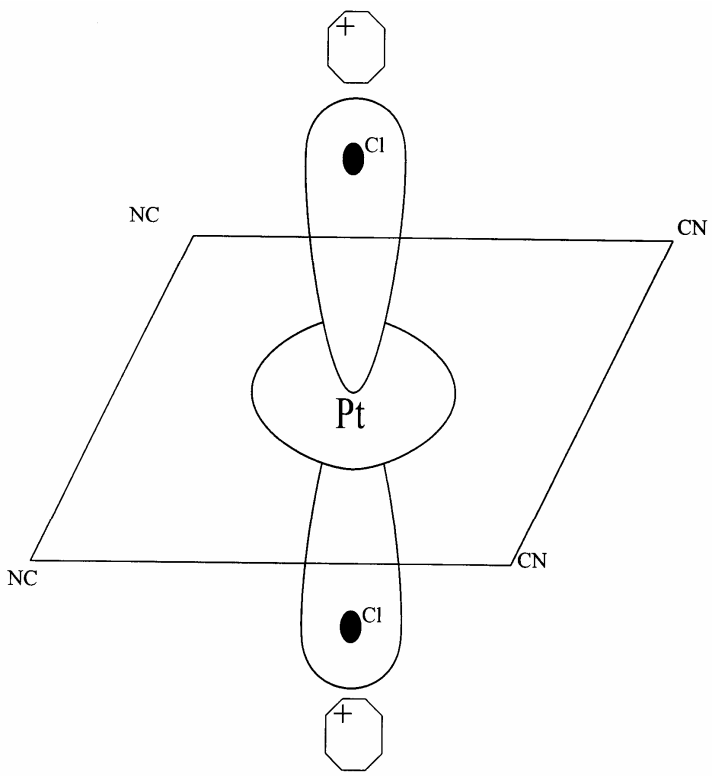

Figure 2. A possible model of the axially distorted [$Pt(CN)_4$ $Cl_3]^{3-}$ complex having d^7 configuration

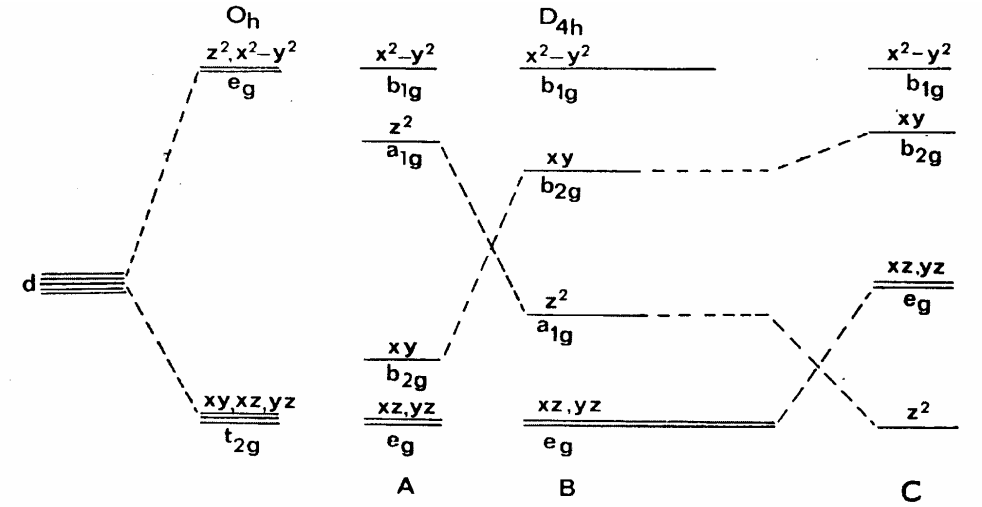

Figure 3. Ordering of the five d orbitals in an octhaedral field with an axially elongated tetragonal distortion increasing from A to C

3. The Spin Hamiltonian parameters for d^7 low spin platinum complexes

The observed EMR spectra in PtMC can be described by the following axial – spin Hamiltonian [6]:

$$H = \mu_B \left[g_{\parallel} S_z B_z + g_{\perp} (S_x B_x + S_y B_y) \right] + \sum_{k=1}^{n} \left[A_{\parallel} S_z \boldsymbol{I}_{zk} + A_{\perp} (S_x \boldsymbol{I}_{xk} + S_y \boldsymbol{I}_{yk}) \right] + \sum_{i=1}^{2} \left[A^{L}_{\parallel,i} S_Z I^{L}_{Z,i} + A^{L}_{\perp,i} (S_X I^{L}_{X,i} + S_y I^{L}_{y,i}) \right] \quad (2)$$

where the first and second term represent the electron Zeeman and magnetic hyperfine interaction with Pt nuclei, respectively. Here, *n* denotes the number of equivalent Pt nuclei over which the charge of spin is delocalized in Q1D conductors, **I** is the total nuclear spin operator and the other notations have their standard meanings. The third term, appropriate for $[Pt(CN)_4Cl_2]^{-3}$ complexes, represents the superhyperfine interaction with two equivalent chlorine ligands ($I^L = 3/2$).

For a C_{4v} or D_{4h}, low spin $5d^7$ system and the unpaired electron (or hole) in a d_{z^2} orbital, the crystal - field g – values can be calculated by carrying the theoretical treatment to second order. After succesively applying the spin-orbit operator and the Zeeman operator over the excited states, in the hole formalism, the following g – values result [19,20]

$$g_{\parallel} = 2N^2 - 3N^2 \left(\frac{\lambda}{\Delta E} \right)^2 \quad (3)$$

$$g_{\perp} = 2N^2 + 6N \frac{\lambda}{\Delta E} - 6N^2 \left(\frac{\lambda}{\Delta E} \right)^2$$

where N is the normalization coefficient of the zero – order configuration in the wave function that arises from the spin – orbit interaction, ΔE the crystal – field splitting between E(e_u) and E(a_{2u}) and λ the spin -orbit coupling constant.

The Pt atom has two stable isotopes with a natural abundance r = 0.337 for ^{195}Pt and r = 0.663 for ^{194}Pt. Only the former one has a non-vanishing nuclear spin, I = 1/2, giving rise to the hyperfine interaction. For the same axially distorded low spin system, the ^{195}Pt hyperfine tensor elements can be expressed by [19]

$$A_{\parallel} = -K + \frac{1}{7} P \left(4N^2 \beta^2 + 12 a^2 - 6 a N \right) \quad (4)$$

$$A_{\perp} = -K + \frac{1}{7} P \left(-2N^2 \beta^2 - 9a^2 + 45 a N \right)$$

where K is the isotropic hyperfine interaction, P is the dipolar hyperfine interaction given by $P = g_N \mu_N g_e \mu_e < r^{-3} >_{5d}$, $a = \lambda / \Delta E$ and β^2 is the total spin density in the d_{z^2} orbitals corresponding to the covalency. If the covalency is ignored ($\beta^2 = 1$) and by taking into account an adequate combinations of signs for the experimental

determined $A_{\|}$ and $A_{\perp}$, the solution to Eq.(4) results is a value for P that agrees in sign and order of magnitude with the theoretical value [21]. The covalency could be estimated from Eq. (4) if we use a value P = 54.4 [mT] for Pt^{3+}, the value obtained by extrapolation from Hartree – Fock calculations of the free ions [19].

The core polarization hyperfine field per unit spin, χ, is obtained from K by [21]

$$\chi\,[\text{u.at.}] \;=\; -\frac{3}{2}\mathrm{K}\left(\frac{\mathrm{h\,c\,a_0^3}}{\mathrm{g_e\;g_N\;\mu_e\;\mu_N}}\right)\cdot 10^{-4} \tag{5}$$

where K is expressed in Tesla units. The effective field at the platinum nucleus due to the core polarization, B_{cp}, can be expressed as

$$B_{cp} = 2S\chi \tag{6}$$

In order to determine the principal values of the ^{195}Pt hyperfine tensor ($A_{\|}$, $A_{\perp}$) and the number *n* of platinum nuclei over which the electron spin is delocalized in Q1D – Pt conductors,we have developed a model in terms of coupled nuclear spins [8].It is based on the first two expressions of Eq.(2) where the coupled representation $M_{\mathbf{I}}$ = **I, I**-1**, ..., -I** with **I** = 1/2 *n* ,1/2 *n*-1,....,1/2 (odd number of equivalent nuclei) and **I** = 1/2 *n*,1/2 *n*-1,...., 0 (even number of equivalent nuclei) is introduced. One obtains the following expressions for the EMR line positions, B(**I**, $M_{\mathbf{I}}$), and the intensities, G(**I**, $M_{\mathbf{I}}$), of the hyperfine lines .

$$\begin{aligned}\mathrm{B}(\mathbf{I},\mathrm{M_I}) = \mathrm{B_0} - \frac{\mathrm{g_0^2}}{\mathrm{g^2}}\Bigg[\frac{\mathrm{g}}{\mathrm{g_0}}\mathrm{K M_I} + \frac{\mathrm{g_{\|}\,g_{\perp}^2}}{\mathrm{g^4}}\,\frac{(\mathrm{A_{\|}^2 - A_{\perp}^2})}{2\mathrm{B_0 K^2}}\,\mathrm{M_I^2}\sin^2\theta\cos^2\theta + \\ + \frac{\mathrm{A_{\perp}^2\,(A_{\|}^2 + K^2)}}{4\mathrm{B_0 K^2}}\,(\boldsymbol{I}\,(\boldsymbol{I}+1) - \mathrm{M_I^2})\Bigg]\end{aligned} \tag{7}$$

$$\mathrm{G}(\boldsymbol{I},\,\mathrm{M}_{\boldsymbol{I}}) = \sum_{2\mathrm{I}\le 2\mathrm{I}'\le \mathrm{n}} \frac{\mathrm{P}(2\mathrm{I}')}{\mathrm{S}_{2\mathrm{I}'}} \tag{8}$$

The meaning of the notation used in Eqs.(7) and (8) can be found in [8].

As already mentioned, for low spin Pt – tetracyanide complexes of the $[Pt(CN)_4Cl_2]^{-3}$ type an superhyperfine interactions with two equivalent chlorine nuclei is expected. When two chlorines couple equivalently, there are three combinations with different probabilities because of the different natural abundance of ^{35}Cl and ^{37}Cl, viz., ^{35}Cl - ^{35}Cl (probability 9/16), ^{35}Cl - ^{37}Cl (probability 6/16) and ^{37}Cl - ^{37}Cl (probability 1/16). Since for the investigated Pt – species the spectrum is not resolved for various isotopic species, we will consider that the superhyperfine interaction of the unpaired electron with two equivalent ^{35}Cl (I_L = 3/2) stands predominantly over the others [18].

Considering the molecular orbital (MO) scenario, the principal values (axial symmetry) of the superhyperfine interaction with the chlorine ligands can be expressed by [22]

$$A_{\parallel}^{Cl} = A_s^{Cl} + 2A_p^{Cl}$$
$$A_{\perp}^{Cl} = A_s^{Cl} - A_p^{Cl} \quad (9)$$

where A_s^{Cl} and A_p^{Cl} are the isotropic and unisotropic(dipolar) contributions to the chlorine superhyperfine interaction, respectively. They correspond to the magnetic interaction between the unpaired spin in the d_{z^2} orbital of Pt and the polarized electron density in the chlorine s and p orbitals.

The existence of transferred hyperfine interaction to the chlorine ligands is a direct measure of the covalency in Pt – tetracyanide complexes. The spin densities at the ligands can be written as [23]

$$f_S = \frac{A_s^{Cl}}{A_{3s}^0} \qquad f_p = \frac{A_p^{Cl}}{A_{3p}^0} \quad (10)$$

where

$$A_{3s}^0 = (8\pi/3)\, g_e\, g_n\, \mu_B\, \beta_n \left| \psi(0) \right|_{3s}^2 \quad (11)$$
$$A_{3p}^0 = (2/5)\, g_e\, g_n\, \mu_B\, \beta_n \langle r^{-3} \rangle_{3p}$$

represent the superhyperfine coupling parameters assuming one unpaired electron occupying a 3s or a 3p chlorine orbital, respectively. By assuming the more recent values for the atomic parameters $\left| \psi(0) \right|_{3s}^2$ and $\left\langle r^{-3} \right\rangle_{3p}$ [25], one gets $A_{3s}^0 = 204.21 \quad \text{mT}$ and $A_{3p}^0 = 6.25 \quad \text{mT}$.

Since in the Pt – complexes of $[Pt(CN)_4Cl_2]^{3-}$ type the superhyperfine interaction implies the interaction with two chlorine nuclei, the total spin density transferred to the ligands amounts to $2(f_s + f_p)$ and corresponds to the hybridization ratio f_s / f_p.

4. Pt – Hyperfine interaction and the charge delocalization in Q1D conductors

EMR experiments on Pt – Q1D conductors can be performed in a wide temperature range and different orientations of the magnetic field with respect to the metal chain axis *c*. In what follows, I will only point at a particular temperature where the EMR linewidth, $\delta B_{1/2}$, goes through a minimum in KCP(Br) [7, 24, 25] or the hyperfine pattern typical of MGS is best resolved [8,14,18]. The analysis of the results presented here will be done within the framework of the mixt – valence model where the thermally excited holes (or electrons) across the energy gap contribute to the electronic and magnetic properties [13] : On the other hand, some of the relaxation and lineshape phenomena observed by NMR in KCP(Br) may be caussed either by spin carrying solitons via hyperfine interaction or by spinless solitons via quadrupolar and chemical shift interactions [26]. A theory of soliton formation in Pt – Q1D conductors was recently proposed [27,28].

The minimum at T = 85 K in the temperature dependence of $\delta B_{1/2}$ in KCP(Br) arises from two competing process: a hole – phonon collision broadening and a motional narrowing at high and low temperatures, respectively.Thus, in our considerations we will refer to this particular linewidth assuming the unresolved hyperfine pattern to be the main source of its broadening.

From Figs. 4a and 5 one can see the appearance of a hyperfine structure for MGS but no such hyperfine splittings are observed in the spectrum corresponding to KCP(Br). In both cases we atribute these resonances to the hyperfine interaction of one hole associated with d_{z^2} orbitals with several coupled Pt nuclei along the linear chain [8].

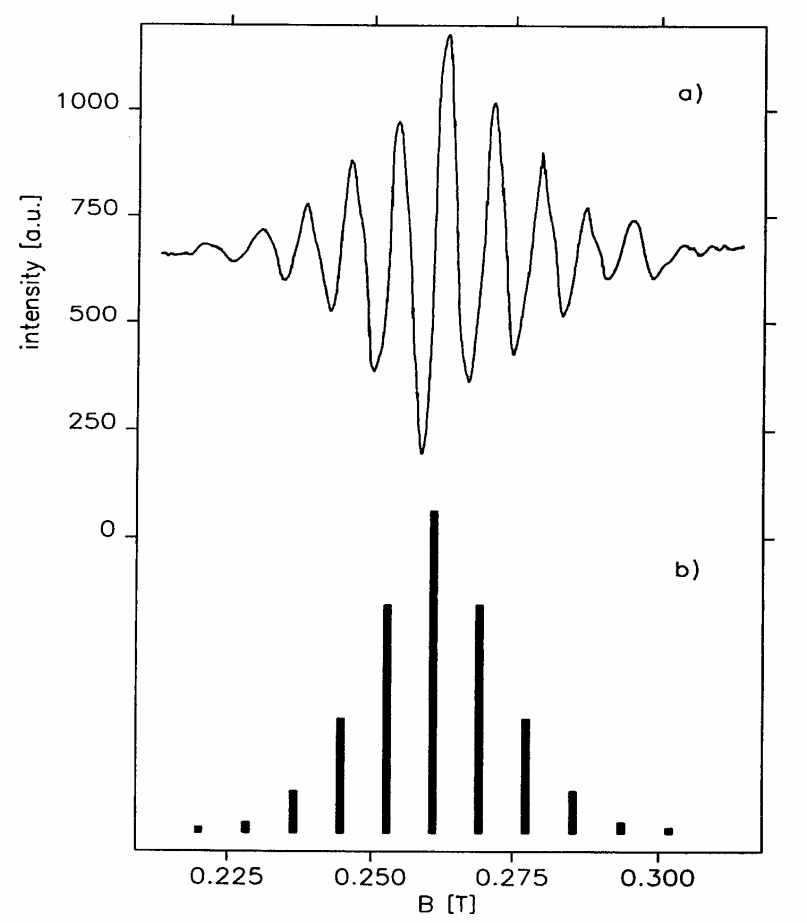

Figure 4: a) Single crystal EMR spectrum of MGS at X-band, T = 77 K and B ⊥ c.
b) Theoretical hyperfine intensity pattern for *n* = 7 coupled Pt nuclei along the chain

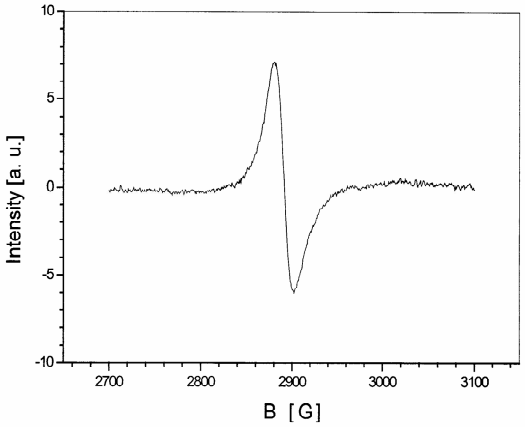

Figure 5. Single crystal EMR spectrum of KCP(Br) at X -band, T = 85 K and B⊥ c.

In the case of MGS the observed intensity distribution of the hyperfine pattern agrees well with the theoretical predictions of hyperfine interaction with n = 7 adjacent Pt nuclei (Fig.4b). By comparing the experimentally determined hyperfine line positions, B($\mathbf{I}$, M_I) and the corresponding intensities, G($\mathbf{I}$, M_I) with the calculated ones (Eqs.7 and 8) the principal values of the hyperfine tensor were extracted.

In order to determine the charge delocalization along the Pt - chain and the platinum hyperfine tensor elements in KCP(Br), the experimental linewidth at T = 85 K having a Lorentzian shape and $\delta B_{1/2}$ = 11.2 mT could be fitted with the spectra obtained from the numerical simulations based on Eqs. (7) and (8). We have considered both, the simplified situation of infinitely narrow hyperfine lines (Fig.6) and the more realistic one where a finit linewidth δB_0 = 3.2 mT [19] was taken into account (Fig.7). In the formal case the resulting EMR spectrum is represented by the envelope of the hyperfine pattern while in the latter one it results from the convolution of the individual hyperfine lines which now overlap.

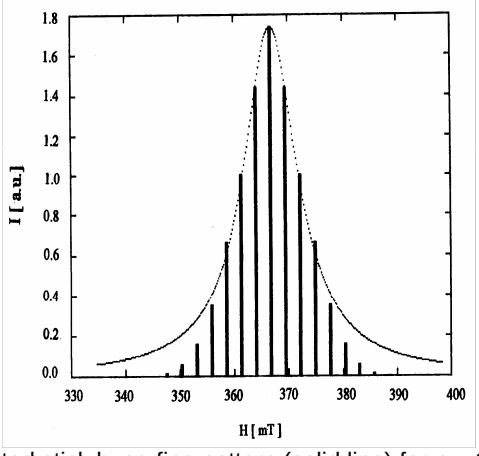

Figure 6. The simulated stick hyperfine pattern (solid line) for n = 11 and $A_{||}$ = 5.2 mT, $A_{\perp}$ = 6.5 mT for the absorbtion EMR line in KCP(Br) at T = 85 K and B ⊥ c (dotted line)

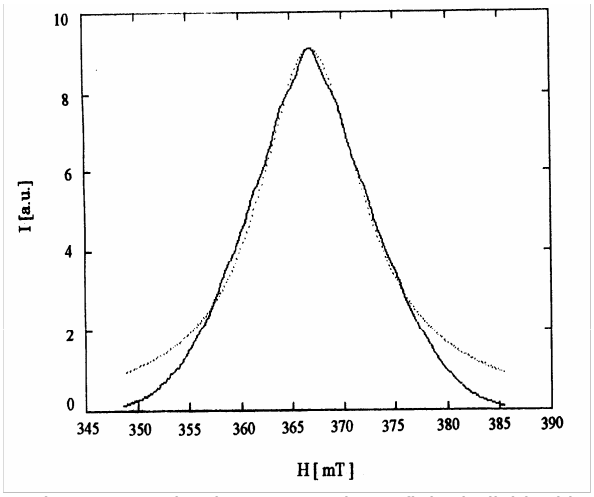

Figure 7. The same as in Fig.6 except that a finite individual hyperfine linewidth δ_0 = 3.2 mT, was considered

The best fit with the experimental EMR spectrum at T = 85 K corresponds to a charge delocalization extended over *n* = 11 Pt – nuclei along the chain and the Pt – hyperfine interaction parameters given in Table 1.

Tabel 1

Hyperfine interaction parameters for $5d^7$ low spin platinum species with d_{z^2} ground state and the unpaired electron delocalized over *n* coupled Pt nuclei

Compus	$A_{\|\|}$ [mT]	$A_{\perp}$ [mT]	*n*	χ [at.u.]	B_{cp} [T]	$< r^{-3} >_{5d}$ [at.u.]
Pt^{3+} free ion				-17.9	- 71.5	13.3
K_2PtCl_4	47.5	66	2	9.3	38.9	12.2
EPO	65	40.5	2	13.3	56	13.0
MGS: Fe^{3+}	9.4	12.6	5	-12.8	-54	11.8
MGS	11.9	15.5	7	-12.9	-54.7	5.7
KCP(Br)	5.2	6.5	11	- 0.8	- 3.1	0.6

The wide extension of the localized orbits along the chain axis is not surprising and the results obtained by EMR are consistent with an assumed localization of the electronic states as a result of disorder over distances of 10 lattice sites [29].

The large charge delocalization in Pt -Q1D, MGS and KCP(Br), finds further confirmation by the largely reduced values of the Pt – hyperfine tensor elements as compared with those measured in K_2PtCl_4 [19], $Pt(en)_2Cl(ClO_4)_2$ (or EPO) [30] and MGS doped with Fe^{3+} [31], where delocalization over *n* =2 Pt nuclei was observed in the first two compounds (Table 1).

By using Eqs. (4), (5) and (6), one could get the hyperfine interaction parameters χ, B_{cp} and $\left\langle r^{-3} \right\rangle_{3p}$ which are summarized in Table 1, together with the parameters corresponding to the above mentioned compounds.

The reduced values of B_{cp} compared with the theoretical one for Pt^{3+} free ion (B_{cp} = -71.5 T [19]) implies the likely existence of a small 6s contribution to the ground state. The spin – unrestricted Hartree – Fock calculations show that the occupancy of an (n+1)s orbital lying outside the partially filled *nd* shell contributes a term in χ opposite in sign to the *nd* core polarization [32]. Under D_{4h} symmetry, the s and d_{z^2} orbitals have the same irreducible representations and the mixture is allowed by symmetry.

Core polarization effects are also expected to produce a negative Knight shift which was confirmed in KCP(Br) by Pt – NMR in the low temperature insulating state [33]. From the P – values one could get the $\left\langle r^{-3} \right\rangle_{5d}$ parameters which are considerably less than the theoretical value of 13.3. at.u.This also reflects a large delocalization of the hole orbit along the Pt -nuclei chain.

Following the procedure described in Cap.3, the evaluated covalency factor $\beta^2 \approx 0.6$ gives strong evidence for quite a large transfer of the $5d_{z^2}$ charge density in to the ligands in Q1D [8].

5. Nature of binding in molecular Pt – tetracyanide complexes

The angular variation investigations of $[Pt(CN)_4Cl_2]^{3-}$ molecular complexes produced by irradiation in KCl and NaCl single crystals revealed a tetragonal symmetry C_{4v} or D_{4h} for the point group of the ground state of Pt^{3+} ion.The EMR spectra show the characteristic platinum hyperfine structure with an additional well-resolved pattern of seven equally spaced lines with the intensity ratio 1:2:3:4:3:2:1 suggesting a superhyperfine interaction with two equivalent chlorine nuclei (I^L = 3/2) [4]. A typical perpendicular component of the EMR psectrum is shown in Fig. 8.

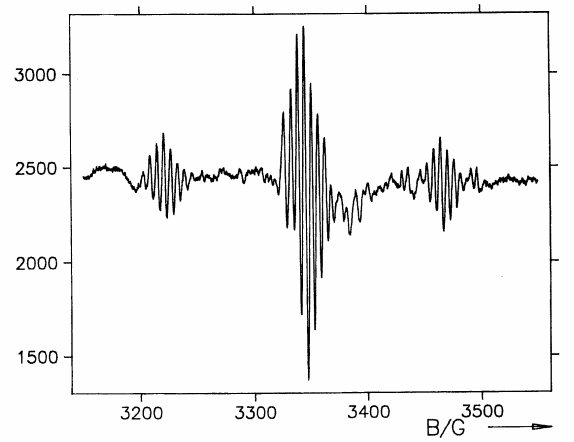

Figure 8. The perpendicular EMR spectrum of $[Pt(CN)_4Cl_2]^{3-}$ complex in KCl at T = 77K and B|| [100]

The analysis of the spectroscopic properties could be done by means of the spin Hamiltonian given in Eq.(2) with *n* = 1. Here x,y and z are the principal axis parallel to the [100], [010] and [001] crystal axis respectively, z axis being perpendicular to the plane of four CN^- ions.

The spin Hamiltonian parameters for $[Pt(CN)_4Cl_2]^{3-}$ molecular complexes stabilized in NaCl [4,12] and KCl [18] single crystals are represented in Table 2. Here, the principal values of the hyperfine and superhyperfine tensors are given in units of mT.

Tabel 2

Spin Hamiltonian parameters for low spin d^7 platinum complexes of $[Pt(CN)_4Cl_2]^{3-}$ type in alkali halides at T = 77K

	NaCl	KCl
$g_{\parallel}$	1.988	1.991
$g_{\perp}$	2.253	2.704
$A_{\parallel}(^{195}Pt)$	27.72	28.33
$A_{\perp}(^{195}Pt)$	41.65	44.78
$A^L_{\parallel}(^{35}Cl)$	4.210	3.690
$A^L_{\perp}(^{35}Cl)$	1.360	1.230

The g – factors, Pt – hyperfine and Cl -superhyperfine coupling parameters are consistent with a low spin d^7 configuration, the unpaired electron being localized in an 5 d_{z^2} orbital.

In order to discuss the influence of the charge state of the metal ion and the host lattice spacings on the metal – ligand binding, one has to consider the folllowing isoelectronic and isostructural sets of $[M(CN)_4Cl_2]^{m-}$ complexes (M = Co, Ni, Rh, Pt).

m	5	4	3
$3d^7$		Co^{2+}	Ni^{3+}
$4d^7$		Rh^{2+}	
$5d^7$			Pt^{3+}

Values of $g_{\parallel}$ for these complexes are very close to the free electron value, g_e = 2.0023, but $g_{\perp}$ - values are larger and vary considerably. This is consistent with excitation from the filled $d_{xy, yz}$ orbitals to the half – filled d_{z^2} orbital when the magnetic field is in the xy plane [34] .

In the MO – picture, $g_{\perp}$ - shift i.e. $\Delta g_{\perp} = g_{\perp} - g_e$ (Eq.(3)) is proportional to the $\beta^2 / \Delta E$ where β^2 is a measure of the covalency [35]. it could serve as the useful guide for discussing the strenght of the metal ligand binding in conjunction with the superhyperfine data. Table 3 shows a comparison between g- shifts and $\beta^2 / \Delta E$ values corresponding to various $[M(CN)_4Cl_2]^{m-}$ complexes.

The following clear – cut trends are observed:

(i) $\beta^2 / \Delta E$ decreases when the oxidation state of the metal ion increases from +2 to +3. It is understandable on the basis of stronger electrostatic attraction of the Cl^- ligands towards to metal ion with increasing positive charge on the metal ion.

Table 3.

$g_\perp$ - shifts for $[M(CN)_4Cl_2]^{m-}$ complexes in alkali halides

Ion	Lattice	$\Delta g_\perp$	$(\alpha^2/\Delta E)\times10^{-5}$
Co^{2+}	KCl	0.303	9.8
	NaCl	0.191	6.2
Ni^{3+}	NaCl	0.151	3.5
Rh^{2+}	KCl	0.294	3.9
	NaCl	0.222	3.0
Pt^{3+}	KCl	0.268	1.2
	NaCl	0.250	1.0

(ii) due to the very nature of the d_{z^2} orbital, its energy and overlap with the ligand orbitals are very sensitive to the changes in the metal ion – axial ligand distance. Therefore, one would expect considerable influence of the lattice size on the $g_\perp$- factor. For $[Pt(CN)_4Cl_2]^{3-}$ complexes in KCl and NaCl, the increase in overlap and the reduction in $\Delta g_\perp$ are consistent with the decrease in lattice size from KCl to NaCl.

(iii) The values of β^2 / ΔE in the isostructural and isoelectronic Ni^{3+} ($3d^7$) and Pt^{3+} ($5d^7$) complexes clearly ilustrate the expected trend that the 5d ions tend to be more covalent than the 3d ions, on account of the larger spread of the d orbitals and consequent increase in the overlap with chlorine ligand orbitals.

The analysis of the experimental Pt -hyperfine tensor elements by means of Eqs. (4) – (6) results in the hyperfine parameters given in Table 4.

Table 4.

^{195}Pt – hyperfine interaction parameters for $[Pt(CN)_4Cl_2]^{3-}$ complexes

	K [mT]	χ [at.u.]	B_{CP} [T]
KCl	53.1	-19.5	-82.0
NaCl	51.2	-18.9	-79.5

The hyperfine field at the Pt nucleus in $[Pt(CN)_4Cl_2]^{3-}$ molecular complexes results mainly from core polarization effects ($\chi < 0$) and the corresponding value is larger than the theoretical one for free Pt^{3+} ion (Table 1). In the Pt – tetracyanide complexes, the polarizing unpaired electron occupies a d_{z^2} molecular orbital which can be strongly delocalized. Therefore, one could attribute the large negative χ values to an expansion of the unpaired electron d_{z^2} molecular orbital [36].

6. Ligand superhyperfine interaction and the spin density distribution

The chlorine superhyperfine structure in $[Pt(CN)_4Cl_2]^{3-}$ molecular complexes showed a tetragonal symmetry. Based on the experimental superhyperfine tensor elements (Table 2), the evaluated isotropic and dipolar contributions, the spin densities transferred to the chlorine s and p orbitals and the hybridization ratio (Eqs. (9) – (11)) are summarized in Table 5.

Table 5.

EMR parameters for chlorine ligands in $[Pt(CN)_4Cl_2]^{3-}$

	A_s^{Cl} [mT]	A_p^{Cl} [mT]	f_s %	f_p %	$2(f_p+f_s)$ %	f_p / f_s
KCl	2.15	0.76	1.05	12.20	26.5	11.6
NaCl	2.41	0.88	1.18	14.08	30.5	11.9

One could compare the ligand field parameters of the Pt – complexes with the corresponding ones for the isoelectronic and isostructural $[M(CN)_4Cl_2]^{m-}$ sets (Table 6).

Table 6.

Chlorine superhyperfine parameters and the axial ligand spin densities for $[M(CN)_4Cl_2]^{m-}$ complexes in alkali halides

Ion	Lattice	A_s^{Cl} [mT]	A_p^{Cl} [mT]	f_s %	f_p %	f_p / f_s
Co^{2+}	KCl	0.81	0.23	0.39	3.80	9.7
	NaCl	1.07	0.28	0.52	4.45	8.5
Ni^{3+}	NaCl	1.70	0.87	0.83	13.77	16.4
Rh^{2+}	KCl	1.87	0.55	0.91	8.76	9.5
	NaCl	2.21	0.66	1.08	10.59	9.8
Pt^{3+}	KCl	2.15	0.76	1.05	12.20	11.6
	NaCl	2.41	0.88	1.18	14.08	11.9

It is clear that the mixing of chlorine 3s and 3p orbitals with the metal d - orbitals increases when the covalency is increased, i.e. from the $3d^7$ to $5d^7$ configuration. As it was pointed out from $g_\perp$ - shift analysis (Cap. 5), the overlap strongly depends on the alkali halide lattice size.

The increased covalency in $[Pt(CN)_4Cl_2]^{3-}$ complexes could be explained by taking into account the strong σ -acceptor character of the chlorine ions, resulting in a very extended molecular wave function with appreciable spin density far from the Pt –nucleus.

In order to evaluate the distribution of the total spin density in $[Pt(CN)_4Cl_2]^{3-}$ complexes, one has to consider the MO – scenario where the ground state could be describe by an antibunding molecular orbital of a_{1g} symmetry made up of platinum $|5d_{z^2}\rangle$ and $|6s\rangle$ atomic orbitals and the ligand $|3p\rangle$ and $|3s\rangle$ levels[22]. The wave function describing this molecular orbital is given by

$$\psi(a_{1g}) = N\left[\Phi_m - \frac{C}{\sqrt{2}}(\overline{\sigma}_1 + \overline{\sigma}_2)\right] \tag{13}$$

where Φ_m represents the metal orbitals and $\overline{\sigma}_1$ and $\overline{\sigma}_2$ are the axial chlorine sigma orbitals.
Now,

$$\Phi_m = \beta \left| 5d_{z^2} \right\rangle \pm (1-\beta^2)^{1/2} \mid 6s \rangle \tag{14}$$

and

$$\overline{\sigma}_i = \alpha \left| 3p_i \right\rangle \pm (1-\alpha^2)^{1/2} \left| 3s_i \right\rangle \tag{15}$$

The spin densities transferred to the chlorine s and p orbitals can be expressed as

$$f_p = \frac{1}{2} N^2 C^2 \alpha^2$$
$$f_s = \frac{1}{2} N^2 C^2 (1-\alpha^2) \tag{16}$$

where N, C and α are the molecular orbital coeficients in Eqs.(13) and (15).

Considering EMR parameters for chlorine ligands (Table 5), the calculated values of NC and α are

	NC	α
KCl	0.51	0.95
NaCl	0.55	0.96

We can now write the ligand σ - antibonding orbitals as

$$\overline{\sigma}_i = 0.95 \left| 3p_i \right\rangle \pm 0.28 \left| 3s_i \right\rangle \quad \text{in KCl} \tag{18}$$

$$\overline{\sigma}_i = 0.96 \left| 3p_i \right\rangle \pm 0.26 \left| 3s_i \right\rangle \quad \text{in NaCl} \tag{19}$$

The orbital coefficients corresponding to Φ_m could be derived by taking into account that the spin density in the $5d_{z^2}$ orbital for a d^7 (Pt^{3+}) ion is given by

$$\beta^2 = \frac{P_{exp}}{P_{teor.}} \tag{20}$$

where P_{exp} and P_{teor} are the experimental and theoretical dipolar hyperfine couplings for Pt^{3+} ion, respectively (Cap.3 and Eq. (4)). Evaluation gives

$$\beta^2 = 0.77 \quad \text{in KCl} \tag{21}$$

$$\beta^2 = 0.73 \quad \text{in NaCl} \tag{22}$$

Therefore, the Pt – molecular orbital has the form

$$\Phi_m = 0.94 \left| 5d_{z^2} \right\rangle \pm 0.48 \left| 6s \right\rangle \qquad \text{in KCl} \qquad (23)$$

$$\Phi_m = 0.86 \left| 5d_{z^2} \right\rangle \pm 0.52 \left| 6s \right\rangle \qquad \text{in NaCl} \qquad (24)$$

Since the experimental EMR spectra correspond to a hyperfine coupling with one ^{195}Pt nucleus and two axial ^{35}Cl ligands, the total spin density is distributed as

$$\beta^2 \left[Pt^{3+}\right] + 2(f_p + f_s)\left[Cl^-\right] \qquad (25)$$

Finally, one obtains the following distributions of the total spin density in $[Pt(CN)_4Cl_2]^{3-}$ molecular complexes stabilized in alkali halides

$$0.77\,(Pt^{3+}) + 0.26\,(Cl^-) \qquad \text{in KC l} \qquad (26)$$

$$0.73\,(Pt^{3+}) + 0.31\,\,(Cl^-) \qquad \text{in NaCl} \qquad (27)$$

It confirms the accuracy of the evaluated hyperfine coupling parameters and the correctness of the molecular model used for the data interpretation.

Conclusions

EMR spectroscopy has proved to be a very sensitive method for the investigation of platinum molecular complexes. In Q1D – platinum conductors a large charge delocalization along the chain axis was found. It is also confirmed by the reduced values of ^{195}Pt – hyperfine tensor elements. The molecular orbitals scenario can well describe the spectroscopic properties of $[Pt(CN)_4Cl_2]^{3-}$ complexes. Due to the high covalency of these complexes there is a considerable amount of spin density transferred to the chlorine ligands. The EMR parameters strongly depend on the alkali halide lattice size in which $[Pt(CN)_4Cl_2]^{3-}$ is stabilized by irradiation.

Acknowledgements

I would like to thank Prof. I.Ursu for the continous support given during the investigation of platinum molecular complexes. I also appreciate many enlightning discussions with Prof. M.Mehring during the visiting scientist program at the University of Stuttgart.

REFERENCES

[1]. Zeller H.R.: Festkörperprobleme **13**, 31 (1973)

[2]. Little W.A.: Phys.Rev. **B13**, 235 (1985)

[3]. Manoharan P.T., Subramanian S., Rogers M.T. : J.Coord. Chem. **3**, 293 (1974)

[4]. Giurgiu L.V., Ursu I., Rogers Max T.: Bull. Magn. Reson. **2**, 171 (1981)

[5]. Vugman N.V., Jain V.K.: Rev. Roum. Phys. **33**, 981 (1988)

[6]. Ursu I.: La Resonance Paramagnetique Eleatronique, Dunod, Paris, 1968

[7]. Knorr S., Filip X., Darabont A., Pana .O., Ordean R, Filip C., Giurgiu L.V., Mehring M.: Appl. Magn. Reson. **19**, 373 (2000)

[8]. Ordean R., Fekete R., Pana O., Filip C., Giurgiu L.V., Kesller C., Mehring M.: Rom. J. Phys. **43**, 481 (1998)

[9]. Williams J.M., Schultz A.J.in : Molecular Metals, Ed.. Hatfield W.E , (Plenum Press, New York) p.337, 1979

[10]. Mehran F., Scott B.A.: Phys. Rev. Lett. **31**, 99 (1973)

[11]. Giurgiu L.V., Ursu I.: Procc. XIX-th Congress AMPERE, Eds. Brunner K., Housser K.H. Schweitzer D. , Heidelberg , Germany, p.594 , (1976)

[12]. Ursu I., Giurgiu L.V.: Extended Abstracts of RAMIS Conference, Eds. Pislewski N., Stankowski J., Poznan, Poland, p.151 (1979)

[13]. Takahashi T., Doi H., Nagasawa H.: J. Phys. Soc. Japan **48**, 423 (1980)

[14]. Ursu I., Giurgiu L.V., Nagy G., Pana O.: Extended Abstracts RAMIS Conference ,Eds. Pislewski N., Stankowski J., Poznan, Poland, p.347 (1983)

[15]. Rüegg W., Kuse D., Zeller H.R.: Phys Rev. **B8**, 952 (1973)

[16]. Bloch A.H., Weisman R.B., Varma C.M.: Phys.Rev. Lett **28**, 753 (1972)

[17]. Mehran F., Scott B.A.: Phys. Rev. Lett. **31**, 1347 (1973)

[18]. Ursu I., Giurgiu L.V.: Procc. XXI-th Congress AMPERE, Eds. Pislewski N., Stankowski J., Poznan, Poland, p. 48, (1998)

[19]. Krigas T., Rogers Max T.: J. Chem. Phys. **55,** 3035 (1971)

[20]. Giurgiu L.V., Nicula A.: Studia Univ. Babes-Bolyai, Physica **2,** 63 (1978)

[21]. Freeman A.J., Malow J.W., Bagus P.: J. Appl. Phys. **41**,1321 (1970)

[22]. Abragam A., Bleaney B.: Electron Paramagnetic Resonance of Transitions Ions , Oxford, Clarendon, 1970

[23]. Owen J. Thornley J.H.M.: Rep. Prog. Phys. **29**, 675 (1966)

[24]. Giurgiu L.V. : Studia, Physica, Special Issue **1** , 55 (2001)

[25]. Giurgiu L.V., Filip X., Pana O., Filip C., Darabont A., Ordean R., Knorr S, Rahmer J , Mehring M.: J. Optoelectronics & Advanced Materials **2**, 371 (2000)

[26]. Mehring M., Kanert O., Mali M., Brinkmann D.: Solid State Comm. **33**, 225 (1980)

[27]. Pana O., Giurgiu L.V., Mehring M.: Solid State Comm. **84**, 651 (1992)

[28]. Pana O., Giurgiu L.V., Knorr S., Rahmer J., Grupp A., Mehring M.: Solid State Comm. **119**, 553, (2001)

[29]. Bloch A.H., Weisman R.B., Varma C.M.: Phys.Rev. Lett **28**, 753 (1972)

[30]. Kuroda M., Ito M., Nishina Y., Kawamori A., Kodera Y., Matsukawa T. : Phys. Rev **B 48** , 4245, (1992)

[31]. Mehran F., Interrante L.V.: Solid State Comm. **18**, 1031 (1976)

[32]. Bleaney B.: Phil. Mag. **42**, 441 (1951)

[33]. Niedoba H., Launois M., Brinkman D., Brugger R., Zeller H.R. : Phys. Stat. Sol. **58B** , 309, (1973)

[34]. Viswanath A.K., Rogers Max T.: J. Chem. Phys. **75**, 4183 (1981)

[35]. Jain S.C., Reddy K.V., Reddy Rs.T.: J. Chem. Phys **62**, 4366 (1975)

[36]. Goodings D., Heine V.: Phys. Rev. Lett. **5**, 370 (1960)

STUDIA UNIVERSITATIS BABEŞ-BOLYAI, PHYSICA, XLVIII, SPECIAL ISSUE, 2003

EPR STUDY OF S-STATE PARAMAGNETIC IONS FROM $4Bi_2O_3 \cdot PbO$ SYSTEM

S. SIMON

Babes-Bolyai University, Faculty of Physics, 3400 Cluj-Napoca, Romania

ABSTRACT. Vitreous samples belonging to $(100-x)[4Bi_2O_3 \cdot PbO]xMO$ system, where MO = Fe_2O_3, MnO or Gd_2O_3 and x = 1, 5, 10 and 20 mol %, were obtained by quickly undercooling of melts from 1100^{o}C to room temperature. The samples were partially crystallised by heat treatment applied for 5 hours at 550^{o}C followed by slowly cooling to room temperature.

The electron paramagnetic resonance study carried out both on glass and vitroceramic samples points out important differences regarding the surrounding of the investigated S-state ions. Clustering tendency favouring the devitrification of the matrix is evidenced in all cases with the increase of MO content. The highest stabilising effect on the vitreous lead-bismuthate network is notified for gadolinium.

Introduction

Generally obtained by quickly undercooling of melts, the glasses are metastable systems wherein several relaxation processes take place, which tend to eliminate the strength incorporated by "frozen" of a certain structural disorder degree typical to melt. The structural relaxation of glasses may imply only local rearrangements of the atoms or, in certain conditions, it may lead to the partial or complete crystallisation of starting glasses. The partial crystallisation results in vitroceramic materials having different properties also with respect to glasses and to crystals of the same composition. These properties of vitroceramics are essential for applications in electronics, electrotechniques, optoelectronics and medicine [1].

The glasses with high content of heavy metals, like Bi_2O_3 and PbO are intensely investigated due to their special properties as high density, high refraction index, excellent IR transmission and high polarisability [2-5]. All these properties recommend them for applications as thermal and mechanic sensors [5], wave-guides nonlinear optics [6], scintillation detectors in high-energy physics [6, 7]. At the same time the study of glasses containing low amounts of classical glass network formers like SiO_2, B_2O_3 or P_2O_5 and of glasses completely without traditional formers is very important for understanding the way in which is possible to form stable glasses in the absence of these classical formers.

After discovery of high temperature superconductivity [8] the bismuthate glasses received an additional interest having in view that the choose of an appropriate composition can represent precursors of oxide bismuth based superconductors [9-11]. It is known the stabilising effect of Pb in Bi(Pb)-Sr-Ca-Cu-O superconducting systems on 2223 phase with highest critical temperature [12] but it is not yet explained how contributes lead to this stabilisation. Therefore it is of great interest the investigation of binary bismuthate systems like Bi_2O_3-PbO for understanding the properties of the mentioned multicomponent systems.

The properties of glasses and vitroceramics are mainly determined by local order type and disorder degree from samples, therefore the local structure investigation is highly desired in order to understand the properties-structure correlation. The electron paramagnetic resonance (EPR), or electron spin resonance (ESR), spectroscopy [13, 14] proved to be one of the most efficient methods for characterisation of the local order and magnetic interactions from non-crystalline systems in general and in glasses in particular [15]. In the last 50 years, since the EPR method have been used for glass investigation [16], the studies carried out offered essential information to understand the correlation between the local order and macroscopic properties of the structural disordered materials [17-21]. The paramagnetic centres from glasses which can be investigated by EPR are either ions of transition metals, of rare earth elements or centres associated with electric charged or neutral defects. The paramagnetic ions are introduced in glass matrices to confer them special electric, magnetic or optic properties, or only in order to investigate indirectly the structural properties of these materials.

In this study we choose as paramagnetic ions Fe^{3+} ($3d^5$, $^6S_{5/2}$), Mn^{2+} ($3d^5$, $^6S_{5/2}$, I = 5/2) and Gd^{3+} ($^4f^7$, $^8S_{7/2}$). All these ions are in the S state and they are frequently used in the EPR investigation of glasses [22-35].

Experimental

The phase diagram for Bi_2O_3-PbO system (Fig.1) indicates that in the entire composition range the melting temperature is under 900°C with a minimum around $Bi_2O_3 \cdot 2PbO$. Beside this crystalline phase also occur the phases $3Bi_2O_3 \cdot 2PbO$ and $4Bi_2O_3 \cdot PbO$. Due to the fact that in the start compositions of bismuth based superconductors the ratio Pb/Bi is up to 0.3, it is interesting the investigation of vitreous and partially crystallised matrices having composition ranging between these phases. Preparation of $4Bi_2O_3 \cdot PbO$ vitreous matrix that corresponds to the highest bismuth content of a crystalline phase in Bi_2O_3-PbO binary system is rather difficult due to the crystallisation tendency and imposes high cooling rates of the melt.

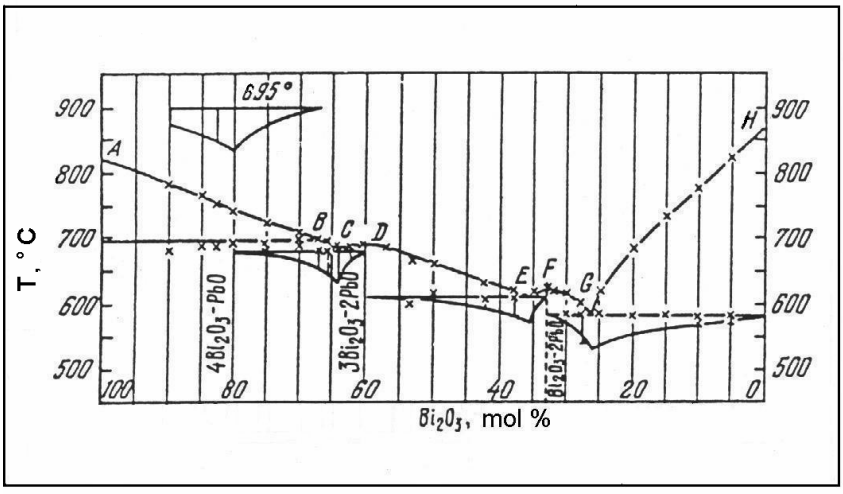

Fig. 1. Phase diagram of Bi_2O_3-PbO system [36].

Vitreous samples belonging to (100-x)[$4Bi_2O_3$·PbO]xMO system, where MO = Fe_2O_3, MnO or Gd_2O_3 and x = 1, 5, 10 and 20 mol % were obtained by quickly undercooling of melts from 1100°C to room temperature by pouring onto a stainless steel plate and pressing with a plate of same material. The samples were partially crystallised by heat treatment applied for 5 hours at 550°C followed by slowly cooling in furnace to room temperature. The crystalline phases developed in samples were identified by X-ray diffraction. The vitreous phase stability is improved by addition of transition metal or rare earth oxides and it proved to be dependent on their content in samples. The most stabilising effect on the vitreous matrix was observed by addition of Gd_2O_3.

EPR spectra of untreated and heat treated samples were recorded at room temperature, in X band (9.3 GHz) using a Bruker spectrometer type EPS 380.

Results and discussion

The main feature of the EPR spectra recorded from the three selected S-state ions introduced in the lead bismuthate matrix is the presence of relatively large lines, characterised by g > 2, occurring in the range of low magnetic fields, B < 2000 G. The energy state of these ions in an external magnetic field $\vec{B}$ is described in a first approximation by the spin Hamiltonian [37]:

$$\mathcal{H} = g_o \beta \vec{B} \vec{S} + D\left[S_z^2 - \frac{1}{3}S(S+1)\right] + E\left(S_x^2 - S_y^2\right)$$

where the first term is the Zeeman term and the next ones are second order terms of crystalline field, D and E are the axial respectively the rhombic constants of energy level splitting in zero magnetic field. Although for Gd^{3+} the upper order terms cannot been generally neglected in case of gadolinium ions in glasses the Gd^{3+} EPR spectra can be described by this Hamiltonian. The lines arising at $g \approx 2$ may be assigned to paramagnetic ions disposed in sites characterised by relatively weak crystalline fields an therefore the main term is the Zeeman term. The lines with g > 2 are attributed to paramagnetic ions disposed in sites of relatively intense crystalline field so that the crystalline field terms from the Hamiltonian are comparative or even larger than the Zeeman term [38].

A common feature of EPR spectra recorded from glass samples is that the line widths are higher than those corresponding to the crystalline samples. This fact is due to the inhomogeneities existing in the local order leading to differences from a resonant centre to other not only by the orientation of symmetry axes like in polycrystals axes but also by the enhancement of the distances to the neighbours from the first coordination sphere of the resonant centres. Taking into account this structural characteristics for simulating the EPR spectra are used distribution functions for the main parameters of the spin Hamiltonian as the components of g tensor and of hyperfine constant A.

The shape of EPR spectra recorded from samples with high content of paramagnetic ions is strongly affected by nature and strength of magnetic interactions between these ions. As the paramagnetic ions content increases the resonance lines become broader in the firs part of the concentration range, due to dipolar interactions and this effect is known as dipolar broadening of EPR lines. As the paramagnetic ions content is further increased between them occurs the superexchange interactions intermediated by oxygen atoms, that leads to the line narrowing and the effect is

know as exchange narrowing of EPR lines. This is a general behaviour in glass samples, with the remark that the concentration of transition metal ions at which the narrowing effect occurs is function of the matrix composition. The vitreous matrix wherein the paramagnetic ions are incorporated also influences the shape of EPR spectra. The neighbourhood of the paramagnetic ions is indeed the result of the competition between the structural characteristics of the vitreous matrix, which tends to impose to paramagnetic ions such a surrounding that will only weakly modify the network of the matrix, and the preference of paramagnetic ion for a certain surrounding. Evidently, the result of this competition is in favour of matrix for low contents paramagnetic ions and it is in favour of paramagnetic ions when their concentration is relatively high. The EPR spectra obtained for samples belonging to $4Bi_2O_3 \cdot PbO$ matrix which contain iron, manganese or gadolinium have different evolution, function on paramagnetic ions concentration and of the thermal history of the samples.

The Fe^{3+} EPR spectra of vitreous samples (Fig. 2a) are dominated by $g \cong 4.3$ line assigned to Fe^{3+} ions disposed in sites of low symmetry characterised by intense crystalline fields. The linewidth increases with iron oxide content as can be seen from Figure 3, showing that the dipolar interaction between the iron ions is increasing.

At the same time one remark an increase of $g \cong 2.0$ line intensity assigned to Fe^{3+} ions disposed in sites of octahedral symmetry, with low crystalline field. Between these ions the same dipolar interaction exists. The dipolar broadening of $g \approx 2.0$ line is given Figure 4.a. Despite the fact that at such high Fe_3O_3 content a narrowing of the linewidth is expected, due to superexchange interactions, the narrowing effect is not observed. We suppose that the iron is homogeneous distributed in the glass matrix and if such an effect could appear in some clusters it is masked by the dipolar broadening.

After heat treatment the shape of EPR spectra is considerably modified (Fig. 2b) especially for the samples with high Fe_2O_3 content. The EPR spectra of these samples consist mainly of a narrow line, extremely intense, with $g \cong 2.0$, typical for crystalline phases of magnetite type [31, 37]. Tacking into account that this line is more narrow (Fig. 4b) for the sample with x = 20 mol % than for that of the sample with x = 10 mol % one can conclude that in the first case the size of microcrystalites of magnetite type is much larger. In the samples with a lower Fe_2O_3 content the main effect of the applied heat treatment consist in the increase of the contribution given by the $g \cong 2.0$ line, and this happens mainly due to the structural relaxation of the neighbourhood surrounding Fe^{3+} ions that leads to a considerable decrease of the crystalline field strength at the sites occupied by these ions. In the EPR spectrum of the sample with x = 5 mol % the g = 2.0 line evidences contributions also from Fe^{3+} ions interacting by superexchange and disposed in crystalline grains. The prevalent presence of the line with $g \cong 4.3$ in the spectrum of the sample with x = 1 mol % Fe_2O_3 indicates that Fe^{3+} ions are placed also after heat treatment in sites typical for vitreous matrices.

The EPR spectra of the vitreous samples containing manganese (Fig. 5a) contain lines with $g \cong 4.3$ and 2.0 assigned to Mn^{2+} ions disposed in sites with intense crystalline field of low symmetry and in sites with weak crystalline field of octahedral symmetry, respectively. One remarks that the number of Mn^{2+} ions disposed in sites of weak crystalline field is larger than that of Fe^{3+} ions in the glasses of similar

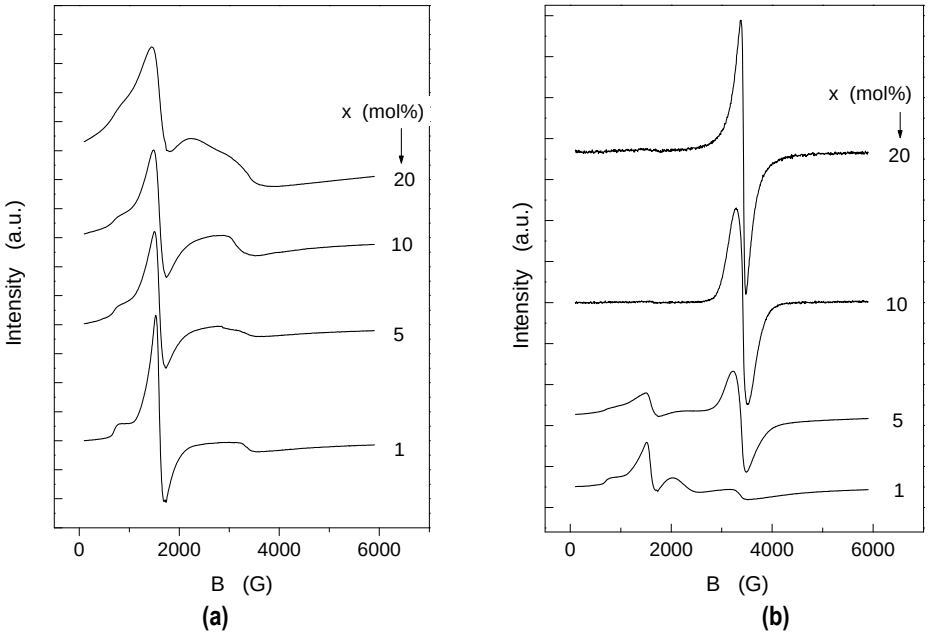

Fig. 2. EPR spectra of $xFe_2O_3(100-x)[4Bi_2O_3 \cdot PbO]$ samples before (a) and after (b) heat treatment.

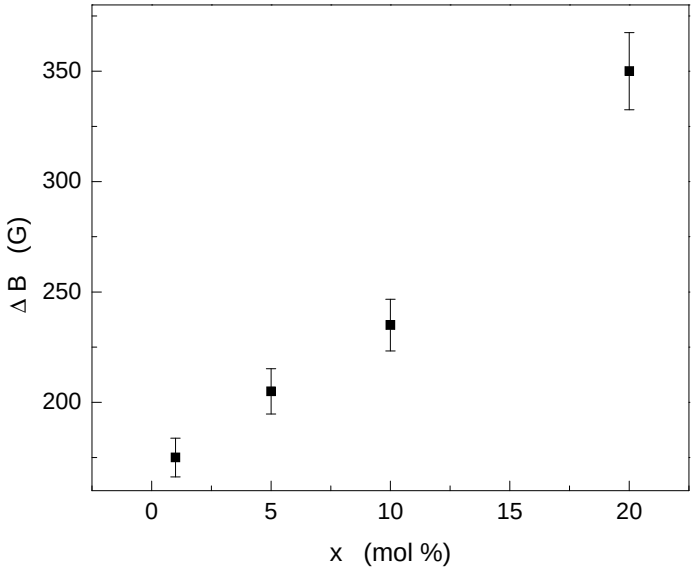

Fig. 3. Composition dependence of the linewidth at g ≈ 4.3 for $xFe_2O_3(100-x)[4Bi_2O_3 \cdot PbO]$ samples before heat treatment.

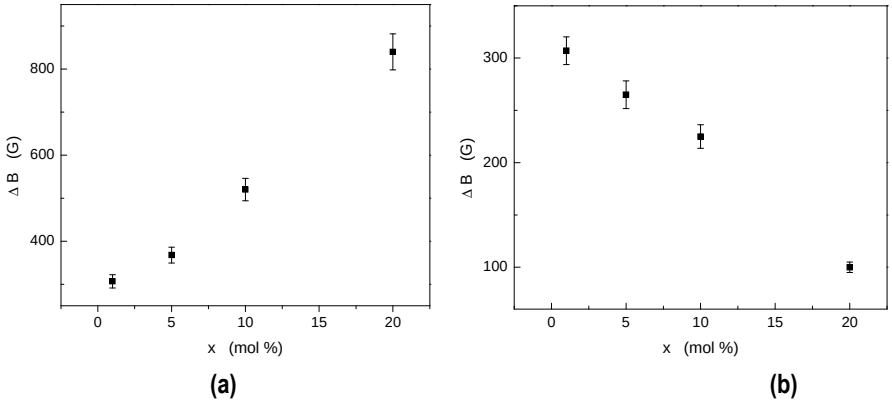

Fig. 4. Composition dependence of the linewidth at g ≈ 2.0 for $xFe_2O_3(100-x)[4Bi_2O_3 \cdot PbO]$ samples before (a) and after (b) heat treatment.

composition. It is surprising the tendency for resolving the hyperfine structure at the line with g ≅ 4.3 while the line with g ≅ 2.0 is without hyperfine structure. The lack of hyperfine structure for the line with g ≅ 2.0 is unusual for Mn^{2+} ions, especially at low contents, and this result is assigned to the fact that the local disorder degree around the sites characterised by octahedral symmetry is higher than around the sites of low symmetry responsible for the line with g ≅ 4.3.

The EPR spectra of the heat treated samples with high content of MnO (Fig. 5b) are dominated by a relative narrow line occurring at g ≅ 2.0, attributed to Mn^{2+} ions from crystalline phases between which there are superexchange interactions. The EPR spectrum of the sample with x = 1 mol % MnO consists of both g ≅ 4.3 and g ≅ 2.0 lines and the last one is more intense and has a well resolved hyperfine structure. This denotes that the heat treatment has induced a major structural relaxation around Mn^{2+} ions that determined both the decreasing of the crystalline field strength and a higher uniformity around the paramagnetic ions.

The Gd^{3+} EPR spectra of untreated samples (Fig. 6a) consist of the superposition of the well known U type spectrum [37, 38] with lines at g ≅ 5.9, 2.85 and 2 specific to Gd^{3+} ions in structural disordered systems, and of a resonance line occurring at g ≅ 4.8 which is unusual intense for vitreous systems. The lines from the U type spectrum are assigned to Gd^{3+} ions disposed in sites with intermediate crystalline field having the coordination number, N, higher than 6, while the line with g ≅ 4.8 is specific to Gd^{3+} ions placed in sites of intense crystalline field and having a low coordination number. Usually such coordinatively unsaturated species occur only at the surface of oxide systems [34]. Their existence in the vitreous system $xGd_2O_3(100-x)[4Bi_2O_3 \cdot PbO]$ proves that the glass matrix $[4Bi_2O_3 \cdot PbO]$ is extremely stiff and imposes to a part of Gd^{3+} ions a less usual coordination for the vitreous oxide matrices.

(a) (b)

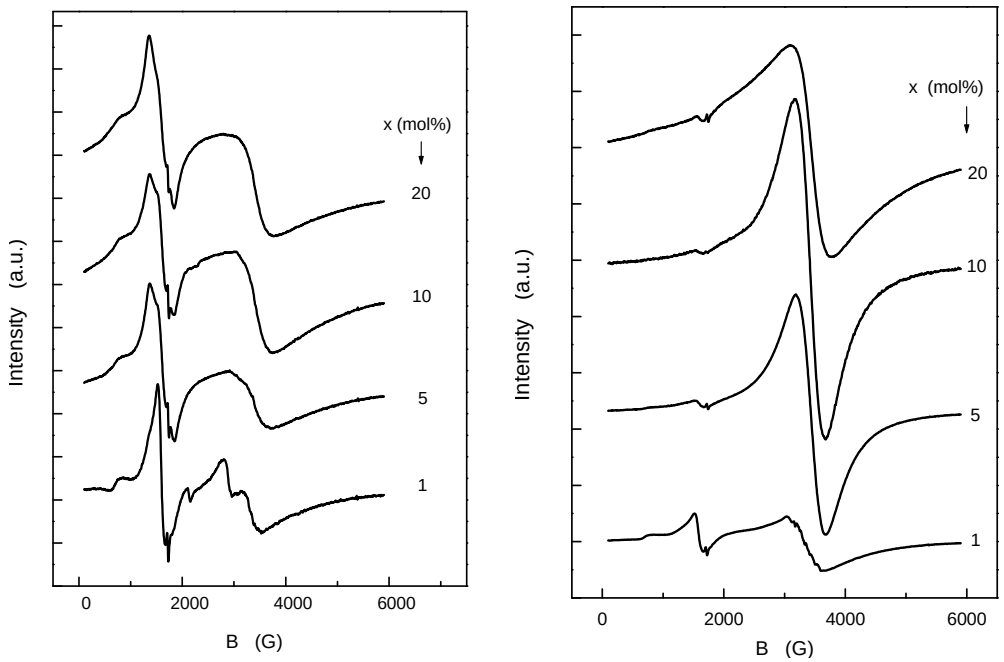

Fig. 5. EPR spectra of xMnO(100-x)[$4Bi_2O_3$·PbO] samples before (a) and after (b) heat treatment.

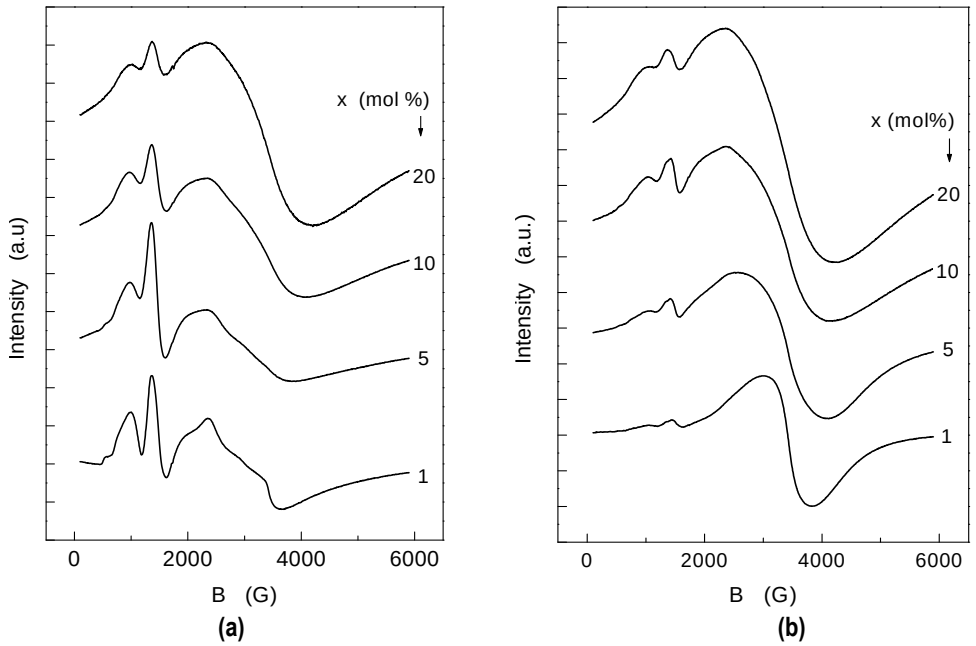

Fig. 6. EPR spectra of xGd_2O_3(100-x)[$4Bi_2O_3$·PbO] samples before (a) and after (b) heat treatment.

After heat treatment the EPR spectra recorded from samples with Gd_2O_3 (Fig. 6b) still contain the lines with $g > 2.0$ but they are dominated by $g \cong 2.0$ line which is relatively large and arises from Gd^{3+} ions disposed in crystalline phases and interacting preponderantly by dipolar interactions. The significant presence of the lines with $g > 2.0$, specific to Gd^{3+} ions in disordered matrices and, especially the insignificant difference between the EPR spectra recorded from the samples with $x = 10$ and $x = 20$ mol % untreated and heat treated, are arguments which support the assumption that gadolinium has a stabilising effect on vitreous matrix network [24].

Conclusions

The electron paramagnetic resonance study carried out on glasses and vitroceramics belonging to $xMO(100-x)[4Bi_2O_3 \cdot PbO]$ system (MO = Fe_2O_3, MnO or Gd_2O_3, $x \leq 20$ mol %) points out differences in the surrounding of the investigated S-state ions. Despite these differences the EPR results for all paramagnetic ions show that the lead-bismuthate matrix imposes to them sites with low coordination number and high crystalline field.

It is evidenced the clustering tendency of Fe^{3+} ions with the increase of Fe_2O_3 content what favours the devitrification of the matrix wherein the magnetite type crystallites act as crystallisation germs.

Mn^{2+} ions are in this lead-bismuthate matrix preponderantly incorporated in sites characterised by strong crystalline field of low symmetry. After heat treatment the Mn^{2+} ions are further disposed in the partially crystallised samples in disordered neighbourhoods but the main part of them occupy weak crystalline field of octahedral symmetry.

Gadolinium has a stabilising effect on the formation of vitreous network in samples. Gd^{3+} ions are relatively uniform distributed in samples so that only dipolar type interactions are evidenced between these ions even for high concentration. Unusual high fraction of Gd^{3+} ions are situated in the sites of high crystalline field and low coordination number as result of the stiffness of the lead-bismuthate matrix.

REFERENCES

1. K.Ohura, M.Ikenaga, T.Nakamura, T.Yamamuro, Y.Ebisawa, T.Kokubo, Y.Kotoura, M.Oka, J. Appl. Biomaterials, 2, 153 (1991)
2. W.H. Dumbaugh, J.C. Lapp, J. Am. Ceram. Soc. 75, 9, 2315 (1992)
3. S. Hazra,A. Ghosh, Phys. Rev, B 51, 851 (1995)
4. Y.Dimitriev, V.T. Mihailova, J. Sci. Lett, 9, 1251 (1990)
5. S. Hazra, A.Ghosh, Phys. Rev, B 56, 13 (1997)
6. C. Stehle, C. Vira, D. Hogan, S. Feller, M. Affatigato, Phys. Chem. Glasses, 39, 2, 836 (1998)

7. S.E. Van Kirk, S.W. Martin, J. Am. Ceram. Soc., 75, 4, 1028 (1992)
8. J.G. Bednorz, K.A. Müller, Z. Phys. B, 64, 189 (1986)
9. T. Komatsu, R. Sato, K. Imai, K. Matusita, T. Yamashita, J Appl. Phys, 27L 550 (1998)
10. T. Minami,Y.Y. Akamatsu, M. Tatumisago Tohge,Y. Kowada, J Appl. Phys, 127L, 777 (1998)
11. S. Simon, M. Cri¿an, Supraconductibilitatea la temperaturi înalte, University Press, Cluj-Napoca, 1998
12. S.M. Green, C. Jiang, Y. Mei, H.L. Luo, C. Politis, Phys. Rev. B, 38, 5016 (1988)
13. I. Ursu, Rezonanß¾ Electronic¾ de Spin, Editura Academiei, Bucure¿ti, 1965
14. Al. Nicula, Rezonanß¾ Magnetic¾, Editura Didactic¾ ¿i Pedagogic¾, Bucure¿ti, 1980
15. D.L. Griscom, J. Non-Cryst. Solids, 40, 211 (1980)
16. R.H. Sands, Phys. Rev. 99, 1222 (1955)
17. R. Stößer, M. Noty, Glastechn. Ber. Glass Sci. Technol., 67, 156 (1994)
18. S.Simon, Al.Nicula, Solid State Commun., 39, 1251 (1981)
19. S.Simon, Al. Nicula, Nucl. Instr. and Methods, 1-2, 199 (1982)
20. S.Simon, Al. Nicula, Glastech. Ber. 56K, 2, 904 (1983)
21. S.Simon, Al .Nicula, J. Non-Cryst. Solids, 57, 23 (1983)
22. D.L. Griscom, Glass Science and Technology, eds. D.R. Uhlman and N.J. Kreidl, vol. 4B, Academic Press, 1990, p.151
23. S.Simon, Al.Nicula, Studia Physica 27, 59 (1982)
24. S.Simon**,** Al.Nicula, Phys. Status Solidi (a), 81, Kl (1984)
25. S.Simon**,** Gh.Ilonca, I.Barbur, I.Ardelean, R.Redac, Physica C, 162-164, 1289-1290 (1989)
26. S.Simon**,** Al.Nicula, Rev. Roum. de Phys., 28, 1, 57 (1983).
27. I.Ardelean, E.Burzo, D.Mitulescu-Ungur, S.Simon, J. Non-Cryst. Solids 146, 256-260 (1992)
28. I.Ardelean, M.Peteanu, V.Simon, S.Filip, M.Flora, S.Simon, Phys. and Chem. of Glasses, 41, 3, 153 (2000)
29. S.Simon, I.Ardelean, M.Peteanu, M.Pop, R.Stefan, Mod. Phys. Lett. B, 14, 2, 59 (2000)
30. R.Stefan, S.Simon, Mod. Phys. Lett. B, 15, 3, 111 (2001)
31. S. Simon, D. Eniu, A. Pasca, D. Dadarlat and V. Simon, Mod. Phys. Lett. B, 15, 21, 921 (2001)
32. S.Simon**,** A. van der Pol, E.J.Reijerse, A.P.M. Kentgens, G.J.M.P. van Moorsel, E.de Boer, J.Chem. Soc. Faraday Trans. 90, 2663-2670, (1994)
33. S.Simon**,** A. van der Pol, E.J.Reijerse, A.P.M. Kentgens, G.J.M.P. van Moorsel, E.de Boer, J.Chem. Soc. Faraday Trans. 90, 2663-2670, (1994)

34. S.Simon, Mod. Phys. Lett. B, 12&13, 375 (2001)
35. S.Simon, I.Ardelean, S.Filip, I.Bratu, I.Cosma, Solid State Commun., 116, 83 (2000)
36. Phase Equilibrium Diagrams, Am. Ceram. Soc. Publ., Westerville, 1998 L. Belladen, Gazz. Chim. 52, 162 (1922)
37. D.L. Griscom, J. Non-Cryst. Solids, 67, 81 (1984)
38. L.E.Iton, C.M.Brodbeck, S.L.Suib and G.D.Stucky, *J. Chem. Phys*., 79, 1185(1983)

STUDIA UNIVERSITATIS BABEŞ-BOLYAI, PHYSICA, XLVIII, SPECIAL ISSUE, 2003

ESR STUDY OF SOME METAL-COMPLEXES WITH THEOPHYLLINE AND NUCLEOTIDES

O. COZAR, L. DAVID, V. CHIŞ

Dept. of Physics, Babeş-Bolyai University, 3400 Cluj-Napoca

ABSTRACT. The $CuT_2L_2 \cdot H_2O$ complexes [T= Theophylline (1,3-dimethylxanthine), L=NH_3, n-propylamine (npa)] where prepared and investigated by ESR spectroscopy. Powder ESR spectrum of $CuT_2(NH_3)_2 2H_2O$ is axial ($g_{\|}$ = 2.255, $g_{\perp}$ = 2.059). ESR spectrum of $CuT_2(npa)_2 2H_2O$ is a superposition of one axial ($g_{\|}$ = 2.299, $g_{\perp}$ = 2.064) and one isotropic component (g_0 = 2.100). The axial spectra of the former complexes are due to a statistic Jahn-Teller effect (E_{JT} = 2880 cm^{-1}). ESR investigation of Cu(II) complexes with guanosine-5'-monophosphate (5'-GMP) and cytidine-5'-monophosphate (5'-CMP) shows the affinity of Cu(II) ion to interact with the base and the phosphate groups. The different modes of the coordination of the metallic ion at the nucleotide and the water molecules lead to octahedral species, distorted by dynamical Jahn-Teller effect (g_0 = 2.106) for Cu(II)–5'-CMP complex and rhombically distorted (g_1 = 2.358, g_2 = 2.126, g_3 = 2.068) or tetragonally distorted ($g'_{\|}$ = 2.299, $g'_{\perp}$ = 2.126) for Cu(II)–5'-GMP complex.

INTRODUCTION

The cooper (II) complexes with organic ligands are intensely studied in the last years owing to theirs medical implications [1]. The biological activity of these compounds is influenced by the manner in which the cooper(II) ions coordinate the ligands molecules. As a part of our work about metal complexes with molecules of biological interest [2-6], we investigate the Cu(II) – theophylline and Cu(II) – nucleotides compounds. Transition metal complexes containing theophylline (1,3-dimethylxanthine) and amine type ligands may serve as model for coordination of metal ions to nucleic acids through their oxopurine base. Structural and thermal stability of these compounds can provide additional data to a better understanding of their possible genetic role and/or anti-tumor activity derived by interactions between nucleic acids and certain metal ions [7-8]. In previous papers, the theophylline (Fig. 1) was studied as a model for guanine-metal ion interaction, of great importance in problems concerning the division and replication of DNA molecules [9,10].

In relation to their mode of coordination at the nucleotides and nucleic acids and their chemical properties the metal ions have been classified in three types [11]: “hard” (a-class), “soft” (b-class) and borderline metals. Hard metals interact especially with the oxygen atoms while the soft metals interact with nitrogen and sulfur atoms. Concerning metal-nucleic acid interaction, it has been proved [12] that metals belonging to the a-group have greater affinity for the phosphate group, b-class metal for the heterocyclic base while the borderline ions form complexes both with the base and the phosphate group. (Fig.2)

The coordination of the Cu(II) ion to the theophylline molecules is usually realised at its N(7) atom, by deprotonation [13]. If the preparation of theophylline complexes is attempted from aqueous solutions of ammonia or primary amines, then coordination compounds consisting of both theophyllinato and amine ligands can occur, whose structure is, in general, not predictable [14]. The amine molecules can alter the local structure around the Cu(II) ion, depending on the mono or bidentate character of these molecules and the interplay between steric and electronic contributions.

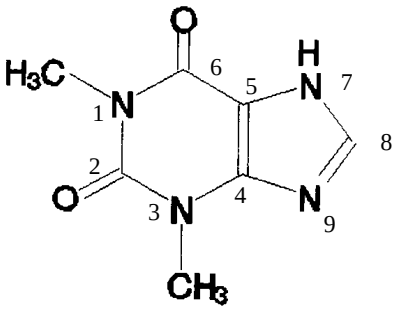

Fig. 1 - The molecular structure of theophylline.

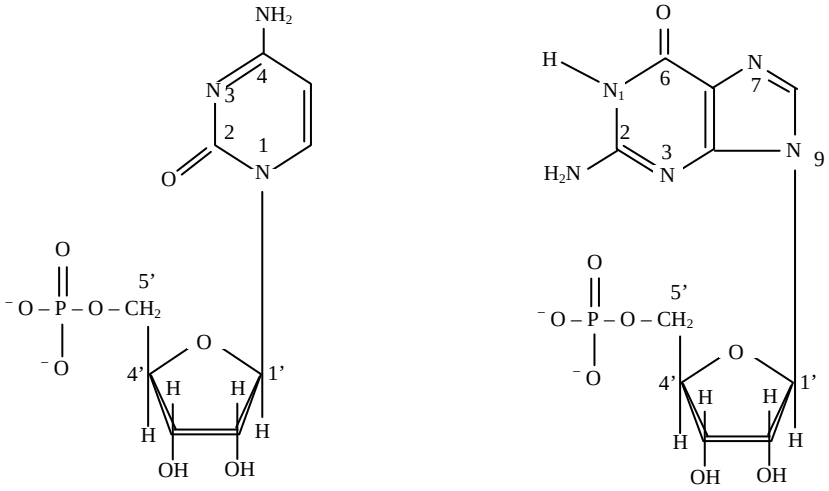

Fig. 2 - The structural formulae of 5'-CMP and 5'-GMP nucleotides.

In the case of Cu(II)–5'-GMP the Cu(II) ion can interact with N7 and/or O6 atoms of the guanosine. In Cu(II)–5'-CMP the N3 and/or O2 are the active sites of the cytidine for the coordination of the metallic ion [15]. The interaction with the phosphate oxygen may be realized either directly, like in a great number of monomeric complexes, or through hydrogen bonds via the water molecules [16].

Our research regards the Cu(II) coordination mode at the nucleotides, the local symetry around the metallic center and also the stability of these complexes in aqueous solution.

2. EXPERIMENTAL

The $CuT_2L_2 \cdot H_2O$ compounds were prepared according to the procedure described in paper [12,13]. The IR spectra indicate a similar behavior of the $CuT_2(NH_3)_2 2H_2O$ and $CuT_2(npa)_2 2H_2O$ complexes, the Cu(II) ion being coordinate in each case by two theophylline and two amine molecules with characteristic $CuN_2N^*_2$ chromophore [17].

These complexes have been investigated in powder samples and in DMF solutions in the 143-293 K temperature range and also in DMF solutions adsorbed on NaY zeolite.

Disodium salt of 5'-GMP from Boehringer Mannheim GmbH, disodium salt of 5'-CMP from Sigma Chemical Co. (99 %) and Cu(II)-nitrate trihydrate (>99 %) from Fluka were used without further purification. The 1:1 Cu(II)–5'-CMP and Cu(II)–5'-GMP complexes were prepared by adding 0.45 mol·dm^{-3} aqueous solution of copper(II)-nitrate trihydrate to 0.45 mol dm^{-3} aqueous solution of the corresponding nucleotide at room temperature. A greenish-blue precipitate was obtained for the Cu(II)–5'-GMP complex and a blue one for the Cu(II)–5'-CMP. Complex-water 1:10 solutions were also prepared for both Cu(II)-nucleotide complexes. A part from these solutions was then adsorbed on SiO_2 (ARCC-4). EPR spectra of copper-nucleotide complexes as powder samples, water solutions and adsorbed solutions on SiO_2 were recorded at 9.4 GHz (X band) using a standard JEOL-JES-3B equipment with a magnetic field modulation of 100 kHz.

3. RESULTS AND DISCUTIONS

a. Cu(II) – theophylline complexes

Powder ESR spectra of the $CuT_2L_2 \cdot H_2O$ are shown in fig. 3. The axial spectrum of $CuT_2(NH_3)_2 \cdot 2H_2O$ compound with $g_{||} = 2.255$ and $g_{\perp} = 2.059$ values suggests a compressed pseudotetrahedral symmetry around the metallic ion. The 4.5 value of the G parameter ($G = (g_{||} - 2.0023)/(g_{\perp} - 2.0023)$), inside of the usually interval (4÷5), indicates that the experimental data suit to molecular g values. The shape of the spectrum and the **g** tensor values remain unchanged by lowering the temperature at 143K.

Powder ESR spectrum of $CuT_2(npa)_2 \cdot 2H2O$ complex (Fig. 4) shows a super-position between an axial ($g_{||} = 2.299$ and $g_{\perp} = 2.064$) and isotropic ($g_o = 2.100$) components. The **g** values remain unchanged when the temperature decreased at T = 143 K, while the amplitude of the isotropic spectrum decreases too.

The axial spectra of the powder complexes containing (NH_3) and (npa) are due to the compression of the CuN_4 tetrahedron lengthwise of one S_4 axis owing to a static Jahn-Teller effect (resulting a flattened tetrahedral local configuration). This effect appear by the vibronical coupling between the electronic states of T_2 symmetry and the active E vibrational mode in the cubic group [18]. The isotropic spectrum which

appear for $CuT_2(npa)_2 2H_2O$ complex correspond to one trigonal specie compressed lengthwise a C_3 axis owing to a dynamic Jahn-Teller effect ($T_2 \otimes T_2$ vibronical coupling). The amplitude of thus spectrum decrease with the lowering of the temperature because of the diminution of the tunnel effect between the three paraboloid of the potential surface (the probability of this effect $P \approx \exp(-3E_{JT}/k_BT)$, where E_{JT} is the Jahn-Teller energy) [18,19].

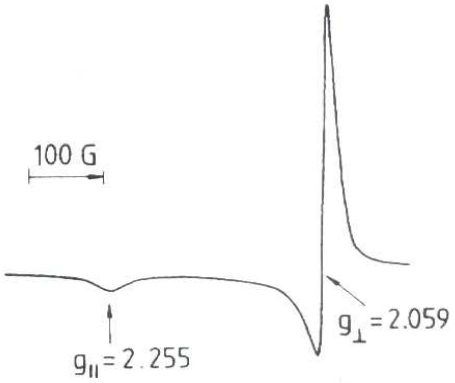

Fig. 3 - Powder ESR spectrum of $CuT_2(NH_3)_2 \cdot 2H_2O$ complex at room temperature.

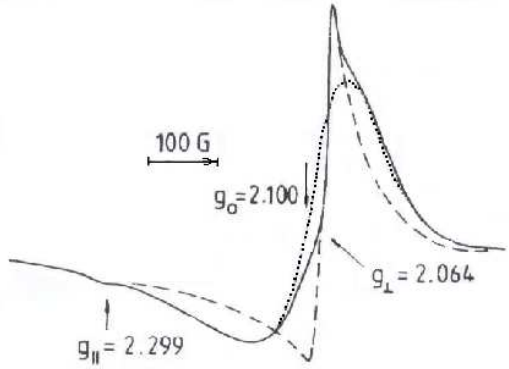

Fig. 4 – Powder ESR spectrum of $CuT_2(npa)_2 \cdot 2H2O$ complex at room temperature.

The monomeric compressed pseudotetrahedral species are present in DMF solutions too (Fig. 5). The isotropic values $g_0 = 2.106$, $A_0 = 62$ G for $CuT_2(npa)_2 \cdot 2H_2O$ and $g_0 = 2.125$, $A_0 = 64$ G for $CuT_2(NH_3)_2 \cdot 2H_2O$ and the shape of the spectra are similar to that obtained for other reported Cu(II)-proteins and Cu(II)-enzymes with the metallic ion surrounded by four nitrogen atoms [20].

Both complexes present axial symmetries around the metallic ion in DMF solutions adsorbed on NaY zeolite (Fig. 6). The $g_{||}$ values correspond to a dominant square-planar local symmetry (or strong compressed pseudotetrahedral symetries) and the $A_{||}$ values are typical to a $CuN_2N^*_2$ chromophore (Table 1).

Table 1

ESR parameters of DMF Cu(II)-theophylline solution adsorbed on NaY zeolite at room temperature

Compound	$g_{\|\|}$	$g_\perp$	$\|A_{\|\|}\|$ (G)	α^2	β^2	δ^2
$CuT_2(NH_3)_2$	2.254	2.060	178	0.83	0.61	0.60
$CuT_2(npa)_2$	2.246	2.057	174	0.81	0.61	0.60

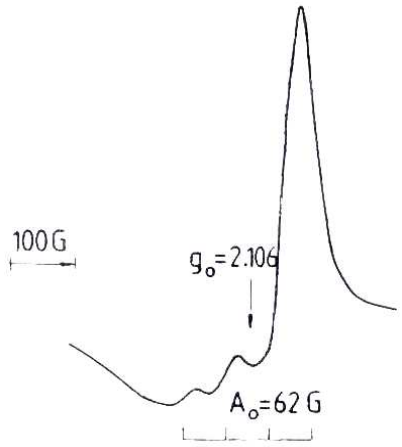

Fig. 5 - ESR spectrum of $CuT_2(npa)_2 \cdot 2H_2O$ in DMF solution at room temperature.

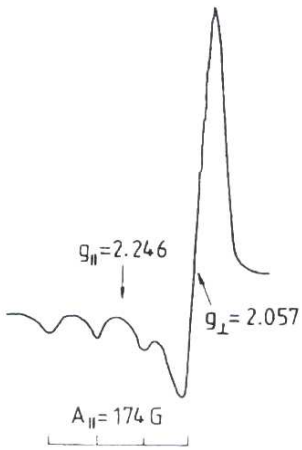

Fig. 6 - ESR spectrum of DMF $CuT_2(npa)_2$ solution adsorbed on NaY zeolite at room temperature.

The average of the g values is the same in powder, DMF solutions and DMF solutions adsorbed on NaY zeolite for the compressed pseudotetrahedral species, this fact suggesting the stability of the complexes in solutions. In the $g_\perp$ region of $CuT_2(npa)_2 \cdot 2H_2O$ spectrum there are resolved nine superhyperfine lines owing to the interaction of the paramagnetic electron with four magnetic equivalent nitrogen atoms (a^N = 15G). For $CuT_2(NH_3)_2 \cdot 2H_2O$ complex, the superhyperfine structure is not resolved and the signals of the parallel band are broader then these given the previous case. This is a result of the small dimension of the (NH_3) molecules which allows the existence of dipolar interactions between the metallic ions.

In the case of species presenting a static Jahn-Teller effect, the molecular coefficients (α, β, δ) have been evaluated with the help of LCAO-MO procedure typical for square-planar configuration [21]. The obtained values (Table 1) show a ionic character of the σ bond in the (xOy) plane and a covalent character of the π bonds in and out the plane.

b. Cu(II) – nucleotides complexes

Powder EPR spectra of the Cu(II)–5'-CMP and Cu(II)–5'-GMP complexes obtained at room temperature suggest different local symmetries around Cu(II) ions.

The simulation of the Cu(II)–5'-CMP experimental spectrum (Fig. 7, thick line) indicates a superposition between an axial spectrum, with the copper(II) hyperfine structure resolved in the parallel band ($g_{||}$ = 2.265, $A_{||}$ = 162 G, $g_\perp$ = 2.076) (Fig. 7, thin line) and an isotropic spectrum (g_0 = 2.106) (Fig. 7, dotted line). Both components have the same contribution at the experimental spectrum.

The $R = g_{||} / |A_{||}|$ = 133 cm value for the axial spectrum indicates a square-planar symmetry around the metallic ion [22]. By comparing the obtained values of the g_{II} = 2.265 and A_{II} = 162 G parameters with those reported in the case of other copper(II) complexes with mixed N and O ligands (peptides in aqueous solutions) [23],

we may conclude that in the xOy plane there are three oxygen atoms and one nitrogen atom ($CuNO_3$ chromophore). The nitrogen atom and one oxygen atom proceed from cytosine (N3,O2) and the other two oxygens from phosphate groups [24].

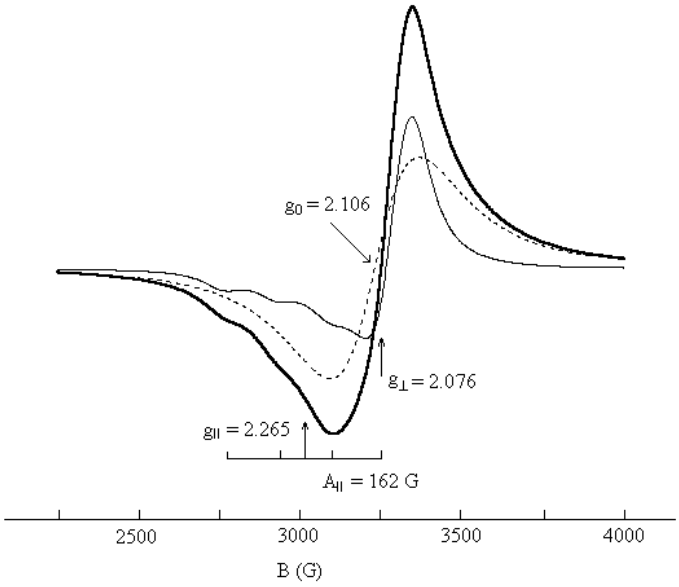

Fig. 7. The powder EPR spectrum of Cu(II)–5'-CMP: the experimental spectrum (thick line), the axial component (thin line), the isotropic component (dotted line).

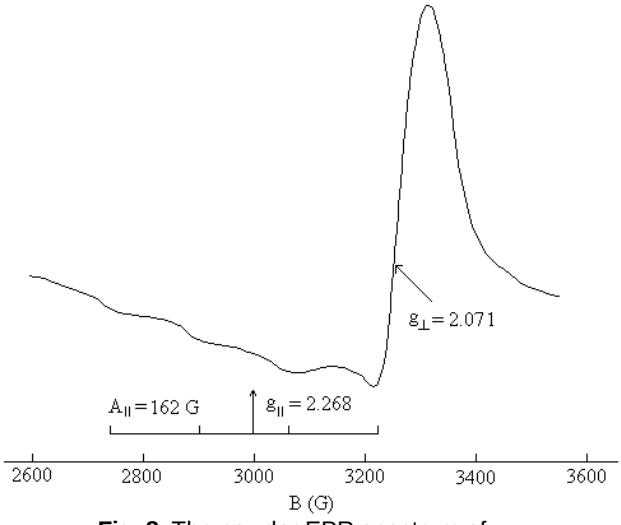

Fig. 8. The powder EPR spectrum of Cu(II)–5'-CMP after one year.

The isotropic spectrum corresponds to an hexacoordinated octahedral symmetry species distorted by a dynamic Jahn-Teller effect [18]. The Cu(II) ion interacts here with the cytosine base, the phosphate group and two coordination water molecules.

The species presenting dynamic Jahn-Teller effect vanishes in time. The spectrum recorded after one year (Fig. 8) reveals only the axial component, with a less resolved hyperfine structure ($g_{\|} = 2.268$, $A_{\|} = 162$ G, $g_{\perp} = 2.071$).

Consequently, the interaction with the cytosine base and phosphate groups is stronger than that with water molecules and thus the square-planar species is more stable in time.

The EPR powder spectrum of Cu(II)–5'-GMP complex (Fig. 9) also suggests the presence of two hexacoordinated nonequivalent species in the 9:10 ratio. One species shows a rhombic spectrum with g_1 = 2.358, g_2 = 2.126, g_3 = 2.068 corresponding to a rhombic distorted octahedral symmetry [13] and the other has an axial spectrum with $g'_{\|}$ = 2.299 and $g'_{\perp}$ = 2.126, corresponding to one tetragonally distorted octahedral symmetry. Thus, it is probable that the interaction of Cu(II) with 5'-GMP nucleotide occurs through the N7 and O6 atoms of guanine and also through the phosphate group. After a period of one year, both components of the spectrum become axial ($g_{\|}$ = 2.351, $g_{\perp}$ = 2.112 and $g'_{\|}$ = 2.310, $g'_{\perp}$ = 2.112, respectively) (Fig. 10). o absorption signal at $g \approx 4$ due to the forbidden $\Delta M_S = \pm 2$ transitions characteristic for coupled copper(II) ions (S = 1) [19] was observed in the spectra of these complexes. Thus even in the solid-state (powder samples) only the Cu(II)-monomeric species prevail.

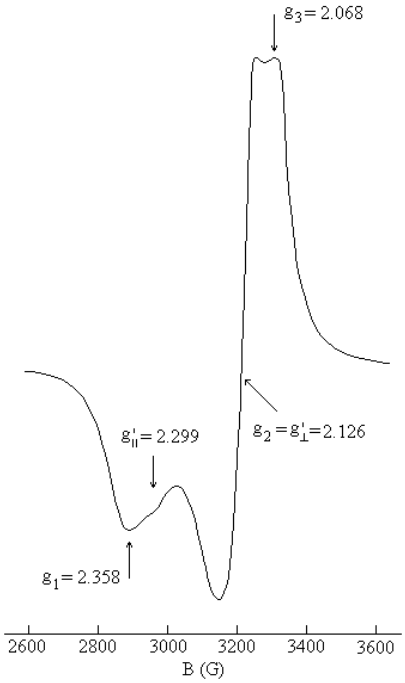

Fig. 9 - The powder EPR spectrum of Cu(II)–5'-GMP.

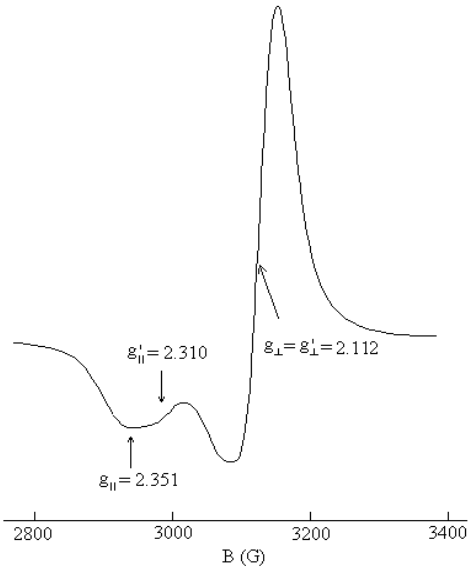

Fig. 10 - The powder EPR spectrum of Cu(II)–5'-GMP after one year.

In aqueous solution, the EPR spectrum of Cu(II)–5'-CMP complex behaves isotropically (g_0 = 2.098) without any hyperfine structure of the copper ion. This is due to the dynamical motion of the molecules in solution correlated with a dynamic

Jahn-Teller effect. The absence of any hyperfine structure of the copper ion suggests that the square-planar species becomes six-coordinated owing to the solvent water molecules.

The Cu(II)–5'-GMP complex has a different behavior in aqueous solution. The EPR spectrum is axial with resolved metallic hyperfine structure in the parallel band ($g_{\|}$ = 2.351, $A_{\|}$ = 152 G, $g_{\perp}$ = 2.099), in agreement with one tetragonally distorted octahedral symmetry [23].

Anisotropic EPR spectra with four hyperfine lines in the $g_{\|}$ region and a strong absorption in the $g_{\perp}$ region were obtained for both studied complexes in aqueous solutions adsorbed on SiO_2 (ARCC-4). Characteristic anisotropic EPR parameters for Cu(II)-5'-CMP complex are: $g_{\|}$ = 2.288, $A_{\|}$ = 160 G, $g_{\perp}$ = 2.057 and $A_{\perp}$ = 29 G. For Cu(II)–5'-GMP complex the obtained values are: $g_{\|}$ = 2.323, $A_{\|}$ = 152 G, $g_{\perp}$ = 2.064 and $A_{\perp}$ = 27 G.

From the analysis of these data and their comparison with those reported for other Cu(II) complexes [26], it may be concluded that in the aqueous solutions of Cu(II)–nucleotide complexes, Cu(II) ions are mainly coordinated by oxygen atoms in a tetragonal-octahedral symmetry. The smaller value of $g_{\|}$ and larger value of $A_{\|}$ obtained for the 5'-CMP complex compared with those of 5'-GMP complex, does not entirely exclude the involvement of the N3 nitrogen atom in the coordination of Cu(II) ion in 5'-CMP complex and the presence of CuO_3N chromophore in its xOy plane.

4. CONCLUSIONS

For the Cu(II)-theophylline complexes with some amine ligands the local symmetry around the Cu(II) ion is strongly influenced by the amines nature.

Two different structural species appear in the $CuT_2(npa)_2 \cdot 2H_2O$ due to the vibronical coupling by the static or dynamic Jahn-Teller effect. These species, one stable and another unstable with the temperature (and not only), could have different biological effects. The local characteristic chromophore is CuN_4.

In the case of $CuT_2(NH_3)_2 \cdot 2H_2O$ complex the great difference between the dimension of the amine and theophylline molecules lead to the stabilization of one state respect to the other, the resulting chromophore being $CuN_2N^*_2$.

The EPR powder spectrum of Cu(II)–5'-CMP complex shows the coexistence of a four coordinated and a six-coordinated species. The six-coordinated species is distorted by dynamical Jahn-Teller effect. The four-coordinated species is square-planar and results from the coordination of the copper(II) ion at the nitrogen and carbonyl oxygen atoms of the base and at the phosphate group oxygens. The six-coordinated species involves two water molecules.

In the case of Cu(II)–5'-GMP complex, two octahedral species occurs, one rhombic distorted and the other tetragonal distorted.

The most stable species in time are that of square-planar symmetry for CMP complex and that tetragonally distorted octahedral symmetry for the GMP compound.

Both these species became tetragonal-octahedral six-coordinated in aqueous solution adsorbed on SiO_2.

REFERENCES

1. J.R.J. Sorenson, *Metal Ions in Biological Systems*, Ed. H. Sigel, vol. 14, Marcel Dekker, New York, 1982
2. L. David, O. Cozar, V. Chis, C. Cosma, A. Negoescu, I. Vlasin, *Appl.Magn. Reson*., **6**, 521 (1994)
3. O. Cozar, L. David, V. Chis, C. Cosma, V. Znamirovschi, G. Damian, I. Bratu, Gh. Bora, *Appl. Magn. Reson*., **8**, 235 (1995)
4. O. Cozar, L. David, V. Chis, E. Forizs, C. Cosma, G. Damian, *Fresenius J. Anal. Chem*., **355**, 701 (1996)
5. L. David, O. Cozar, L. Sumalan, V. Chis, R. Tetean, C. Craciun, *Appl. Magn. Reson*., **13**, 571(1997)
6. M. Fuente, O. Cozar, L. David, R. Navaro, A. Hernany, I. Bratu, *Molec. and Biomolec. Spectrochimica Acta A*, **53**, 637 (1997)
7. S.B. Howell (Ed), *Platinum and Other Metal Coordination Compounds in Cancer Chemotherapy*, Plenum Press, New York (1991)
8. S. Steinkopf, A. Garoufis, W. Nerdal, E. Sletten, *Acta Chem. Scand*., **49**, 495 (1995)
9. D.J. Hodgson, *Progr. Inorg. Chem*., **23**, 211 (1997)
10. T.J. Kirstenmacher, D.J. Szalada, C.C. Chiang, M. Rossi, L.G. Manzilli, *Inorg. Chem*., **17**, 2582 (1978)
11. J.J.R. Frausto da Silva, R.J.P. Williams, *The Biological Chemistry of the Elements. The Inorganic Chemistry of Life*, Oxford, Oxford University Press, 1994
12. H.G. Seiler, A. Sigel, H. Sigel (eds): *Handbook on Toxicity of Inorganic Compounds*, New York, 1998
13. N.S. Begum, H. Manohar, *Polyhedron*, **13**, 307 (1994), and references therein
14. W.J. Birdsall, *Inorg. Chim. Acta*, **99**, 59 (1985) and references therein
15. G. Bemski, M. Rieber, M. Wust, *FEBS Lett*., **14**, 177 (1971)
16. L.A. Herrero, J.J. Fiol, F. Mas, V. Cerda, A. Teron, *Inorg. Chem*., **35**, 3786 (1996)
17. L. David, O. Cozar, A. Hernanz, R. Navarro, I. Bratu, E. Forizs, M. de la Fuente, C. Craciun, in *Spectroscopy of Biological Molecules: Modern Tends*, P. Carmona, R. Navarro, A. Hernanz (Eds.), Kluwer Academic Publishers, Netherlands, 1997, p. 627
18. A. Abragam, B. Bleaney, *Electron Paramagnetic Resonance of Transition Ions*, Claredon Press, Oxford, 1970
19. D. Reinen, *Comments Inorg. Chem*., **2**, 227 (1983)
20. S.A. Chiznahov, V.I. Volkov, A.V. Vorobiev, V.V. Valuev, *Russian Journal of Physical Chemistry*, **7**, 67 (1993)
21. D. Kivelson, R. Neiman, *J. Chem Phys.,* **35**, 149 (1961)
22. U. Sakaguchi, A.W. Addison, *J. Chem. Soc. Dalton Trans,* **600** (1979)
23. G. Formicka-Kozolowska, H. Kozlowski, B. Jezowska-Trzebiatowska, *Inorg. Chim. Acta,* **1**, 24 -25 (1977)

24. K. Aoki, G.R. Clark, J.D. Orbell, *Biochim. Biophys. Acta,* **425**, 369 (1976)
25. O. Cozar, L. David, Rezonanta electronica de spin pe sisteme paramagnetice cuplate, Ed. Presa Universitara Clujeana, 1999
26. H. Pezzano, F. Podo, Chem. Rev., **80**, 365 (1980)

STUDIA UNIVERSITATIS BABEŞ-BOLYAI, PHYSICA, XLVIII, SPECIAL ISSUE, 2003

WHICH RADICALS ARE FORMED BY ELECTROCHEMICAL REDUCTION OF THE NO_2 GROUP IN DINITROFURYL-HYDRAZID HYDRAZONE? AN ESR AND DFT STUDY

V. CHIŞ*, **V. MICLĂUŞ****, **L. MUREŞAN****, **G. DAMIAN***, **L. DAVID***, **O. COZAR***

** Babes-Bolyai University, Faculty of Physics, 3400 Cluj-Napoca, Romania*
*** Babes-Bolyai University, Faculty of Chemistry and Chemical Engeneering, 3400 Cluj-Napoca, Romania*

ABSTRACT. This work deals with the possible paramagnetic products obtained during the electrochemical reduction of NO_2 group from dinitrofuryl-hydrazid-hydrazone (DNFHH) compound and is based on the analysis of experimental data obtained by ESR spectroscopy and the theoretical results provided by Density Functional Theory (DFT) calculations.

The pronounced asymmetry and complexity of the ESR spectrum, recorded during the electrochemical reduction of DNFHH, suggests the superposition of the spectra due to more radicals simultaneously present in the sample. The principal pattern of the ESR hyperfine structure was simulated assuming the interaction of the unpaired electron with one nitrogen nucleus, with isotropic hyperfine coupling constant (hfcc) of 9.73G and two protons with 5.07G and 1.01G hfcc's, respectively. Based on the structure of DNFHH compound, the ESR parameters deduced by simulation, and in conjunction with the theoretical results provided by DFT calculations, we propose a radical of RNO_2H-type to be responsible for the hyperfine structure of the experimental ESR spectrum.

Introduction

Nitrofurans are bactericides containing the 5-nitrofuryl moiety and show a high and wide range of antibacterial activity. These compounds are quickly decomposed in all the tissular liquids excepting the blood. Moreover, they are easily eliminated from organism and in addition, the sensitive microorganisms do not become immune to them. DNFHH (Fig.1), obtained by condensing 5-nitro-2-furaldehide with the appropriate hydrazide has been shown to have the largest range of antibacterial action, and also the highest biological activity among a large series of synthetized compounds which include in their structure the furan nucleus [1]. The structure of this compound has been previously confirmed by elemental chemical analysis, UV-VIS and NMR spectroscopies [2].

This work is dealing with the possible paramagnetic products obtained during the electrochemical reduction of nitrofuryl group of the DNFHH compound. The importance of this study is argued by the fact that the identity of the reduction products of nitro group, especially the short-lived free radicals responsible for DNA damage (strand breaks and helix destabilization) [3,4] is not accurately determined and, in addition, the antibacterial effect of these compounds is based just on the oxidation-reduction processes of the nitro group.

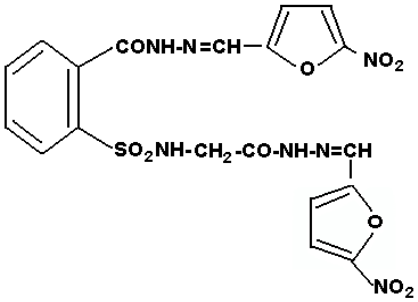

Fig.1 *Structural formula of DNFHH*

Reduction of this group is a prerequisite for biological action [3,5] and the $RNO_2^{-\bullet}$ radical is believed to play a very important role in this process. However, previous studies [6-8] failed to confirm clearly the identity of NO_2 group reduction product even though they sustain that the nitro radical anion must be either the damaging species itself or an obligate intermediate in subsequent reactions or electron addition steps.

Although the ESR spectroscopy [40] is the most useful experimental technique for the detection and identification of the free radicals, however, at least to our knowledge, no other ESR studies are reported on the identity of the nitro group reduction in similar compounds.

On the other hand, ESR spectroscopy does not provide the sign of the spin density or the spin density on nuclei for isotopes having zero nuclear spin. For these reasons, it is always convenient to combine the experimental studies with molecular orbital calculations since the latter provide directly the strength and sign of the spin density on all nuclei, including those with zero nuclear spin. Moreover, theoretical studies provide geometries, energy differences between possible conformers, partial charges, dipole or multipole moments and various other properties, which can be very useful for a complete analysis of the radicals under investigation.

DFT methods, particularly hybrid functional methods [9], are increasingly being shown to provide excellent electronic structures for both, radicals and non-radicals [10-19]. For these methods, the computational cost and memory requirements are considerably less than those of conventional correlated *Ab Initio* procedures. As a consequence, the number of basis functions, and hence the number of atoms, is not a limiting a factor at the DFT level as it is for the *Ab Initio* approaches. However, a problem with DFT methods, including the gradient-corrected variants, is that the density functionals cannot be systematically improved. Nevertheless, because of demonstrations of their good performance, of their lower cost and hence their ability to treat larger systems and their surroundings by explicit consideration of the latter, the DFT methods are now a powerful alternative to conventional *Ab initio* calculations in the computation of hyperfine coupling constants (hfcc's).

Experimental

The radicals have been generated by chemical reduction on a platinum cathode in an aprotic environment of dimethylformamide (DMF/Bu_4NBF_4, 0.1M, 15 ml solution, I=30 μA).

ESR spectra were recorded at room temperature on a ER 200D Brucker spectrometer, at X (ν=9.5 GHz), frequency modulation 100 kHz, sweeping a field range of 50 G with a scan time of 500 s. Due to the recombination of the radicals, the ESR spectrum was only stable for few minutes.

Computational Details

Geometry optimizations and hyperfine coupling calculations have been performed by using DFT methods [9].

All calculations utilized the B3LYP hybrid functional [20] in conjunction with 6-31G(d)-type [21], and EPR-type basis sets [10,11,22]. The latter are optimized for the computation of hyperfine coupling constants by DFT methods (particularly B3LYP). EPR-II is a double-zeta basis set with a single set of polarization functions and an enhanced s part. The contraction schemeis (6,1)/[4,1] for H atom and (10,5,1)/[6,2,1] for B to F atoms. EPR-III is a triple-zeta basis set including diffuse functions, double d-polarizations and a single set of f-polarization functions. Also in this case, the s-part is improved to better describe the nuclear region, by using (6,2)/[4,2] contraction scheme for H atom and (11,7,2,1)/[7,4,2,1] for B to F atoms.

The influence of the solvent on the molecular structure and the spin density distribution of the radicals was investigated by applying the Self Consistent Reaction Field (SCRF) method, in the framework of the Isodensity Polarizable Continuum Model (IPCM) [23,24].

The isotropic hyperfine coupling constants have been calculated with the equation [11]

$$a_{iso}^{(N)}(MHz) = \frac{2}{3}\mu_0 g_e \beta_e g_N \beta_N \frac{10^{-6}}{h} \frac{1}{a_0^3} \rho(r_N) \qquad (1)$$

were g_e and g_n are the electron and nuclear g factors, μ_B and μ_N are the Bohr and the nuclear magneton respectively, μ_0 is the vacuum magnetic permeability, h is the Planck constant, a_0 is the first Bohr radius and $\rho(r_N)$ represents the spin density at the nucleus N. Whereas $g_e\beta_e g_N\beta_N$ is a constant for a specific nucleus, $\rho(r_N)$ have to be obtained by electronic structure methods.

All the calculations were performed using the Gaussian 98W program package [25].

Results and Discussions

The electrochemical reduction measurement made at a constant intensity on a platinum cathode in a medium of DMF/Bu_4NBF_4 0.1M (7mg product in 15 ml of solution) led to an observable ESR spectrum obtained at I=30μA by sweeping 50 G in 500 s. This spectrum (Fig.2) with a total width of about 26 G contains a rather large number of hyperfine lines and decays in few minutes.

The pronounced asymmetry and complexity of the spectrum suggests the superposition of the signals due to more radicals simultaneously present in the sample. Due to the complexity of the spectrum we did not try a full analysis but we focused on the hyperfine structure marked by circles in the experimental spectrum. This structure with 12 lines can be interpreted as a triplet of doublets of doublets and due to the non-degeneracy of the lines it was simulated assuming the interaction of

the unpaired electron with one nitrogen nucleus and two non-equivalent protons. The best agreement between the experimental spectrum and the simulated one has been obtained with the following parameters: g=2.07965, line-width peak-to-peak ΔH_{pp}=0.19G and the isotropic hyperfine coupling constants: A_N=9.73G, $A_H^{(1)}$=5.07G and $A_H^{(2)}$=1.01G. Based on the structure of DNFHH compound, the ESR parameters deduced by simulation and the calculated hfcc's by DFT methods (see bellow) we propose the free radical given in Fig.3 to be responsible for the hyperfine structure marked in the experimental spectrum. For such a radical, the unpaired electron should interact with the nitrogen nucleus, the proton of the H atom from hydroxil group (β-proton) and another proton from the furan ring.

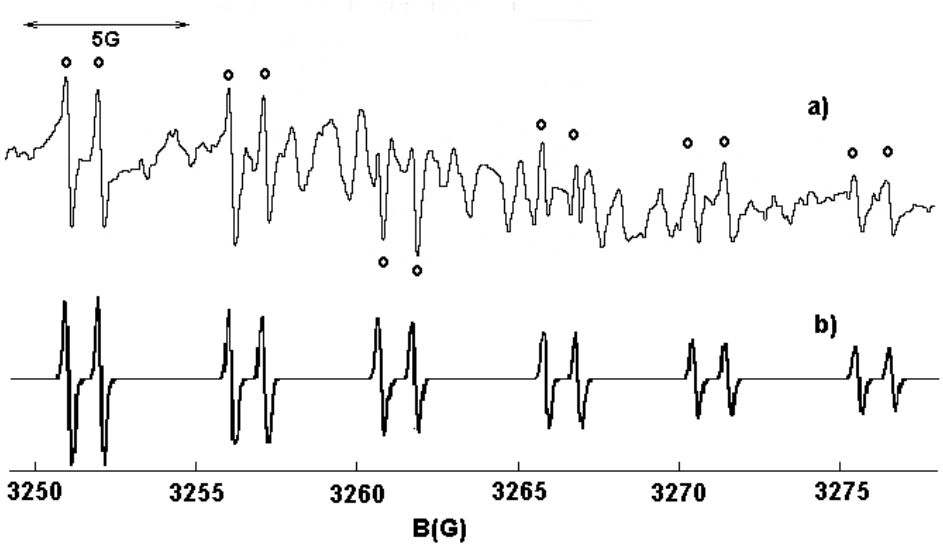

Fig.2 a) *Experimental ESR spectrum obtained by electrochemical reduction of DNFHH compound on a platinum cathode in 0.1M DMF/Bu_4NBF_4 solution.*
b) *Simulated hyperfine structure marked by circles in the experimental spectrum*

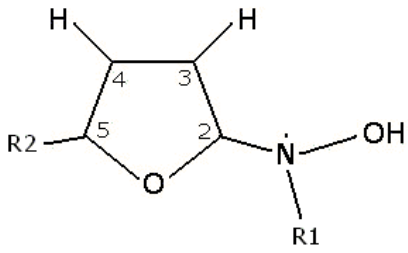

Fig.3 *Proposed structure for the free radical obtained by electrochemical reduction of DNFHH*

The experimental isotropic coupling constants determined by us are comparable with those corresponding to others radicals in which the odd electron is delocalized on similar fragments [26-28]. The unpaired spin density on nitrogen atom can be evaluated using the McConnell equation [29]

$$A_{iso}^{N} = Q^{N}\rho_{\pi}^{N} \tag{2}$$

where A represents the isotropic hyperfine coupling constant of the nitrogen nucleus, ρ is the unpaired spin density on nitrogen atom and Q is an empirical parameter. Using for Q^N a value of 20G [30], one obtains 0.49 for the unpaired spin density ρ_{π}^{N} on nitrogen atom, value which is comparable to other similar radicals [31]. Now, with ρ_{π}^{N} we can obtain the isotropic hfcc for the beta proton by using the equation [32]

$$A_{iso}^{H_\beta} = \rho_{\pi}^{N}[Q_0^{\beta} + Q_2^{\beta}\cos^2\theta] \tag{3}$$

Here, θ is the torsional angle between the symmetry axis of the p_z orbital of the nitrogen atom and the direction of the O-H_β bond. Q_0 and Q_2 are empirical parameters and their values are 12.67 and 78.5G, respectively [31]. Assuming a planar structure of the radical at the nitrogen site, we calculated $A_H^{\beta} = 6.2G$ in a fairly good agreement with the experimentally determined one.

To our knowledge, there are very few data in the literature, concerning the hyperfine structure of free radicals which contains the furan ring. Furthermore, some studies reported till now, refers either to charged radicals [27,28] or to radicals formed by hydrogen addition in irradiated furoic acid [33], so that no consistent comparisons, regarding the hyperfine or molecular structure, can be made with our radical.

For these reasons we used quantum chemical calculations as a help in assigning the observed ESR spectrum and to decide which radical is responsible for it. For computational purposes different models were chosen in which the long R2 chain (see Fig.1), connected to the furyl ring, was truncated to a CHNH group. The geometry of the radical models have been optimized by using DFT methods, with different functionals and basis sets, placing particular emphasis on B3LYP hybrid functional and EPR-II basis set.

As seen in the preceding section, the ESR spectrum given in Fig.2 can only be assigned by assuming the interaction of the unpaired electron with one nitrogen nucleus and two non-equivalent protons. In addition, the odd electron is localized on the nitrogen nucleus whose isotropic splitting is 9.73G and the p_z unpaired electron spin density was estimated to 0.49. In the following, these will be the reference data when comparisons will be made between the theoretical results provided by different models and the experimental findings.

In Fig.4 to Fig.7 are given the models used in our calculations to reproduce the free radical which could be responsible for the ESR spectrum obtained by electrochemical reduction of DNFHH. By geometry optimizations, planar structures were obtained for all the models investigated.

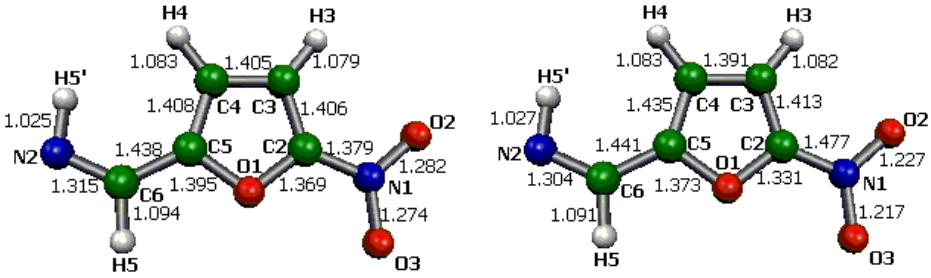

a) anion b) cation

Fig.4 *M1 model (anion and cation) used for calculation purposes*

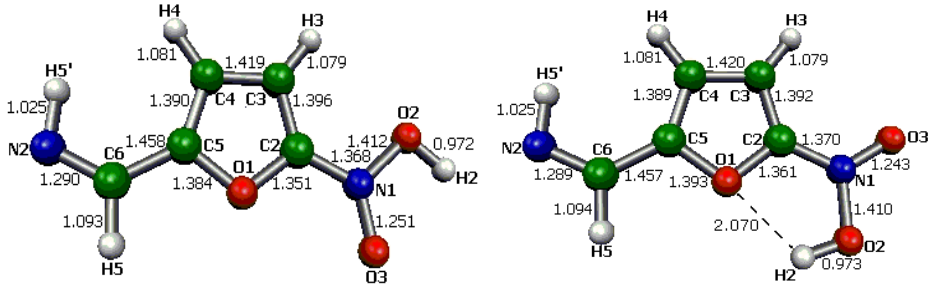

a) conformer 1 b) conformer 2

Fig.5 *M2 model (two conformations) used for calculation purposes*

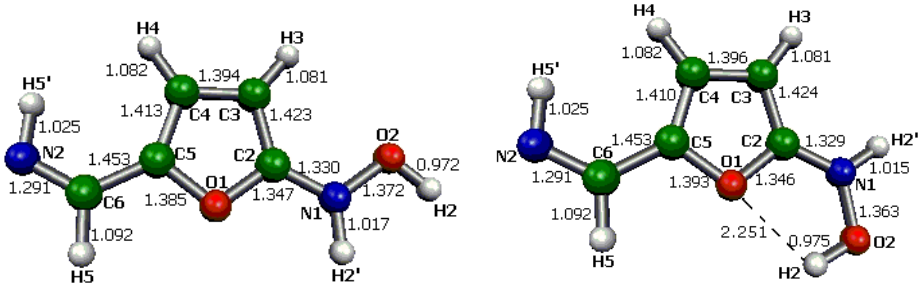

a) conformer 1 b) conformer 2

Fig.6 *M3 model (two conformations) used for calculation purposes*

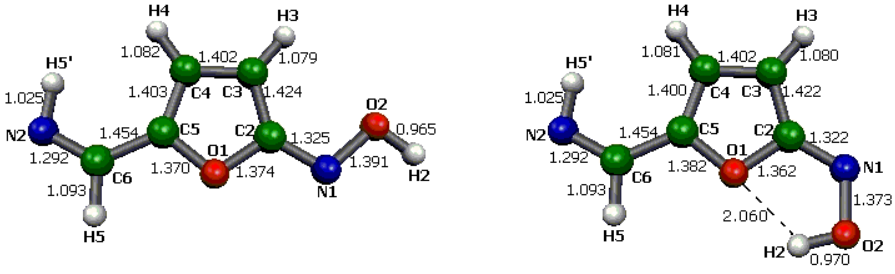

a) conformer 1 b) conformer 2

Fig.7 *M4 model (two conformations) used for calculation purposes*

Table 1.
Calculated isotropic hyperfine coupling constants (in Gauss) for some models of the radical supposed to be obtained by electrochemical reduction of NO_2 group in dinitrofuryl-hidrazid hydrazone (see Fig.4 to Fig.8 for model structures).

Model	Conformer	Method/ Basis set	ρ_π^{N1}	A^{N1}	A^{H3}	A^{H4}	A^{H2}	$A^{H2'}$	A^{H5}	A^{N2}	$A^{H5'}$
M1 $RNÓ_2$	Anion	B3LYP/6-31G(d)	0.12	2.16	-2.01	0.81	-	-	-0.85	3.66	-5.17
	Anion	B3LYP/EPR-II	0.14	1.66	-2.00	0.96	-	-	-0.76	2.91	-4.90
	Cation	B3LYP/EPR-II	-0.02	-1.79	-0.74	-3.36	-	-	2.37	3.92	-9.02
M2 RNO_2H	1	B3LYP/6-31G(d)	0.29	10.17	-6.30	2.54	-1.22	-	1.34	2.63	-3.46
	1	B3LYP/6-31+G(2df,p)	0.32	7.02	-5.14	2.08	-0.77	-	0.98	1.71	-3.02
	1	B3LYP/EPR-II	0.30	7.36	-5.73	2.17	-1.18	-	0.94	1.63	-3.14
	1	B3LYP/EPR-II[a)]	0.30	7.60	-5.54	2.24	-1.11	-	0.64	1.70	-3.06
	2	B3LYP/EPR-II	0.28	6.27	-5.61	2.22	-1.59	-	0.90	1.62	-3.13
M3 RNHOH	1	B3LYP/EPR-II	0.22	5.00	-6.67	0.70	-1.54	-8.25	2.42	3.17	-6.84
	2	B3LYP/EPR-II	0.24	5.39	-7.19	1.35	-2.10	-8.76	2.44	3.16	-6.83
M4 RNOH	1	B3LYP/6-31+G(d)	0.42	8.96	-8.10	2.58	-2.62	-	1.49	3.20	-4.85
	1	B3LYP/6-31+G(d)[b)]	0.42	8.81	-7.94	2.84	-2.56	-	1.04	3.35	-4.82
	1	B3LYP/EPR-II	0.43	7.31	-7.85	2.52	-2.75	-	1.47	2.49	-4.85
	1	B3LYP/EPR-III	0.42	7.37	-7.71	2.40	-2.55	-	1.38	2.52	-4.70
	2	B3LYP/EPR-II	0.41	7.09	-8.12	3.11	-3.19	-	1.61	2.79	-5.42
	2	B3LYP/EPR-II[b)]	0.41	7.09	-8.26	3.20	-2.87	-	1.39	2.92	-5.37
Experimental			**0.49**	**9.73**	**5.07**	**n.d.**	**1.01**	**n.d.**	**n.d.**	**n.d.**	**n.d.**

[a)] SP IPCM in BuOH isodensity=0.004

[b)] SP IPCM in DMF isodensity=0.004

n.d. – not detected

The optimized geometrical parameters given in figures 4-7 correspond to the B3LYP/EPR-II calculations. Compared with the experimental [34] and theoretical results [35] of the furan molecule, these parameters suggest a significant elongation of the radical along the C_2 symmetry axis of the furan ring. Excepting the C2-C3 and C4-C5 bond lengths, for which the experimental counterparts in the furan molecule are 1.361Å, the other bond distances and angles of the furan ring in our models are rather close to the experimental data of the furan molecule. This is obviously for the CH bond lengths (experimental 1.077Å in furan) which are reproduced within 0.05Å mean deviation. The CO bonds are longer than those corresponding to the furan molecule (1.362Å) by about 0.001Å to 0.03Å, depending on the model. The C3-C4 bond seems to be also significantly changed when passing from furan (1.431Å) to our radical models. All the bond angles of the furan ring in our models are reproduced very close to the experimental values of the furan molecule.

M1 model

The one electron addition product $RNÓ_2^-$ anion radical is believed [6-8] to be a key radical in reduction of nitroheterocyclic compounds of biological interest, and has consequently attracted considerable attention. The reactivity, and hence

the lifetime of this radical, seem to be highly dependent on the molecule to which the nitroheterocycle belongs. Thus, for a series of drugs, the $T_{1/2}$ time was found to vary from $1.4 \cdot 10^{-2}$s for nitrofurazone, to 11.75s for M&B 4998 drug [8].

Our first attempt was to clarify if the ESR spectrum given in Fig.2 could be due to a charged $RNÓ_2$ species. For this purpose we optimized and then calculated the isotropic hfcc's for both $RNÓ_2^-$ and $RNÓ_2^+$ radicals. Their optimized bond lengths obtained at B3LYP/EPR-II level of theory are given in Fig.4. The calculated geometrical parameters reveal that C3-C4, O1-C2, O1-C5 and N-O bonds are larger for anion than for cation, while the opposite is true for C2-C3, C4-C5 and C-N bonds. The bond angles remain essentially the same in the two charged radicals.

Their hyperfine structure parameters given in Table 1 are very different from the experimental ones. As seen, the unpaired spin density on nitrogen atom is much too low and also the N1 isotropic hyperfine coupling constant. As revealed by theoretical results this is due to the localization of the unpaired electron primary on the oxygen atoms of the radical.

The agreement between experiment and theory does not improves by replacing the exchange and/or correlation functionals or by using more sophisticated basis sets. In conclusion, this radical can not explain the hyperfine structure of the ESR spectrum given in Fig.2. In addition, allowing that $RNÓ_2^-$ radical it is produced as the first step of the NO_2 group reduction process, as stated by Tocher *et al*.[6,7], it is clear that the radical is very reactive, decaying in less than few seconds.

M2 model

As seen in Fig.5, for M2 model the two conformers differ in the orientation of the NO_2H group with respect to the furan ring. By geometry optimizations at B3LYP/EPR-II level of theory it comes out that conformer 1 is 3.02Kcal/mol lower in energy than conformer 2. This is somewhat surprising because it should be expected a more stabilization for conformer 1 due to a possible O2H2...O1 hydrogen bond whose calculated bond length is 2.070Å. This contradiction implies that coulombian repulsion between the atoms of NO_2 group play a more important role than hydrogen bonding in stabilization of the radical.

The optimized bond lengths of this model for the two conformations are very close, the largest difference being noted for N1-O3, O1-C2 and O1-C5 distances. These minor differences between the conformers' geometries are however reflected in the calculated hyperfine parameters. Thus, by using the B3LYP/EPR-II method (see Table 1), A^{N1} hfcc is 15% lower and A^{H2} hfcc is 35% higher in absolute magnitude for the second conformer with respect to conformer 1. All the others theoretical hfcc's, but also the ρ_π^N are essentially the same for the two conformers.

Due to the satisfactory accuracy in predicting the hyperfine structure of the radical, this model represents a good candidate for the radical type obtained by electrochemical reduction of the nitro group in DNPHH. Especially very good agreement is obtained with this model for A^{H2} and A^{H3} hfcc's. Good agreement can be also noted for A^{N1} and ρ_π^N. However, like for all the other models, A^{H4} is predicted to have a substantial value, while experimentally it is not detected. This discrepancy could be due to the environmental effects of the R2 chain which has been truncated in our models to the CHNH group.

It is noteworthy also here the very good match between theoretical and experimental A^{N1} hfcc provided by 6-31G(d) basis set. However, increasing the quality of the basis set, less agreement is obtained. This behavior of the 6-31G-type basis sets has been observed also in other studies [13,19,36,] and an explanation for this could be that the spin density introduced through the use of a larger basis set is cancelled by correlation effects.

M3 model

For model M3, for which one of the two oxygen atoms in NO_2 group is replaced by an H atom, the intramolecular H-bonded conformer 2 is more stabilized than conformer 1 by 7.5cal/mol. This very small energy difference is reflected in a rather long H-bond O1H2...O1 distance, calculated at 2.251Å in conformer 2. Although the barrier energy between the two conformers is very low, there are significant differences between their calculated hyperfine structures (see Table 1). These differences are especially noted for A^{H3} and A^{H2} isotropic hfcc's which change substantially from one conformer to the other.

Large discrepancies are noted between the experimental and calculated values of ρ_π^{N1} and A^{N1}. The very low theoretical values of the π-unpaired spin density on nitrogen N1 atom (0.22 and 0.24 for the two conformers, respectively) lead to very small calculated values of hfcc A^{N1} (5.00G and 5.39G, respectively) with respect to the experimental one of 9.73G. Moreover, a very large value is expected for A^{N2} in this model, which is in a total disagreement with the experimental findings. In conclusion, this model is sustained neither by the calculated ρ_π^{N1} spin densities nor by nitrogen atoms' theoretical hfcc's.

M4 model

Finally, the M4 model was investigated as a possible candidate for the radical whose ESR spectrum is given in Fig.2. Again, two conformers, with different orientations of the OH group with respect to the furan ring, were tested. The minor differences between the B3LYP/EPR-II optimized geometries of the two conformers resides only in O-C bonds of the furan ring and N1-O2 bond length. However, the intramolecular hydrogen bonded conformer 2 is much more stable than conformer 1, their energy difference being 45.6Kcal/mol with a hydrogen bond length O2H2...O1 in conformer of 2.060Å.

From Table 1, one can easily be seen the very good match between the experimental and theoretical unpaired spin density on nitrogen atom. However this agreement is not reflected in the calculated isotropic hyperfine coupling constant for nitrogen nucleus for all the basis sets used in calculations, but only for 6-31+G(d). Anyway, even with this basis set, the other hfcc's are predicted too far away from the experimental data and they are not improved by considering the solvent effects in the framework of the IPCM solvation model.

From the results given in Table 1 for M4 model seems that diffuse functions added to the 6-31G basis set greatly improve the calculated hfcc of nitrogen nucleus. The same conclusion has been reached by Bauschlicher *et al.* [37] in a theoretical study of the nitrogen atom hyperfine coupling constant, using several methods and basis sets.

In order to ensure that differences in the calculated and experimental N1 and H2 couplings do not arise due to differences in the hydrogen bonding environment at O2, a series of calculations (results not shown) were performed in which the OH bond length and dihedral angle formed by OH group with the rest of the radical in M2 model, were varied. From these results it comes out that the isotropic hfcc of N1 decreases to a value of 4.85G by increasing the dihedral H2O2N1C2 angle to 90^o. In addition, the hfcc of H2 proton is greatly affected by this variation of the dihedral angle, its value reaching 14.34G for 90^o. The rest of hfcc's remain essentially unmodified as the result of this variation.

Thorough this investigation we focused on the use of the B3LYP functional which proved its ability in predicting with high accuracy not only hfcc's but also geometries, vibrational structures, dipole moments, etc. However we have to keep in mind that part of the success of the B3LYP method has been attributed to a fortuitous cancellation of errors, at least in some systems [14,38,39] and this explains why higher quality basis sets do not always provide hfcc's closer to the experimental results. Moreover, being a hybrid method, B3LYP provides isotropic hyperfine coupling constants which are affected by spin contamination, due to the inclusion of the exact exchange energy given by Hartree-Fock theory. However, the spin expectation values lie much closer to the theoretical one than those given by *Ab Initio* calculations, the deviation from the exact value of 0.750 being too small to indicate a severe spin contamination.

It is very surprising that the small 6-31G basis set yields better results compared with more elaborated basis sets. This may reflect the effect that spin polarization effects arising from using a larger basis set would compensate for in a multi-reference calculation by including configurations which contribute to spin polarization in the opposite sense.

It should be also noted that the solvent effects were not taken explicitly into account in present study. This offers a possible explanation for some discrepancies between theory and experiment.

Conclusions

The geometries, spin density distributions and hyperfine coupling constants in radicals that are possible products of electrochemical reduction of NO_2 group in dinitrofuryl-hidrazid hydrazone have been studied through the use of density functional theory.

Possible charged and neutral radical models were examined and the calculated isotropic hyperfine coupling constants were compared to those obtained by ESR spectroscopy. It was concluded that $RNÓ_2^-$ anion radical can not reproduce the experimental ESR spectrum due to the large discrepancies between theoretical (hfcc's and spin density on nitrogen atom) data obtained on the basis of this model and the experimental findings. A reasonable candidate for the radical responsible for the ESR spectrum is RNO_2H model for which we obtained the best agreement between theoretical and experimental data.

However, more detailed experimental, as well as theoretical investigations are required in order to definitely identify the radical (or radicals) produced by the reduction of NO_2 group in DNFHH.

Acknowledgements

The authors are gratefully indebted to Prof. Anne-Marie Martre, Laboratoire d'Electrochimie Organique, Universite Blaise Pascal for recording the spectra and very useful discussions.

REFERENCES

1. V.Miclăuş, *Ph.D. Thesis*, Babeş-Bolyai University, 1998; G.Campan, M.Hadaruga, V.Miclăuş, *J. Chromatography A*, 869,49(2000)
2. F.Jugrestan, V.Miclăuş, M.Toşa, G.Câmpan, D.Homorodean, *Studia UBB Chemia*, 115, 39 (1993)
3. D.I.Edwards, *Biochem.Pharmacol*., 35,53 (1986)
4. P.L.Olive in*: Radiation Sensitizers*, L.W.Brady, Ed., Masson, New York, p.39 (1980)
5. R.J.Knox, D.I.Edwards, R.C.Knight, *Int.J.Radiat.Oncol.Biol.Phys*., 10,1315 (1984)
6. J.H. Tocher, D.I. Edwards, *Int.J.Radiat.Biol*., 57,45 (1990)
7. J.H. Tocher, D.I. Edwards, *Int.J.Radiat.Biol*., 9,49 (1990)
8. J.H. Tocher, D.I. Edwards, *Free Rad.Res.Comms*., 16(1), 19(1992)
9. R.G.Parr, W.Yang, *Density-Functional Theory of Atoms and Molecules*, Oxford University Press, New York, 1989
10. C.Adamo, V.Barone, A.Fortunelli, *J.Chem.Phys.*, 102,384(1995)
11. V.Barone, in: D.P.Chong (Ed.) *Recent Advances in Density Functional Methods*, Part I , World Scientific Publishing, Singapore, Chapter 8, 199
12. V.G.Malkin, O.L.Malkina, L.A.Eriksson, D.R.Salahub, in: J.M.Seminario and P.Politzer (Eds.) *Modern Density Functional Theory: A Tool for Chemistry*, p.273, Elsevier Science, 1995
13. S.D.Wetmore, R.J.Boyd, L.A.Eriksson, *J.Chem.Phys*., 106,7738(1997); S.D.Wetmore, R.J.Boyd, L.A.Eriksson, *J.Phys.Chem. B*, 102,9332(1998)
14. J.Cirujeda, J.Vidal-Gancedo, O.Jurgens, F.Mota, J.J.Novoa, C.Rovira, J.Veciana, *J.Am. Chem. Soc.,* 122,11393(2000)
15. S.Sinnecker, W.Koch, W.Lubitz, *Phys.Chem.Chem.Phys.,* 2,4772(2000)
16. M.J.Raiti, M.D.Sevilla, *J.Phys.Chem. A*, 103,1619(1999)
17. P.J.O'Malley, *J.Phys.Chem. B*, 104,2176(2000)
18. B.Giese, D.McNaughton, *Phys.Chem.Chem.Phys*., 4,5161(2002; B.Giese, D.McNaughton, *Phys.Chem.Chem.Phys*., 4,5171(2002).
19. V.Chiş, A.Nemeş, L.David, O.Cozar, *Studia UBB Physica*, XLVII(1),157(2002)
20. A.D.Becke, *J.Chem.Phys*., 98,5648(1993)
21. W.J.Hehre, L.Radom, P.v.R.Schleyer, J.A.Pople, "*Ab Initio" Molecular Orbital Theory* , John Wiley & Sons, New York, 1986
22. N.Rega, M.Cossi, V.Barone, *J.Chem.Phys.*, 105,11060(1996)
23. S.Miertus, S.Scrocco, J.Tomasi, *Chem.Phys.* 55,117(1981); S.Miertus, J.Tomasi, *Chem. Phys.* 65,239(1982)
24. J. B. Foresman, T. A. Keith, K. B. Wiberg, J. Snoonian and M. J. Frisch, *J.Phys.Chem.*, 100, 16098(1996); J.B. Foresman, A.Frisch, *Exploring Chemistry with Electronic Structure Methods*, 2nd ed., Gaussian Inc., Pittsburg, PA,(1996)

25. *Gaussian 98, Revision A.7*, M. J. Frisch, G. W. Trucks, H. B. Schlegel, G. E. Scuseria, M. A. Robb, J. R. Cheeseman, V. G. Zakrzewski, J. A. Montgomery, Jr., R. E. Stratmann, J. C. Burant, S. Dapprich, J. M. Millam, A. D. Daniels, K. N. Kudin, M. C. Strain, O. Farkas, J. Tomasi, V. Barone, M. Cossi, R. Cammi, B. Mennucci, C. Pomelli, C. Adamo, S. Clifford, J. Ochterski, G. A. Petersson, P. Y. Ayala, Q. Cui, K. Morokuma, D. K. Malick, A. D. Rabuck, K. Raghavachari, J. B. Foresman, J. Cioslowski, J. V. Ortiz, A. G. Baboul, B. B. Stefanov, G. Liu, A. Liashenko, P. Piskorz, I. Komaromi, R. Gomperts, R. L. Martin, D. J. Fox, T. Keith, M. A. Al-Laham, C. Y. Peng, A. Nanayakkara, C. Gonzalez, M. Challacombe, P. M. W. Gill, B. Johnson, W. Chen, M. W. Wong, J. L. Andres, C. Gonzalez, M. Head-Gordon, E. S. Replogle, and J. A. Pople, Gaussian, Inc., Pittsburgh PA, (1998)
26. N.V.Vugman, M.F.Elia, R.P.A.Muniz, *Mol.Phys.,* 30,1813(1975)
27. M.Scholz, G.Gescheidt, U.Schoberl, J.Daub, *J.Chem.Soc.Perkin Trans.,* 2,2137(1992)
28. M.Schmittel, G.Gescheidt, L.Eberson, H.Trenkle, *J.Chem.Soc. Perkin Trans*., 2,2145(1997)
29. H.M.McConnell, D.B.Chesnut, *J.Chem.Phys*., 28,107(1956)
30. A.Carrington, J.dos Santos-Veiga, *Mol.Phys*., 5,21(1962)
31. W.Gordy, *Theory and Applications of Electron Spin Resonance*, John Wiley & Sons, New York, 1980
32. C.Heller, H.M.McConnell, *J.Chem.Phys.,* 32,1535(1960)
33. R.J.Cook, J.R.Rowlands, D.H.Whiffen, *Mol.Phys*., 7,57(1963)
34. B.Bak, D.Christensen, W.B.Dixon, L.Hansen-Nygaard, J.Rastrup-Andersen, M.Schotlander, *J.Mol.Spectrosc*., 9,124(1962)
35. L.A.Montero, R.Gonzalez-Jonte, L.A.Diaz, J.R.Alvarez-Idaboy, *J.Phys.Chem.,* 98, 5607 (1994)
36. M.J.Cohen, D.P.Chong, *Chem.Phys.Lett*., 234,405(1995)
37. C.W.Bauschlicher, Jr., S.R.Langhoff, H.Partridge, *J.Chem.Phys.,* 89,2985(1988)
38. V.Barone, *Chem.Phys.Lett.,* 226,392(1994)
39. I.Carmichael, *J.Phys.Chem. A*, 101,4633(1997)
40. I.Ursu, *La Resonance Paramagnetique Electronique*, Dunod, Paris, 1968

STUDIA UNIVERSITATIS BABEŞ-BOLYAI, PHYSICA, XLVIII, SPECIAL ISSUE, 2003

EPR STUDY OF TWO SANDWICH-TYPE HETEROPOLYOXOMETALATES WITH TRINUCLEAR VANADIUM CLUSTERS (V^{IV}_3 AND $V^{IV}_2V^{V}$)

L. DAVID, O. COZAR, V. CHIŞ

Department of Physics, "Babeş-Bolyai" University,
1, M. Kogălniceanu, RO-3400 Cluj-Napoca, Romania

ABSTRACT. The sandwich-type $K_{12}[(VO)_3(BiW_9O_{33})_2]\cdot 31H_2O$ (**1**) and $K_{11}[(VO)_3(BiW_9O_{33})_2]\cdot 21H_2O$ (**2**) heteropolyoxotungstates were investigated by means of EPR spectroscopy. The powder EPR spectrum of the complex **1** obtained at room temperature was simulated as a superposition of one axial component with $g_{\parallel} = 1.899$, $g_{\perp} = 1.974$, $A_{\parallel} = 184$ G and $A_{\perp} = 69$ G for the S = 1/2 ground state of the V^{IV}_3 cluster and a broad component (≈ 500 G) with $g_{iso} = 1.974$ for the excited S = 3/2 state and accounting for a combined effect of unresolved **g** and **A** anisotropies and V–V dipolar coupling. The powder spectrum of the complex **2** presents the same features, but with the EPR parameters: $g_{\parallel} = 1.908$, $g_{\perp} = 1.968$, $A_{\parallel} = 186$ G, $A_{\perp} = 60$ G for the axial component and $g_{iso} = 1.968$, $\Delta B_{iso} = 500$ G for the isotropic component.

1. Introduction

During the last years, interest for heteropolyoxometalates (HPOM) substituted by early transition metals (3d) has been continuously growing [1-4]. These complexes have the capacity to include more transition metals, which interact by means of dipolar or exchange coupling [5-7]. This aspect recommends heteropolyoxometalates as potential hosts of high dimensional clusters [5]. Heteropolyoxometalates have also received much attention because of the vast range of applications, in material science, medicine, catalysis [3,6].

A special class of heteropolyoxometalates is the unsaturated trilacunary Keggin-type $[X^{n+}W_9O_{33}]^{(12-n)-}$ structure, where the heteroatom X is one of the Bi^{III}, As^{III} or Sb^{III} ions [9-11]. The main characteristic of these ions is the presence of one pair of electrons, which prevents further condensation to a saturated Keggin structure [12]. However, transition metal ions could link the lacunars units, resulting a sandwich-type structure. Our interest was focused on structures with two trivacant Keggin fragments linked by a trinuclear cluster of vanadium ions. Recently, the magnetic properties of sandwich-type HPOM with As^{III} as heteroatom and containing a mixed valence cluster V^{IV}_2/V^{V} [12] and respectively with Sb^{III} as heteroatom and containing a V^{IV}_3 cluster [13] were reported. Distances of 4.2–5.7 Å prevent the direct overlapping of the vanadium ions orbital. The HPOM framework favorites the superexchange, thus leading to a small antiferromagnetism between the vanadium ions.

In this paper we investigate the new $K_{12}[(VO)_3(BiW_9O_{33})_2]\cdot 31H_2O$ (**1**) and $K_{11}[(VO)_3(BiW_9O_{33})_2]\cdot 21H_2O$ (**2**) sandwich-type complexes by EPR spectroscopic method. The main goal was to obtain information about the vanadium ions coordination to the trilacunary ligands, the local symmetry around the vanadium ions and the presence of possible vanadium-vanadium couplings. The investigated compounds contain two identical α-B-$[BiW_9O_{33}]^{9-}$ heteropolyanion fragments [14,15], related by a center of inversion and facing each other with their open sites (Fig. 1). A belt of three vanadium ions connects the trilacunary anions. The Bi^{III} ions are surrounded by three oxygen atoms in a trigonal pyramidal geometry, with the lone pair of electrons located at the apex of the pyramid and presenting a low availability to be used in dative bonds [16].

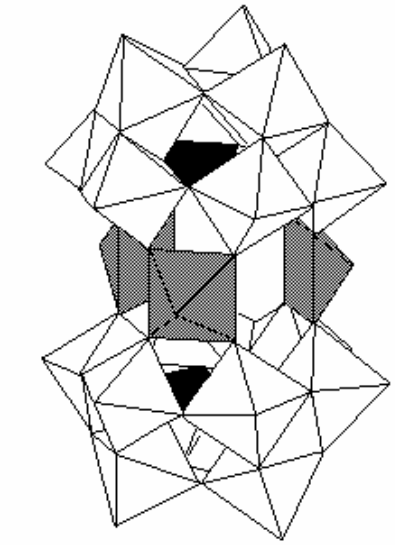

*Fig. 1. Structure of the complexes **1** and **2**. Empty polyhedral are WO_6 octahedral, the black triangles are BiO_3 pyramids and the shaded polyhedral are $(VO)O_4$ pyramids.*

The spectroscopic and electrochemical investigation of the $K_{12}[(VO)_3(BiW_9O_{33})_2]\cdot 31H_2O$ (**1**) and $K_{11}[(VO)_3(BiW_9O_{33})_2]\cdot 21H_2O$ (**2**) complexes indicate the coordination of the vanadium ions at two corner-sharing octahedral from each α-B-$[BiW_9O_{33}]^{9-}$ heteropolyanion. Cyclic voltammograms confirm the presence of three V^{IV} ions in the complex **1** and two V^{IV} and one V^{V} ions in the complex **2**. The vanadyl ions are five coordinated by oxygen atoms in C_{4v} local environments, with $^2B_2(d_{xy})$ ground state. The electronic d levels are more distantly in the case of the complex **2** with mixed valence vanadium ions.

2. Experimental

All chemicals were of reagent grade and used as received. $Na_9[BiW_9O_{33}]\cdot 14H_2O$ have been synthesized as previously described [17]. For both complexes, the total number of water molecules has been checked by TG studies.

All measurements were performed at room temperature. EPR spectra on powdered solids were recorded at *ca.* 9.6 GHz (X band) using a Bruker ESP 380 spectrometer.

3. Results and discussion

Powder EPR spectrum of the $K_{12}[(V^{IV}O)_3(BiW_9O_{33})_2]\cdot 31H_2O$ (**1**) sample (Fig. 2a), obtained in the X band at room temperature contains a series of signals superposed on a very broad component. Such types of spectra were previously reported for other HPOM involving vanadium ions [18-20]. The experimental spectrum was simulated as a superposition of two Gaussian components, one axial and another isotropic, in the 2:3 ratio (Fig. 2a).

One contributing species exhibits eight components, both in the perpendicular and parallel bands due to the hyperfine coupling of the unpaired electron spin with the nuclear spin of the ^{51}V isotope (I = 7/2). It can be described by an axial spin Hamiltonian characteristic for S = 1/2 system with C_{4v} local symmetry [21,22]:

$$H = \mu_B[g_{II}B_zS_z + g_{\perp}(B_xS_x + B_yS_y)] + A_{II}S_zI_z + A_{\perp}(S_xI_x + S_yI_y) \qquad (1)$$

where g_{II}, $g_{\perp}$ and A_{II}, $A_{\perp}$ are the axial principal values of the ***g*** and hyperfine tensors respectively, μ_B is the Bohr magneton, B_x, B_y, B_z are the components of the applied magnetic field in direction of the principal ***g*** axes, S_x, S_y, S_z and I_x, I_y, I_z are the components of the electronic and nuclear spin angular momentum operators, respectively.

EPR parameters of the axial component, derived from the simulation, are: g_{II} = 1.899, $g_{\perp}$ = 1.974, A_{II} = 184 G, $A_{\perp}$ = 69 G and the linewidths ΔB_{II} = 57 G, $\Delta B_{\perp}$ = 32 G for a Gaussian lineshape. The principal axes of the ***g*** and ***A*** tensors were presumed to be coincident. The hyperfine structure of the complex containing eight lines in each of the parallel and perpendicular bands indicates the fact that the unpaired electrons of the three V^{IV} ions are prevalently trapped on the parent ions. For the assignment of the isotropic component, characterized by g_{iso} = 1.974 and ΔB_{iso}(p-p) = 500 G we took into account the fact that polyoxometalates with more vanadium ions present such broad EPR signals with a resolved hyperfine structure either due to the electron hopping between the vanadium ions in a thermally activated process or to a clustered system in undiluted powder samples [24-26]. The intermetallic distance longer than 4.2 Å prevents the direct electron hopping between the vanadium ions. The broad component of the spectrum could be interpreted in therms of the presence of very weak extended exchange interactions within the vanadyl triangular cluster, as recently reported for the sandwich-type complex with Sb^{III} [13]. These lead to the appearance of two doublets (S = 1/2) and an excited quartet (S = 3/2). This last state together with the presence of dipolar interactions between the vanadium ions and the unsolved hyperfine structure and possible ***g*** and ***A*** tensors anisotropies could be responsible for the appearance of the broad component of the spectrum.

The axial EPR components of the ***g*** and ***A*** tensors were used for the estimation of the molecular coefficients by means of the LCAO-MO approach for the V^{IV} ion with antibonding $B_2(d_{xy})$ ground state in a C_4 local symmetry. The covalence degrees of the in-plane V–O π (β_2^2) bonds has been evaluated from [27]:

$$\beta_2^2 = \frac{7}{6}\left[-\frac{A_{II} - A_{\perp}}{P} + (g_{II} - g_e) - \frac{5}{14}(g_{\perp} - g_e)\right] \qquad (2)$$

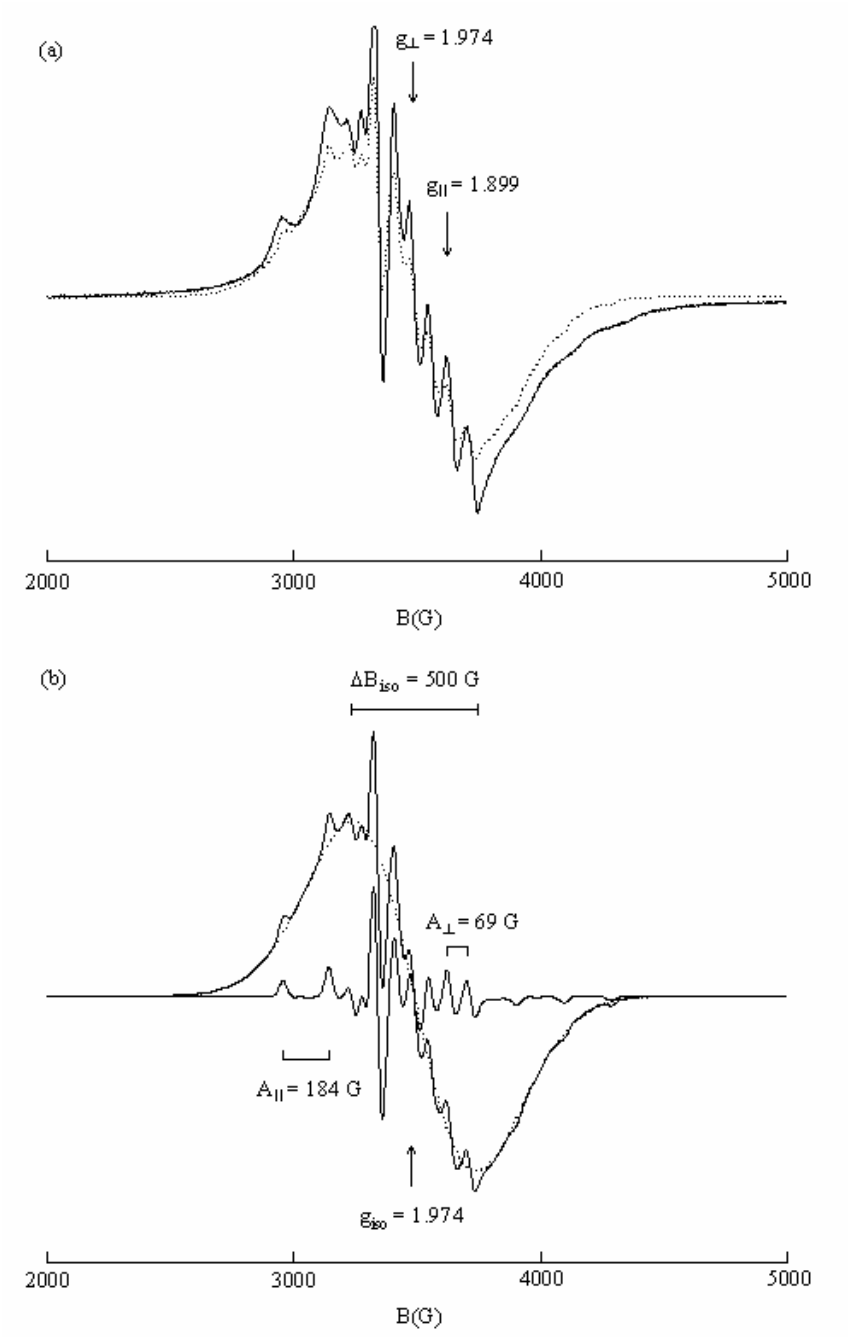

*Fig. 2. (a) Experimental (solid state) and simulated (dotted line) EPR spectra of the powder complex **1**, at room temperature. (b) The components of the simulated spectrum*

where $P = g_e\mu_B g_N \mu_N \langle r^{-3} \rangle$ = 0.0128 cm^{-1} is the dipolar interaction term for the vanadyl ion and g_e = 2.0023 is the *g* factor of the free electron [27,28]. The Fermi contact term was determined as $K = -(A_0/P)-(g_e-g_0)$, where $A_0 = (A_{||}+2A_{\perp})/3$ and $g_0 = (g_{||}+2g_{\perp})/3$. The obtained coefficient (β_2^2 = 0.876) corresponds to a dominant ionic character of the in-plane π V–O bonds. However, there is also an important degree of covalence of these bonds. The low Fermi contact term *K* = 0.705 and the negative signs of $A_{||}$ and $A_{\perp}$ agree with the delocalization of the unpaired electrons of the V^{IV} ions towards the neighboring oxygen atoms.

The powder EPR spectrum of the $K_9[(V^{IV}O)_2V^{V}(BiW_9O_{33})_2]\cdot 21H_2O$ (**2**) sample (Fig. 3) also exhibits two components in the 2:3 ratio as those described for the

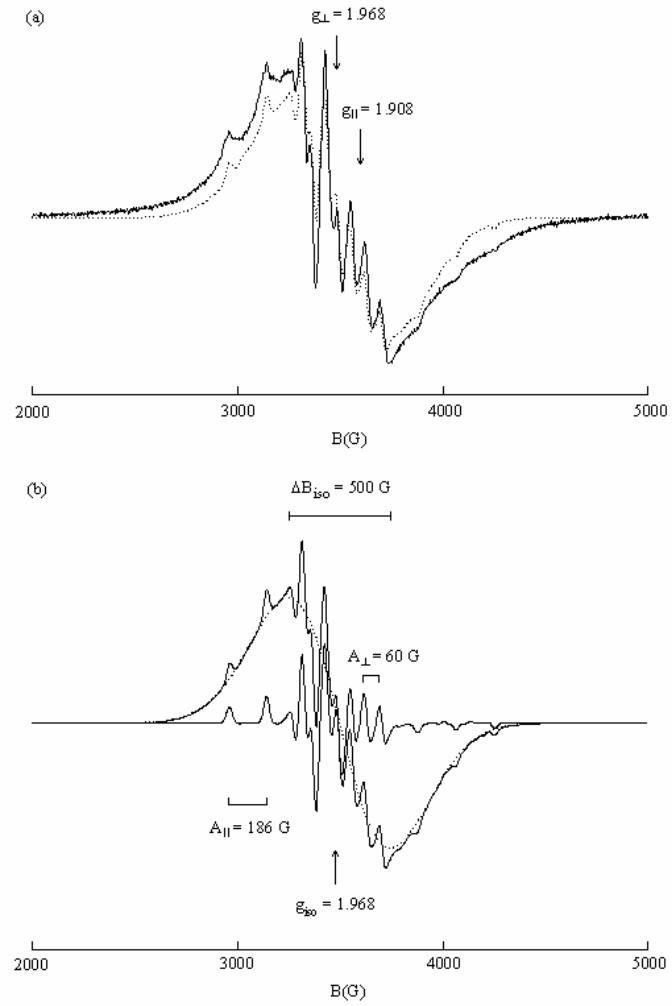

*Fig. 3. (a) Experimental (solid line) and simulated (dotted line) EPR spectra of the powder complex **2**, at room temperature; (b) The components of the simulated spectrum.*

complex **1**. EPR parameters obtained for the axial component by simulating the spectrum are the spin state S = 1/2, g_{II} = 1.908, $g_{\perp}$ = 1.968, A_{II} = 186 G, $A_{\perp}$ = 60 G and the linewidths ΔB_{II} = 46 G, $\Delta B_{\perp}$ = 28 G. These parameters belong to each vanadium (IV) ion. The isotropic component has g_{iso} = 1.968 and ΔB_{iso} = 500 G and suits from dipolar coupling of the vanadium ions. Using the EPR parameters, the molecular coefficient β_2^2 = 0.907 and the Fermi contact term K = 0.662 have been calculated. This time, the in-plane π bonding are more ionic than for the complex **1** with three V^{IV} ions, but the delocalization of the unpaired electrons continues to be realized especially through π rather than σ bonds.

The agreement between the g values obtained for the two complexes is due to the fact that for the complex **1**, g_{II} = 1.899 and $g_{\perp}$ = 1.974 are due to the ground state S = 1/2 of the V^{IV}_3 cluster and for the complex **2**, g_{II} = 1.908 and $g_{\perp}$ = 1.968 values are due to the individual V^{IV} ions. These behavior is sustained by the in plane π bonding β_2^2 molecular coefficient, which is lower for the complex **1** (0.876) than for the complex **2** (0.907), so the delocalisation of the unpaired electrons of the vanadium ions towards the oxygen atoms of the polyoxometalate is higher in the complex **1** and this justify the small extended superexchange interactions present in this complex.

4. Conclusions

EPR parameters obtained after the simulation of the experimental spectra of the $K_{12}[(VO)_3(BiW_9O_{33})_2]\cdot 31H_2O$ and $K_{11}[(VO)_3(BiW_9O_{33})_2]\cdot 21H_2O$ complexes indicate the trapping of the unpaired electrons at the parent V^{IV} paramagnetic ions and the absence of direct delocalization towards the neighboring vanadium ions. The very broad component observed in the EPR spectra are proofs for the existence in both samples of dipolar coupled vanadium(IV) ions.

REFERENCES

[1] D.E. Katsoulis, Chem. Rev. 98 (1998) 359.

[2] M.T. Pope, Heteropoly and Isopoly Oxometalates, Springer–Verlag, Berlin, 1983.

[3] X. Zhang, Q. Chen, D.C. Duncan, C.F. Campana, C.L. Hill, Inorg. Chem. 36 (1997) 4208.

[4] D. Rusu, C. Crăciun, A.-L. Barra, L. David, M. Rusu, C. Roşu, O. Cozar, Gh. Marcu, *J. Chem. Soc. Dalton Trans.*, 19 (2001) 2879

[5] A. Müller, F. Peters, M.T. Pope, D. Gatteschi, Chem. Rev. 98 (1998) 239.

[6] C.J. Gómez-Garcia, E. Coronado, P. Gómez-Romero, N. Casañ-Pastor, Inorg. Chem. 32 (1993) 89.

[7] L. David, C. Craciun, V. Chis, R. Tetean, *Solid State Comm.* 121 (2002) 675

[8] N. Mizuno, M. Misono, Chem. Rev. 98 (1998) 199.

[9] I. Loose, E. Drost, M. Bösing, H. Pohlmann, M.H. Dickman, C. Rosu, M.T. Pope, B. Krebs, Inorg. Chem. 38 (1999) 2688.

[10] C. Tourné, A. Revel, G. Tourné, M. Vendrell, C. R. Acad. Sci. Paris C277 (1973) 643.

[11] A. Mazeud, N. Ammari, F. Robert, R. Thouvenot, Angew. Chem. 35 (1996) 1961.

[12] P. Mialane, J. Marrot, E. Rivière, J. Nebout, G. Hervé, Inorg. Chem. 40 (2001) 44.

[13] T. Yamase, B. Botar, E. Ishikawa, K. Fukaya, Chem. Letters 1 (2001) 56.

[14] Y. Ozava, Y. Sasaki, Chem. Lett. 923 (1987).

[15] B. Botar, T. Yamase, E. Ishikawa, Inorg. Chem. Comm. 3 (2000) 579.

[16] C. Silvestru, H.J. Breunig, H. Althaus, Chem. Rev. 99 (1999) 3277.

[17] B. Krebs, R. Klein, in Polyoxometalates: From Platonic Solids to Anti-Retroviral Activity, M.T. Pope and A. Müller (Eds.), Kluwer Publishers, Dordrecht, 1994.

[18] J. Park, H. So, Bull. Korean Chem. Soc. 15 (1994) 752.

[19] L. David, C. Crăciun , *Appl. Magn. Reson* 20 (2001) 357

[20] C.W. Lee, H. So, Bull. Korean Chem. Soc. 7 (1986) 318.

[21] I. Ursu, "Rezonanță Electronică de Spin", Ed. Academiei RSR, Bucureşti, 1965

[22] Al. Nicula, "Rezonanță Magnetică", Ed. didactică şi pedagogică, Bucureşti, 1980

[23] M. Otake, Y. Komiyama, T. Otaki, J. Phys. Chem. 77 (1973) 2896.

[24] Y.H. Cho, H. So, Bull. Korean Chem. Soc. 16 (1995) 3.

[25] O. Cozar, I. Ardelean, I. Bratu, S. Simon, C. Crăciun, L. David, C. Cefan, J. Mol. Struct., 421 (2001) 563

[26] H. So, Bull. Korean Chem. Soc. 8 (1987) 111.

[27] A. Bencini, D. Gatteschi, Transition Metal Chemistry, vol.8, Marcel Dekker, New York, 1982.

[28] P.R. Klich, A.T. Daniher, P.R. Challen, Inorg. Chem. 35 (1996) 347.

STUDIA UNIVERSITATIS BABEŞ-BOLYAI, PHYSICA, XLVIII, SPECIAL ISSUE, 2003

THE INFLUENCE OF B_2O_3- BI_2O_3 VITREOUS MATRIX ON COPPER IONS EPR ABSORPTION SPECTRA

R. STEFAN[1] and S. SIMON[2*]

[1] University of Agricultural Sciences and Veterinary Medicine, 3400 Cluj Napoca, Romania
[2] Babes-Bolyai University, Physics Department, 3400 Cluj Napoca, Romania

ABSTRACT. Results of EPR investigations performed on glasses from (100-y)[(xB_2O_3(1-x) Bi_2O_3]yCuO system with $0.07 \leq x \leq 0.8$ and y = 0.5 and 1 mol % are reported. The changes in EPR spectra point out the modification of the copper ions vicinity due to the variation of the B_2O_3/Bi_2O_3 ratio in the glass matrix. The hyperfine structure is observed in the parallel band only for samples with high boron oxide content wherein the Cu^{2+} paramagnetic ions can be disposed in sites of octahedral symmetry, while in the samples with high bismuth oxide content Cu^{2+} ions are experiencing a more disordered surrounding.

Introduction

Bismuth oxide is an unusual glass network former. The network of bismuthate glasses is built up of [BiO_3] pyramidal units, while multicomponent bismuth - transition metal glasses are built up of both [BiO_6] octahedral and [BiO_3] tetrahedral units.[1-3] The boron oxide is one of the vitreous structure classical formers; it is disposed in oxide glasses as BO_3 planar and BO_4 tetrahedral units in a ratio depending on the modifier oxide and the added impurities.[3,4] The properties of heavy metal oxide glasses, such as high refraction index, very good infrared transmission and wide nonlinear susceptibility[1] as well as their applicability in the field of optoelectronic devices, and mechanic and thermal sensors[5] determined the investigation of vitreous bismuthate materials. They proved to be also good amorphous precursors for superconducting materials.[5,6]

The data obtained about glass systems by means of electron paramagnetic resonance (EPR) spectroscopy, a very used technique in local order studies, are offering different structural details like paramagnetic ions coordination and the arrangement of their neighbours.[7] The Cu^{2+} ions were intensively used as paramagnetic sensors of the local structure in different glasses.[8-13]

This paper investigates the way in which the changing ratio between boron and bismuth and the paramagnetic ions doping degree influence the local structure of the bismuth borate glasses, particularly in the region of high bismuth content.

Experimental

Glass samples of 99%[(xB_2O_3(1-x)Bi_2O_3]0.5%CuO and 99.5%[(xB_2O_3(1-x) Bi_2O_3]1%CuO systems ($0.07 \leq x \leq 0.8$) were prepared using as starting materials H_3BO_3, $Bi(NO_3)_3 \cdot 5H_2O$ and CuO of reagent purity grade. The mixtures were melted in sintered corundum crucibles introduced into electric furnace with normal atmosphere, directly at 1100°C and maintained for 15 min at this temperature. They were quickly undercooled at room temperature by pouring onto stainless steel plates. The colour of

the samples was red-brown typical for bismuth ions, masking the green-blue colour typical for other glass matrices containing copper ions. The EPR measurements were carried out at room temperature in X band (9.45GHz) with 100 kHz field modulation, using a JEOL type spectrometer.

Results and discussion

The EPR absorption spectra are presented in Figure 1 for 99.5%[(xB_2O_3(1-x) Bi_2O_3]0.5%CuO composition. They are due to unpaired electrons of Cu^{+2} ions with electronic configuration $3d^9$ and nuclear spin (I=3/2). Both for samples with 0.5 mol % Cu_2O and for those with 1 mol % Cu_2O no perpendicular hyperfine structure was detected. The widths of individual components of perpendicular absorptions exceed the separation between absorption peaks $|A_\perp|$.

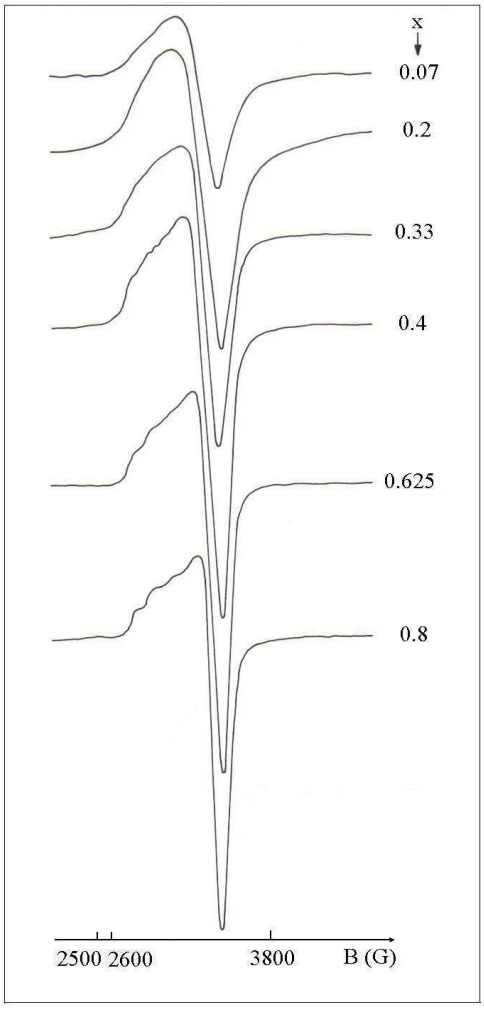

Fig. 1 EPR absorption spectra for 99.5%[(xB_2O_3(1-x)Bi_2O_3]0.5%CuO ($0.07 \leq x \leq 0.8$) glasses.

The absorption lines in the spectra recorded from samples with y = 0.5 are symmetric, wide and unresolved for low B_2O_3 concentrations, proving the high degree of local disorder[8-10]. For $x \geq 0.4$ the parallel hyperfine structure (hfs) is well resolved for m=-3/2 and -1/2 magnetic quantum numbers and the absorption line becomes more asymmetric. This shows that in the samples with high boron content the copper ions are disposed in their typical symmetry, that is a one axis elongated octahedron[8]. Bismuth oxide acts like a glass network modifier determining the vitreous matrix disorder.

The absorption spectra for glasses of 99%[$(xB_2O_3(1-x)Bi_2O_3$]1%CuO composition with ($0.07 \leq x \leq 0.8$) are shown in Figure 2. The parallel hfs appears only for $x \geq 0.6$. The hyperfine structure is more pronounced when x values become higher but is less resolved than in y = 0.5 case for the same B_2O_3 concentration due to the dipolar broadening effect. For high bismuth oxide content the ligand field fluctuations broaden the absorption line and consequently the parallel hyperfine structure disappears.

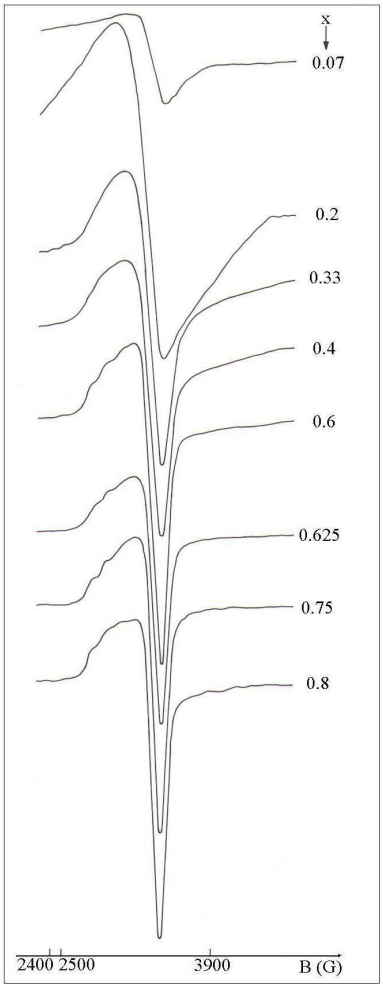

Fig. 2 EPR absorptions spectra for 99%[$(xB_2O_3(1-x)Bi_2O_3$]1%CuO ($0.07 \leq x \leq 0.8$) glasses.

The cupric ions occupy the positions of bismuth cations having an octahedral coordination.[15] For glasses with high bismuth oxide content the intensity of the EPR signal is lower than for the samples with higher boron oxide content, denoting that a part of Cu^{2+} paramagnetic ions are reduced to Cu^{+} non-paramagnetic ions. Our earlier studies showed a similar behaviour for manganese and iron ions hosted in boron-bismuthate glasses.[16] The broad and unresolved EPR absorption line for $x \leq 0.4$ shows a disordered disposal of copper ions into the glass structure or it could be assigned to copper ions clusters even for this low CuO content or both situations could be involved.

The EPR parameters values dependence on boron content in matrix is presented in Table 1. The hyperfine structure constant was estimated using the distance between the first two parallel absorptions. We assume[8] from these data that the coordination sphere of cupric ions is a one-axis elongated octahedron when $g_{\parallel} > g_{\perp} > 2$. The values of $g_{\perp}$ factor were determined using the middle point of perpendicular absorption line with an error up to 10 %.

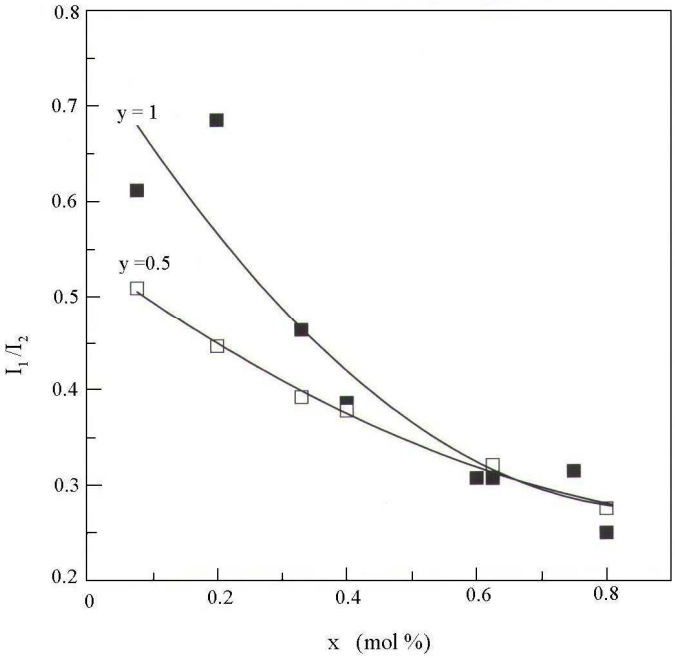

Fig. 3 The asymmetry factor dependence on B_2O_3 content for y = 0.5 and 1.

Figure 3 shows the dependence on boron oxide content of the asymmetry factor expressed as I_1/I_2, where I_1 and I_2 represent the height of resonance lines in the region of the parallel and perpendicular band of the EPR spectrum respectively. The asymmetry factor decreases for both y = 0.5 and y = 1, when the boron oxide content increases in the glass. The second system slope is steeper, showing a greater tendency to a disordered structure when the cooper content increases form 0.5 to 1 into the vitreous matrix.

Table 1

EPR parameters for (100-y)[(xB_2O_3(1-x)Bi_2O_3]yCuO glass samples.

x	g_{II}		A_{II} (G)		$g_{\perp}$	
	y = 0.5	**y = 1**	**y = 0.5**	**y = 1**	**y = 0.5**	**y = 1**
0.07	-	-	-	-	2.098	2.110
0.2	-	-	-	-	2.108	2.138
0.33	-	-	-	-	2.095	2.099
0.4	2.378	-	128	-	2.090	2.095
0.6	-	2.340	-	128	-	2.091
0.625	2.356	2.340	128	128	2.091	2.091
0.75	-	2.351	-	128	-	2.091
0.8	2.357	2.363	128	128	2.082	2.082

Conclusion

Homogenous oxide glasses with high bismuth oxide content beside boron oxide and doped with 0.5 or 1 mol % CuO were obtained. Only parallel hyperfine structure was detected when boron oxide concentration in the vitreous matrix was higher than 0.4 for y = 0.5 and than 0.6 for y = 1.

High boron oxide content allows to Cu^{2+} ions to occupy axially elongated octahedral environments as EPR parameters indicate. High bismuth oxide content in B_2O_3-Bi_2O_3 matrix destroys during the glass formation the copper unstressed environment and these ions are randomised or clustered into the glass matrix structure.

REFERENCES

1. W. H. Dumbaugh, J.C. Lapp, J. Am. Ceram. Soc., 75**,** 9, 2315 (1992).
2. J. Krogh-Moe, Phys.Chem. Glasses, 15, 190 (1962).
3. H. Zheng, R. Xu, J.D. Mackenzie, J. Mater. Res., 4, 911 (1989)
4. C. Stehle, C. Vira, D. Hogan, S. Feller, M. Affatigato, Phys. Chem. Glasses, 39, 2, 83, (1998).
5. L. Baia, D. Maniu, T. Iliescu, S. Simon, S. Schlucker, W. Kiefer, Asian J. of Physics, 9,1, 51 (2000).
6. T. Komatsu, R. Sato, K. Imai, K. Matusita, T. Yamashita, J. Appl. Phys, 27, L550 (1998).
7. D.L. Griscom, Glass Sci. Techn., 48 (1990).
8. H. Imagawa, Phys. Stat. Solidi 30, 469 (1968).
9. L.P. Bogolomova, V.A. Zhachkin, V.N. Lazukin, N.F. Shapovalova, V.A. Shmukler, Soviet Phys. Dokl., 15, 1031 (1971).

10. S. Simon, Al. Nicula, Solid State Commun., 39, 1251 (1981).
11. Al. Nicula, M. Peteanu, Rev. Rom. Phys. 26, 8-9,1047 (1981).
12. S. Simon, Al. Nicula, Nucl. Instr. and Methods, 1-2, 199 (1982).
13. O. Cozar, I. Ardelean, V. Simon, L. David, N. Vedean, V. Mih, Appl. Magn. Res., 16, 473 (1999)
14. S. Simon, Al. Nicula, Studia, Physica, 25, 2, 39 (1982)
15. R.H.Sands, Phys. Rev. 99, 1222 (1955).
16. R.Stefan, S.Simon, Mod. Phys. Lett. B, 15, 3, 111 (2001).